FINAL TECHNICAL REPORT

Federal Agency and Organization: DOE EERE – Geothermal Technologies Program

Recipient Organization: West Virginia University Research Corporation
DUNS Number: 191510239
Recipient Address: 885 Chestnut Ridge road.
PO Box 6845
Morgantown, WV 26506
(304) 293-6709

Award Number: DE-EE0008105
Project Title: Feasibility of Deep Direct-Use Geothermal on the West Virginia University Campus-Morgantown, WV
Project Period: October/2017 – September/2019

Principal Investigator: Dr. Nagasree Garapati
Research Assistant Professor,
Chemical and Biomedical Engineering
nagasree.garapati@mail.wvu.edu
(304) 293-5028
Report Submitted: Jennifer Hause
(If other than PI) Project Manager, WVU Energy Institute
jhause@wvu.edu
(304) 293-6564

Date of Report Submission: September 22, 2021
Reporting Period: October 1, 2017 to September 30, 2019
Report Frequency: Final

Project Partners:
West Virginia Geological & Economic Survey, Morgantown, WV
Lawrence Berkeley National Laboratory, Berkeley, CA
Cornell University, Ithaca, NY

DOE Project Team: DOE Contracting Officer – Laura Merrick
DOE Project Officer – Arlene Anderson
Project Monitor – Angel Nieto

Signature Jennifer D. Hause **Date** September 22, 2021
***The Prime Recipient certifies that the information provided in this report is accurate and complete as of the date shown.**

ACKNOWLEGEMENT
This material is based upon work supported by the U.S. Department of Energy's Office of Energy Efficiency and Renewable Energy (EERE) under the Geothermal Technologies Offices, under Award Number DE-EE0008105.

TABLE OF CONTENTS

LIST OF FIGURES

LIST OF TABLES

FEASIBILITY OF DEEP DIRECT-USE GEOTHERMAL ON THE WEST VIRGINIA UNIVERSITY CAMPUS – MORGANTOWN, WV

EXECUTIVE SUMMARY

In 2010, research completed by the Southern Methodist University (SMU) Geothermal Laboratory estimated temperatures at reasonable drilling depths in the state of West Virginia (WV) were in the temperature range desirable for district heating. This higher temperature region extends from north-central WV (Monongalia County) to southeastern WV (Greenbrier County). The Morgantown campus of West Virginia University (WVU) is located within the north-central region, and as part of the 2016 study on Low-temperature Geothermal Play Fairway Analysis for the Appalachian Basin (GPFA-AB), Morgantown is identified as one of the priority locations for further analysis of the potential for deep direct-use (DDU) of geothermal energy. In this project, the feasibility of developing a Geothermal District Heating and Cooling (GDHC) system for the WVU campus in Morgantown, WV, to replace the current coal-fired steam heating and cooling system, is evaluated.

In conjunction with our project partners, the West Virginia Geological and Economic Survey (WVGES), Lawrence Berkeley National Laboratory (LBNL), and Cornell University, our overall project objectives were to: 1) decrease the uncertainty and risk associated with developing the geothermal resource for use on campus at WVU, and 2) complete an optimized design for the geothermal system that minimized the delivered Levelized Cost of Heat (LCOH) across a range of possible DDU utilization scenarios.

WVGES research focused on characterization of the target geothermal reservoir formation, the Tuscarora Sandstone. Multiple types of analyses were performed to estimate permeability, porosity, and other important reservoir parameters that were required to inform thermal-hydraulic models of heat extraction from the reservoir. These analyses included: measuring permeability via a minipermeameter, petrography, digitization of geophysical well log curves and estimating reservoir properties from those logs, facies analysis, and analyzing computed tomography (CT) scanned data to semi-quantitatively assess fracture volume.

The Tuscarora Sandstone is identified as a very fine- to very coarse-grained, poorly- to well-sorted, quartz sandstone. Permeability measurements were taken on all small-scale deformation features observed in available drill cores. Matrix permeabilities are generally less than 10 milliDarcy (mD). Permeabilities associated with deformation features, especially the larger, open fractures, can exceed one Darcy (D) anywhere within the Tuscarora. The shallower portion of the Tuscarora seems to have more frequent permeable zones than the deeper portion. This may be related to an increase in the amount of silt- and clay-sized sediment towards the bottom of the formation. Porosity is estimated visually through thin-section analysis and digital well log data and average porosity values are in the range of 2-4%. Fracture density is estimated using CT scan data and is in the range of 0.027%-7.7%. The Tuscarora attains maximum thickness in northeastern WV, in proximity to the WVU campus, Morgantown. The geothermal gradient is estimated to be in the range of 22-29°C/km, using bottom hole temperature information from five Tuscarora wells closest to the target location. Estimation of temperatures at the top of the Tuscarora formation (about 3 km depth) using temperature data from within about 30 km of Morgantown provides a

mean value of 88°C with a 5th and 95th percentile estimates of about 74.5°C and 104°C, respectively.

A 3-D geological structural surface was generated by correlating the formation top depths of thirty wells surrounding the proposed geothermal wellsite. The 2D-3D surface modeling is performed in Geological Evaluation System (GES) modeling software (a product of GPT Reservoir Characterization Professionals). Conformable gridding methodology is employed to develop a meaningful structural interpretation for the Tuscarora. The cross-section displays a gently southeast dipping Tuscarora surface, into a syncline separating the proposed geothermal site from the South Burns Chapel Field (a NE-SW trending anticline). While the final structural interpretation of the Tuscarora is reasonable, in the context of regional structural trends, the structural model has a significant amount of uncertainty due to the lack of subsurface data to precisely constrain the structure under the proposed geothermal project site in Morgantown.

A 3-D geological model centered on the proposed well location based on the structural model is constructed with the 3-D GeoModeller, Groundwater Modeling System (GMS). The numerical reservoir model is derived from this geological model and the estimated reservoir properties are used for numerical simulations to analyze reservoir performance using vertical and horizontal well configurations.

iTOUGH2/EOS1 is used to perform the numerical simulations for the analysis of the fractured geothermal system. The iTOUGH2 simulation–optimization code provides inverse modeling capabilities as well as formal (local and global) sensitivity and uncertainty propagation analyses for TOUGH2, a simulator for multiphase, multicomponent, non-isothermal flows in fractured-porous media. EOS1 of TOUGH2 was specifically developed for geothermal applications.

Simulations are performed on single-K and dual-K models using a pair of vertical wells for injection and production. It was found that dual-K models behave like a porous media due to the long residence time and relatively small fracture spacing; the heat exchange between fracture and matrix is dominated by the matrix volume rather than the heat exchange area between fracture and matrix. Therefore, only the single-K model is considered for further analysis. The reservoir behavior using vertical and horizontal well configurations is analyzed. The thermal breakthrough and reservoir productivity are higher for a horizontal configuration and the well-head LCOH is comparable; therefore, a horizontal well configuration is considered. WVU's experience drilling horizontal wells in the Marcellus Shale under the Marcellus Shale Energy and Environment Laboratory (MSEEL) project, and the close relationship with industrial partners provides an advantage to apply this technology for geothermal systems.

Impact of reservoir heterogeneity is analyzed, and it is found that the heterogeneity has a huge impact on thermal breakthrough curves and reservoir productivity. The reservoir parameters that contribute to the most uncertainty is identified as: correlation length and sill variance (i.e., geostatistical parameters used to generate the heterogeneous flow field), permeability, and porosity. Therefore, it would be beneficial to further characterize these influential parameters at the well location through an exploratory well with a full-logging program.

A stochastic estimation of geothermal reservoir productivity for the Tuscarora near Morgantown assuming: 1) fracture-dominated productivity, and 2) matrix flow productivity was also performed. These reservoir productivity estimates are used to update the 2016/2017 Reservoir Risk Factor favorability and uncertainty maps made for the GPFA-AB project (https://gdr.openei.org/submissions/899). Among the reservoirs considered in that play fairway analysis, it is found that a fracture-dominated Morgantown Tuscarora location would be among the most favorable and least uncertain reservoirs to develop a DDU geothermal system in the Appalachian Basin.

The energy consumption data for the WVU campus is measured to characterize the energy demand. Servers are installed at five main distribution points to record steam temperature, pressure, flow rate, and return condensate temperature and flow rate in 5-minute intervals. The data is compared to the monthly invoice from Morgantown Energy Associates (MEA), the current steam supplier. The steam demand fluctuates based on the daily weather. The peak usage is observed in the month of January and the minimum usage is in July.

A centralized, hybrid natural gas geothermal system is proposed to deliver steam to the distribution points at the required conditions; thus, the current distribution system will be used. A heat pump is considered to improve the performance of the system and increase geothermal heat extraction. The surface plant is modeled using ASPEN simulation package, where the surface model is simulated using HYSYS, the plate heat exchanger for geothermal heat extraction is designed using Exchange Design and Rating (EDR), and the capital costs are calculated using the Economic Analyzer or vendor quotes.

The economic analysis of the hybrid GDHC system is performed using GEOPHIRES [GEOthermal energy for the Production of Heat and electricity (IR) Economically Simulated, with "IR" representing electric current and resistance and referring to the electricity mode], developed at Cornell University. GEOPHIRES is modified to account for a hybrid geothermal natural gas system, and the BICYCLE levelized cost model is applied to calculate LCOH. The LCOH for the entire campus steam supply is in the range of 7.0 - 12.5 $/MMBTU, which is below the current cost of $15/MMBTU.

Due to the high latent heat needed for conversion of hot water to steam, the hot water-based geothermal contribution to the current steam-based hybrid system would be low. Therefore, conversion of the steam-based system to a hot water-based system is considered in this analysis. Due to the large water flow rates needed for the system, multiple horizontal configurations are considered. Each configuration has two production wells and one injection well with a total production rate of 80 kg/s. The LCOH obtained for this hot water system is higher than the current cost. However, the LCOH estimated is based on a maximum production rate of 40 kg/s from a single production well; hence, well drilling costs for multiple wells are too high for the system to be economical. Therefore, the feasibility of the hot water-based system depends on the ability to produce high volumes of geothermal hot water from the Tuscarora sandstone to meet the peak demand.

A geothermal DDU system at WVU is feasible to replace the existing coal-based system, given the geological and techno-economic analyses completed in this study. A DDU system would not

only serve the campus of 33,000 students, but it would also serve Ruby Memorial Hospital, the largest hospital in West Virginia and West Virginia's only nationally certified Level 1 trauma center. It would also advance the efforts to achieve a reliable and clean energy source for the central steam generation system as part of WVU's Sustainability Plan, which is managed under the WVU Office of Sustainability and the WVU Energy Institute.

SUMMARY OF PROJECT ACTIVITIES

Original Project Hypotheses

In 2010, research completed by the Southern Methodist University (SMU) Geothermal Laboratory estimated temperatures in the range desirable for district heating could be achieved at reasonable drilling depths within West Virginia (WV) state boundaries (Blackwell et al., 2010; Frone and Blackwell, 2010). An area of particular interest with elevated heat flows was estimated to extend from northcentral WV (Monongalia County), to southeastern WV (Greenbrier County), as shown in Figure 1 (Frone and Blackwell, 2010). Geothermal resource assessment completed using additional well data in the Geothermal Play Fairway Analysis of the Appalachian Basin (GPFA-AB) also estimated a region of elevated heat flows in northcentral WV (Cornell University, 2017). The Morgantown campus of West Virginia University (WVU) is located within this region and offers a desirable and unique combination of critical factors necessary to develop a deep direct-use geothermal system. Specifically, we will be able to leverage an existing surface district heating and absorption cooling infrastructure currently deployed on campus resulting in year-round utilization of the deep direct-use (DDU) geothermal system and thereby lowering the levelized cost of heat (LCOH) by fully amortizing the system over 12 months.

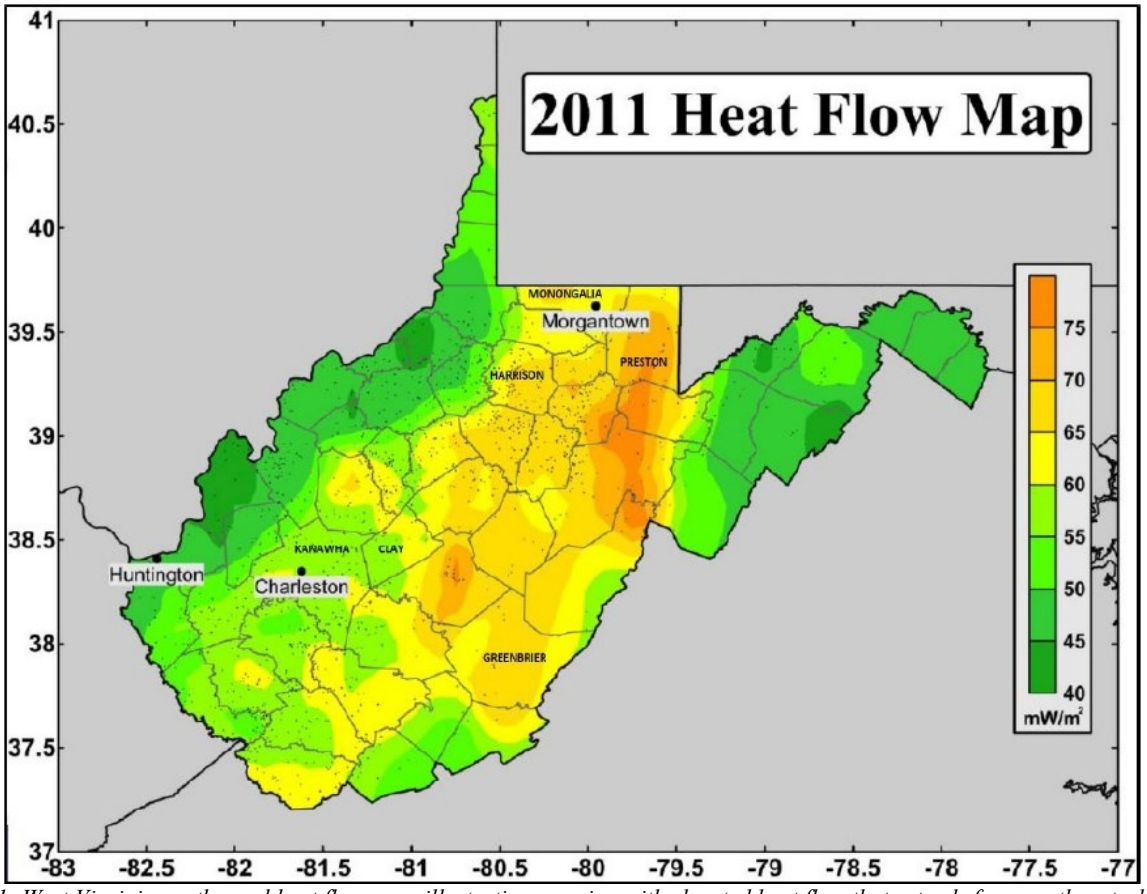

Figure 1: West Virginia geothermal heat flow map, illustrating a region with elevated heat flow that extends from northcentral West Virginia (Monongalia County), to southeastern West Virginia (Greenbrier County) (Frone and Blackwell 2010). Small black circles indicate locations of wells for which the surface heat flow was estimated from bottom-hole temperatures.

WVU's project team has identified the target geothermal reservoir formation as the Tuscarora sandstone. An ongoing project called the Marcellus Shale Energy and Environment Laboratory (MSEEL) has given the project team unprecedented access to subsurface data, including equilibrated geothermal temperatures along the 13,874 ft (total depth, which includes a long lateral component) fiber optic distributed temperature sensor in the well showing a temperature of 167.5°F at 7,412 ft (2,259 m) true vertical depth (TVD). These new data have given the project team confidence in the local heat flux and projected geothermal temperatures. In addition to the temperature information provided by this well, resistivity logs, and previous core analysis from local wells drilled to the depths of the Tuscarora indicated a fracture-dominated reservoir with significant potential porosity and permeability. The elevated temperatures and potential for high flow conductivity makes the proposed site an ideal geothermal resource for direct use.

In this project, the feasibility analysis of developing a Geothermal District Heating and Cooling (GDHC) system for the WVU campus in Morgantown is performed. The two main primary goals of this project are:
1) collect local information on the critical factors (temperature and flow rate) to understand the uncertainty and reduce the risk associated with developing the geothermal resource for use in a WVU campus GDHC system, and
2) complete an optimized design for the GDHC system by minimizing the delivered Levelized Cost of Heat (LCOH).

This report is organized into the following sections:

- **Summary of Project Activities**: original project hypotheses, approaches used, problems encountered, departure from planned methodology, and impact on project results.
- **Methodology:** underlying scientific theory and key assumptions, steps in the workflow, summary of the strengths and limitations of the process, mathematics used (including formulas and calculation methods), potential sources of error, software used, and results of tests to demonstrate satisfactory model performance.
- **Discussion of Results:** primary conclusions and comparison of actual accomplishments with original goals and objectives.
- **Recommendations for Next Phase:** objectives, description of planned activities, and outcome for next phase.
- **Project Output:** List of publications, conference papers, other public releases of results, and networks/collaborations fostered.
- **References:** Major works cited in this report.
- **Catalog of Supporting Files:** a list of datasets used to include the source(s), limitations on rights, custom code/scripts/configuration files used to process data, risk factor, and final favorability map, numerical modeling ASCII data files and processed figures, ASPEN files used for surface plant modeling, GEOPHIRES input and output files and data collected in excel files.

Approaches Used

The Statement of Project Objectives (SOPO) outlines the Project Plan as a series of five objectives, each with several subtasks, as summarized below. Objectives 1 and 3 comprise the Geothermal Resource Assessment, Objective 2 comprises the surface end-use demand estimation, Objective 4 comprises methods to estimate costs and benefits, and Objective 5 is related to the market transformation plan. The plan was followed very closely with only minor adjustments needed as described in the next section, Accomplishments and Challenges. The following is the condensed list of our original project objective tasks including a description of each one.

1. **Objective 1.0 Characterize the Geothermal Site:** The purpose of this objective and its several subtasks are to characterize the proposed geothermal site based on the geological information available from the cores and well logs of nearby existing wells and develop a 3-D representative model for numerical modeling.
   Deliverable: Deliver properties (porosity, permeability, geothermal gradient) of the target formation by processing the raw data obtained by CT scans and minipermeameter measurements. Deliver a 3-D Geological structural surface map of the proposed site and a corresponding 3-D reservoir model for numerical modeling.
2. **Objective 2.0 Characterize Existing Infrastructure:** The purpose of this objective is to characterize energy demand on the campus and the current existing district heating and cooling system (DHCS). A base case surface facility is modeled using ASPEN simulations.
   Deliverable: Deliver year-round steam consumption data (temperature, pressure, and flow rate) for the entire campus. Assess existing distribution system and develop a base case for surface infrastructure.
3. **Objective 3.0 Create Subsurface Model and Design:** The purpose of this objective is to perform subsurface modeling to determine optimum well configuration and uncertainty quantification. Also, update the 2016/2017 Reservoir Risk Factor favorability and uncertainty maps made for the Geothermal Play Fairway Analysis of the Appalachian Basin project.
   Deliverable: Deliver optimum well configuration and quantify the effect of uncertainty in reservoir properties on geothermal fluid production. Deliver an updated risk favorability map with the Morgantown location added for the target Tuscarora sandstone.
4. **Objective 4.0 Develop and Optimize Integrated Geothermal District Heating and Cooling (GDHC) System:** The purpose of this objective is to estimate capital costs and LCOH using GEOPHIRES (GEOthermal energy for the Production of Heat and electricity Economically Simulated) and determine feasibility of geothermal direct use on the WVU Morgantown campus by comparing estimated energy costs and benefits with the current existing system.
   Deliverable: Deliver LCOH and results of feasibility analysis of proposed geothermal direct-use system.
5. **Objective 5.0 Maintain & Update Market Transformation Plan:** The purpose of this objective is to unify the results obtained in Objectives 1-4 and to report them through quarterly and final technical reports.
   Deliverable: Deliver quarterly and final reports in accordance with the Federal Assistance Reporting Checklist. Uploading the data and outputs to DOE Geothermal Data Repository (DOE-GDR).

COMPARISON OF ACTUAL ACCOMPLISHMENTS WITH ORIGINAL GOALS AND OBJECTIVES

Referring to the "Feasibility of Deep Direct-Use Geothermal on the West Virginia University Campus-Morgantown, WV" project's major tasks and deliverables described under Approaches Used in this report, all goals and objectives were achieved. WVGES team members are experienced with large collections of data from oil and gas wells; Cornell is experienced in analyzing datasets using statistical methodologies; LBNL is the lead development team of the TOUGH family of reservoir simulation codes and has extensive experience and expertise in geothermal reservoir simulation; the WVU Geology department is experienced in analyzing well data and developing geological surface model; the WVU Chemical Engineering department is experienced in surface plant modeling and economic analysis; and the WVU Facilities team owns, manages, and maintains a 2 billion BTU/year system for 245 buildings on 1,892 acres and are involved in multi-phase performance contract projects across the campus to improve the university facilities, increase energy efficiency, and safety.

The project had few departures from the original SOPO. In response to surface landowner and lay down space concerns with the initially proposed WVU Arboretum site location, the team sought to investigate other possible locations on the WVU campus for the DDU project installation. New sites are proposed on the Evansdale and Health Sciences campuses due to lack of inholdings on the downtown campus. The main variance in the planned activities include: (a) collection of the utility temperature, pressure, and flow rate; and (b) utilizing a geothermal boiler hybrid system to meet steam requirements on campus. As the current piping for the entire campus is steam-based, changing these pipelines to hot water could be uneconomical. Therefore, it was decided to supply steam using a geothermal hybrid (geothermal-natural gas boiler) system to the distribution points and use the current distribution system across the campus requiring minimal changes and reducing costs. Thus, energy demand is characterized by using measurements at the five main distribution points collected over the project duration. As per a prior DOE suggestion, a preliminary analysis of conversion of steam infrastructure to hot water system is also performed.

The project accomplished all SOPO tasks and exceeded what was required. For instance, Computed Tomography (CT) scans on Preston-119, Harrison-79 and Clay-513 cores are performed at National Energy Technology Laboratory (NETL) and a semi-quantitative fracture density estimation using CT scan data on Preston-119 core is also conducted. Digitization of geophysical well logs curves in WV is completed and reservoir properties are estimated from those logs. Permeability measurements were made for the Preston-119 core using a CoreLab^{TM} PPP-250 Portable Probe minipermeameter. A 3-D geological structural surface is generated by correlating thirty wells surrounding the proposed geothermal wellsite using Geological Evaluation System (GES) modeling software. Fracture analysis for the Marcellus shale from the nearby MSEEL site data was compiled as potential proxy for regional stresses and potential fracture patterns in the Tuscarora sandstone. TOUGH2 simulations are conducted for reservoir performance analysis and uncertainty quantification analysis is performed using iTOUGH2. A Monte Carlo analysis of uncertain reservoir and fluid properties is used to estimate the geothermal reservoir productivity for the Tuscarora and is used to update the 2016/2017 Reservoir Risk Factor favorability and uncertainty maps made for the Geothermal Play Fairway Analysis of the Appalachian Basin project. The end-use surface demand is characterized by year-round steam consumption data and assessment of the existing district heating system (DHS) is also performed. Surface modeling for

the hybrid GDHC is performed using the ASPEN simulation suite. In addition, the usage of steam across the campus is analyzed for conversion of steam-based to hot water-based system and a preliminary analysis is performed to assess the capital costs needed to convert the current steam infrastructure to a hot water system using only the geothermal resource. The economic analysis is performed using modified GEOPHIRES with BICYCLE levelized cost models and the feasibility is determined by comparing the costs and benefits with existing coal-powered steam DHS. Next, each of the Tasks are discussed to highlight changes from the planned methodology.

Objective 1.0 Characterize the Geothermal Site:

Completed Activities

Task 1.1: Perform Core Analysis and Estimate Temperatures

The proposed geothermal site for DDU was characterized based on the geological information available from the cores and well logs of nearby existing wells.

Performed core analysis

- Permeability measurements via a minipermeameter
- CT scanning in collaboration with DOE-NETL
- Fracture density estimations using CT scan data

Collected geological data of cores and nearby existing wells

- Thickness
- Porosity
- Permeability
- Fracture network configuration
- Geothermal gradient

Task 1.2: Estimate Reservoir Properties for Modeling

The data obtained from Task 1.1 were processed to determine the reservoir properties such as thickness, porosity, permeability, fracture network configuration, and geothermal gradient. The reservoir thickness was determined from gamma ray logs indicating extent of the high porosity zone.

Task 1.3: Development of 3-D Geological Model

A 3-D structural surface model is generated by correlating 30 wells surrounding the proposed geothermal wellsite. While the final structural interpretation of the Tuscarora Sandstone is reasonable, in the context of regional structural trends, the structural model has a significant amount of uncertainty due to the lack of subsurface data available near the proposed site for this study. Based on the geological studies, a 3-D numerical reservoir model centered on the proposed well location is constructed, which is subsequently used for numerical modeling using TOUGH2/iTOUGH2 (Pruess et al., 1999; 2011), in Objective 3.

Challenges: There was a delay in collecting permeability measurements using minipermeameter, due to significant technological updates between new instrument and the previous instrument used by WVGES geoscientists to collect permeability measurements, which resulted in a longer than anticipated training period for its use. The main differences involve the configuration of the measurement wand and the apparatus to hold the core samples during measurement, as well as the type, collection method, and temperature of inert gas used for injection. We have mitigated these issues by effectively communicating with the Core Lab Company with detailed questions

regarding the differences in the minipermeameter instrument. Due to the irregular shape, high level of core loss, and extensive breakage of samples from the Harrison-79 and Clay-513 cores precludes the ability to collect reliable, repeatable minipermeameter measurements from these cores.

Objective 2.0 Characterize Existing Infrastructure:
Completed Activities

Task 2.1: Characterize Energy Demand

The year-round energy consumption data for the WVU campus during the project period is collected to characterize the energy demand. Particularly, the steam temperature, pressure, and flow rates at the five distribution meter points, average and peak heating and cooling demand of the campus, and monthly energy usage per meter point was determined over a year.

Task 2.2: Perform Integration Assessment for Current District Heating System (DHS)

The current piping system and the equipment for district heating and cooling across the campus are analyzed. The retrofit capability, lifetime, and economics of the current distribution system integrated with the proposed hybrid GDHC system is quantified.

Task 2.3: Develop Base Case Surface Facility Design

Based on the geothermal production flow rate and temperatures obtained from Task 3.1 and available infrastructure, a base case surface facility is designed. The surface plant model is simulated using ASPEN HYSYS models and heat exchanger is designed using Aspen Exchanger Design and Rating (EDR).

Challenges: The main variance in planned activities is measurement of fluid steam temperatures and flow rates. These measurements are being recorded at the five main distribution points. This change is made because the piping across the entire campus is based on steam delivery; therefore, changing these pipelines to hot water will be too expensive and uneconomical. Instead, it was decided to supply steam using a geothermal hybrid (geothermal natural gas boiler) system to the distribution points and use the current distribution system across the campus thus requiring minimal changes.

Objective 3.0 Create Subsurface Model and Design:
Completed Activities

Task 3.1: Simulate Base Case Vertical and Horizontal Well Configurations

The production simulations are carried out for two different well configurations, one with a pair of vertical wells and the other configuration with a pair of horizontal wells. Simulations are performed using TOUGH2/EOS1 (Pruess et al., 1999; 2011) in a fractured geothermal system. EOS1 of TOUGH2, developed mainly for geothermal applications, can simulate water in both liquid and steam phase. The performance of both configurations is evaluated based on production fluid temperature, thermal drawn down period and reservoir impedance (RI).

Task 3.2: Determine Well Configuration and Orientation/Economic Analysis

To determine an optimum well configuration, different well spacing is evaluated for both vertical and horizontal well configurations. Preliminary economic analysis of well-head LCOH, (i.e., the capital costs for drilling wells and pumping costs for production and fluid injection) for different arrangements is performed using GEOPHIRES. Based on the performance and cost, the final well

configuration is selected to be a pair of horizontal wells for further analysis. WVU's experience drilling horizontal wells in Marcellus shale in the MSEEL project provides an advantage to applying the technology for the proposed geothermal systems.

Task 3.3: Perform Subsurface Uncertainty Analysis

Uncertainty quantification analysis is performed to identify the most influential subsurface parameters (porosity, permeability, and heterogeneity). A stochastic estimation of geothermal reservoir productivity for the Tuscarora Sandstone near Morgantown assuming: 1) fracture-dominated productivity, and 2) matrix flow productivity was performed. These reservoir productivity estimates are used to update the 2016/2017 Reservoir Risk Factor favorability and uncertainty maps made for the Geothermal Play Fairway Analysis of the Appalachian Basin project. The original maps did not include the Morgantown Tuscarora, and the updated maps do include estimates for a potential Morgantown Tuscarora reservoir.

Challenges: The major challenge is lack of the subsurface data available in proximity of the proposed site location for this study, specifically; there is not enough data to characterize the flow in fracture. The existing well core data used in this study is far (about 30 miles) from the WVU geothermal site location, which led to uncertainty in the reservoir property estimations. Therefore, to consider the uncertainty in the parameters and identify the main influential parameters, uncertainty quantification analysis is performed for reservoir thermal-hydraulic modeling using iTOUGH2.

Objective 4.0 Develop and Optimize Integrated Geothermal District Heating and Cooling (GDHC) System:

Completed Activities

Task 4.1: Estimate Base Case Levelized Cost of Heat (LCOH)

The GEOPHIRES code is modified to account for hybrid geothermal natural gas system to perform an overall economic analysis. The BICYCLE (Hardie, 1981) levelized cost model is applied to calculate LCOH.

Task 4.2: Optimize Integrated GDHC System

To improve the performance of the hybrid GDHC system, a heat pump is employed to extract the heat from the return condensate and use it to heat the geothermally preheated water before sending into the boiler thereby improving the geothermal heat extraction and reducing the natural gas usage. Also, preliminary analysis was performed for conversion of steam-based system to the geothermal hot-water based system and determined the LCOH is higher than the current price. While steam-based system that is used to supply for entire campus has LCOH values lower than current price; hence, it is an optimal system design.

Task 4.3: Quantify Minimized System Uncertainties & Development Risks

The aim of this task is to incorporate the uncertainties quantification data obtained from Task 3.3 into the economic model for the optimal system design and to quantify the uncertainty in the LCOH.

Challenges: The main challenge in this task is the uncertainty in the well drilling and completion, surface equipment, and distribution pipeline costs. Therefore, LCOH is calculated using a range

of surface capital and operating and maintenance costs. For well drilling costs, we considered GEOPHIRES default correlations as the upper range and the quotes obtained through Northeast Natural Energy (NNE) as the lower bound.

Objective 5.0 Maintain & Update Market Transformation Plan:
Completed Activities

Task 5.1 – Maintain & Update Market Transformation Plan

The project team developed a framework to assess end-use load, as defined in Objective 2 above, and performed simulations to determine the feasibility of the estimated thermal energy supply, as defined in Objective 3.

REGULATORY COMPLIANCE PLAN

Currently, there are no regulations in place for geothermal development in the State of West Virginia. However, WVU owns mineral and land rights at the proposed location. Under West Virginia law, that ownership is unsevered from the coexisting water rights. The project team has a successful history of collaborating with local drilling companies and experience in obtaining the drilling permits in and near the proposed site through our performance of the MSEEL project. We have worked closely with the West Virginia State Department of Environmental Protection (WVDEP) on drilling.

METHODOLOGY

Objective 1 – Characterize the Geothermal Site

Task 1.1: Perform Core Analysis and estimate temperatures

Permeability measurements

More than 2,000 permeability measurements (in milliDarcy, mD) were made for the Preston-119 core using a CoreLab™ PPP-250 Portable Probe minipermeameter (Figure 2). The experimental permeability was determined by the unsteady state method of Honarpour and Mahmood (1988) where pressure decay was measured as a function of time to compute k_{gas}. Injected gas was air at ambient temperatures and initial pressures of 20-25 psig.

Associated measurements include observations and description of the core, recording depths and parameters of vertical and horizontal fractures (e.g., orientation, length, width, mineral filled fracture spacing, fracture interactions), matrix grain size, and the presence of notable features (e.g., stylolites, fossils, bioturbation and burrow fill, bedding contacts). The process involved systematically investigating all visible fractures on individual segments of the core, starting at the top and working downwards. Orientation, for our purposes, is relative to vertical (parallel to the length of the core) and relative to horizontal (90° to the length of the core). All measurements and observations are recorded in an Excel worksheet (See supporting document, Preston-119_FINAL_core_permeability_illustrated.xlsx).

Figure 2: Core Labs PPP-250 Minipermeameter in operation. The instrument's probe is held tightly against the face of a core sample (on the right) while air is injected into the rock at approximately 26 psig. The instrument itself (on the left) measures the rate of gas uptake by the sample and computes the sample's permeability which is stored digitally on a small tablet computer (also on the left). The quantity being measured is k_{hAir} (horizontal permeability to air) in millidarcies (mD).

In addition to permeability, fracture dimension measurements, general observations, and digital photographs of each core segment and selected core features have been captured and have a hyperlinked for each core segment for reference within the Excel data sheet. Figure 3 shows an example of how permeability changes with depth and between the fractures and matrix.

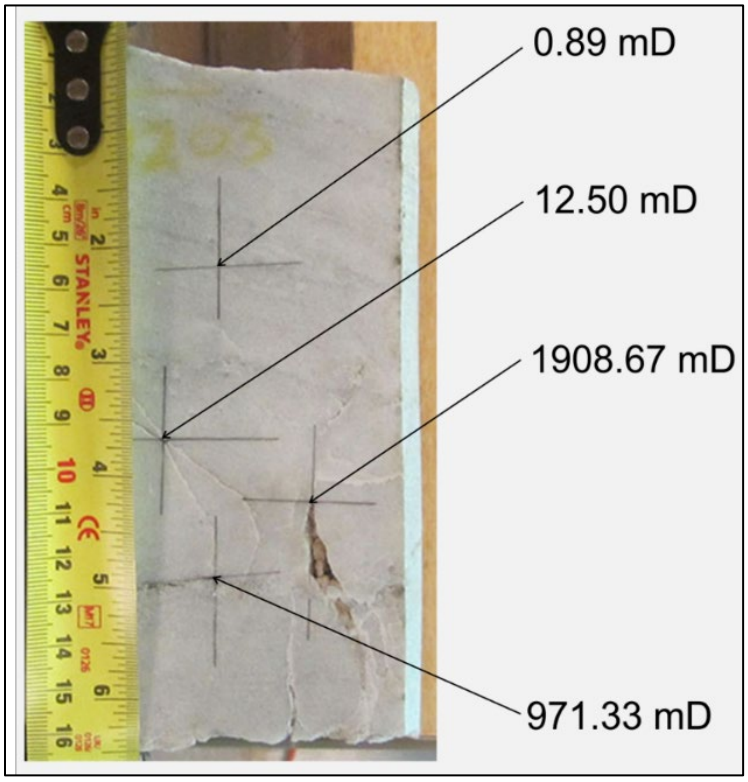

Figure 3: Example of permeability measurements in the Preston 119 core. Crosses mark minipermeameter measurement locations, and annotations are the resultant permeability in millidarcies (mD).

X-Ray Computed Tomography (CT) Scans

CT scan data were collected with a Toshiba® Aquilion TSX-101A/R medical scanner at NETL in Morgantown, WV. The CT scanner generates images with a resolution in the millimeter range, with scans having voxel resolutions of 0.43 x 0.43 mm in the XY plane and 0.50 mm along the core axis. The scans were conducted at a voltage of 135 kV and at a current of 200 mA. Subsequent processing and combining of stacks were performed to create three-dimensional (3D) volumetric representations using *ImageJ* (Rasband, 2018) to produce .TIFF stacks. The variation in grayscale values observed in the CT images indicates changes in the CT number obtained from the scans, which is directly proportional to changes in the attenuation and density of the scanned rock; darker regions are less dense and absorb fewer X-rays (Figure 4).

The grayscale values in the .TIFF stacks were used to isolate and visually differentiate objects of interest in the scans (in this case: matrix, fractures, and air/outside) using the interactive learning and segmentation toolkit *ilastik* (Sommer et al., 2011). The premise of isolating features is to first segment out the feature based on its unique grayscale value. Once this isolation has occurred, the

next steps are to differentiate multiple isolated features and then combine them into one coherent visual representation.

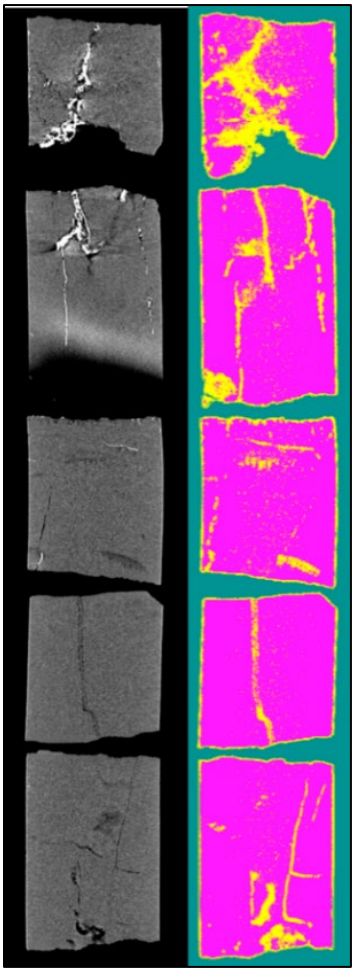

Figure 4: Example of segmentation of a CT scan that allows fracture volume calculation in the Preston 119 core, depths 7165 to 7168 ft., with 3.3% fracture volume.

After segmentation, the data are exported back into *ImageJ* where the volume percentages are calculated for each segmented section. The background (air/outside) was subtracted, and the percent volume of fractures was determined for the entire sample. These segmentations and associated calculations were performed on entire scans (2- to 3-foot sections of core, one length of core box), these can be refined to a smaller subset. Approximately 113 feet of core was processed using the technique described above and filtering for edge effects, which can add potential error to the fracture volume estimation. This filtering of data focuses on interior fractures within intact core and disregards fracture space between individual segments in a core section (i.e., empty space between 'broken' pieces of core is disregarded as its volume can be related to how close the operator placed the core segments into the core boat during scanning). This provides a more conservative estimation of fracture volumes, which range from a low of 0.027% (interval from 7,310 to 7,313 ft.) to a high of 7.7% (7,221 to 7,223 ft.). Two intervals (7,310 to 7,313 ft.; 7,415 to 7,417 ft.) had no fracture volume identified from the CT image processing. All segments, volume estimations, and instructions for users have been provided in supporting documents

(CT/Preston119/CT scan data). Figure 5 displays the fracture volume percentage (fracture porosity) with depth, as well as a comparison of matrix and fracture permeability.

Reservoir thickness

All wells in West Virginia penetrating the Tuscarora Sandstone with geophysical logs were identified and digitized, for a total of 695 curves from 120 wells. Digitized geophysical log data allowed us to determine facies relationships in each well and across key areas, following the methodology of Castle and Byrnes (2005, see Figure 6). Following log digitization, the Tuscarora sandstone was correlated across most of the state using a total of 155 logs. The Tuscarora sandstone tops and bases are picked primarily using the gamma ray log in the subsurface. The Tuscarora sandstone has a relatively low gamma ray signature and occurs between the Juniata and Rose Hill formations, which display a much higher gamma ray signature. Tuscarora tops from the WVGES database along with those tops picked in the Wellbore Integrity project (Sminchak, 2018) and from the Lower Silurian study (R. Diecchio, pers. comm., 2014) were loaded into IHS Petra software and used to correlate the Tuscarora Sandstone regionally. The unit attains maximum thickness (~450 ft in Preston County) in northeastern West Virginia, in proximity to Morgantown and WVU's Evansdale campus.

Three discrete stratigraphic sequence types (Figure 7) are identified in Lower Silurian siliciclastic units of the Appalachian basin: two coarsening-upward types (Type A and Type B), and a fining-upward type. Each of these sequence types exhibits a unique geophysical log signature, which reflects stacking patterns of facies assemblages in discrete depositional environments.

Coarsening-upward Type A assemblages are characterized by aggradation marine, fluvial, and estuarine deposits deposited in relative proximity to source area; where high rates of sedimentation kept pace with accommodation space created by basin subsidence, resulting in thick accumulations of sandstone. These sandstone beds exhibit the highest permeability for a given porosity.

Coarsening-upward Type B is characterized by a complex assemblage of nearshore and shallow marine deposits, shallow subtidal, tidal flat, and tidal channel environments grading from marine shale at the base upward to sand-dominated tidal facies. These deposits represent a progradation shoreline complex that formed as accommodation space was filled.

The last of the three sequences is a fining-upward type in shallow marine and upper/lower shoreface environments characterized by a thick, basal sandstone fining upward to shale, deposited as progressive infill of incised valleys during marine transgression. These deposits represent upper and lower shoreface environments that grade into shallow marine.

In this portion of the study area, the rate of sedimentation is outpaced by creation of accommodation space by basin subsidence and/or marine transgression. A graphic log was created for the Clay 513 well **(**Figure 8), with sedimentary structures including bi-directional cross-laminations, scour surfaces and pebble lags, graded bedding, bioturbation, which illustrates stacking patterns and structures closely resembling those identified by Castle and Byrnes (2005) as deposited in their coarsening-upward Type B sequence type, which was interpreted to represent deposition in shallow subtidal, tidal flat, and tidal channel environments.

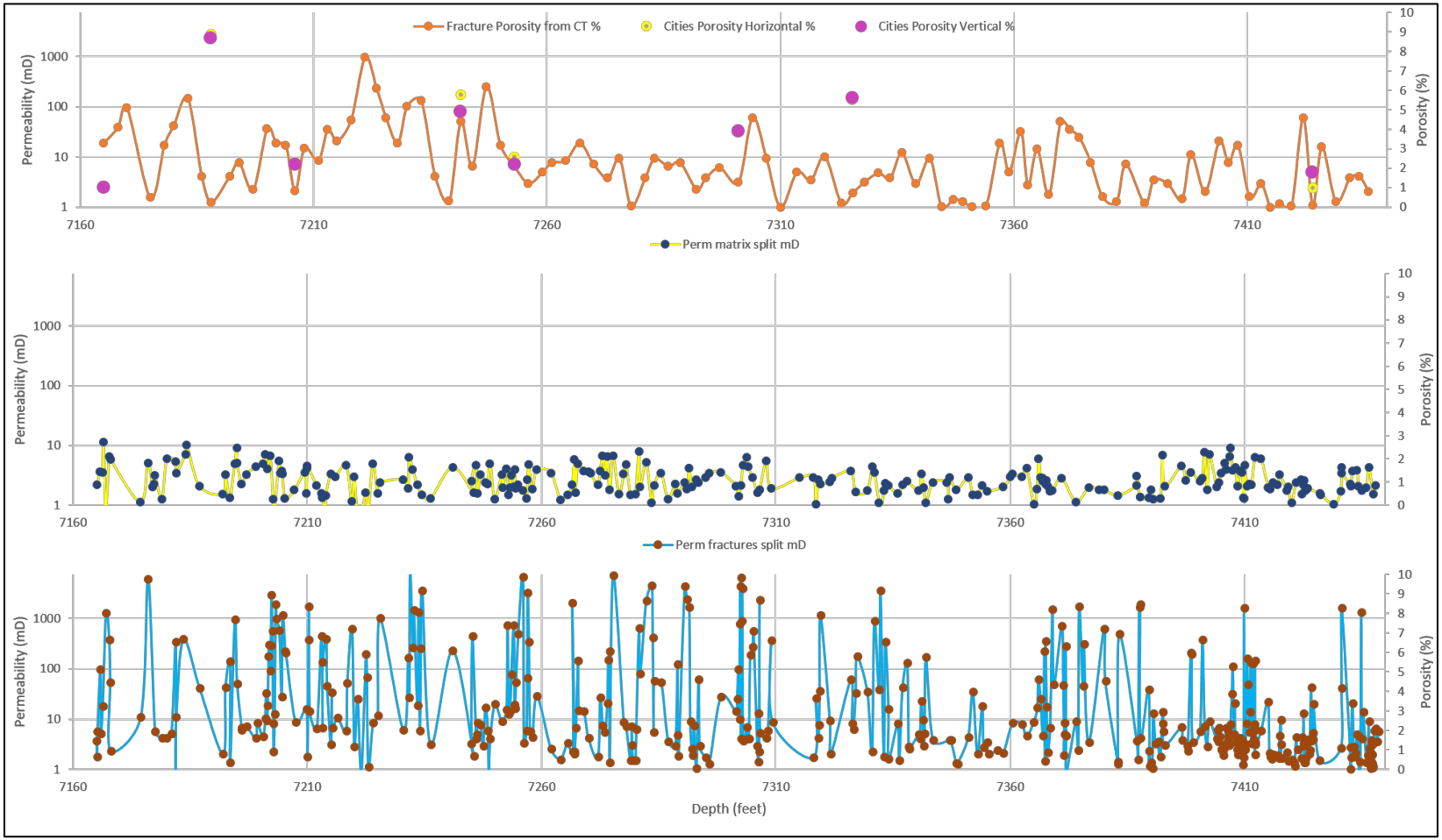

Figure 5: The top graph displays the fracture porosity calculated from CT images in percentage as well as lab porosity results versus depth in feet. The middle graph displays permeability measurements of the matrix (mD) using the permeameter while the bottom graph displays permeability measurements of fractures (mD) using the permeameter. Point data relate to lines for illustrative purposes; lines do not necessarily indicate geologic trends.

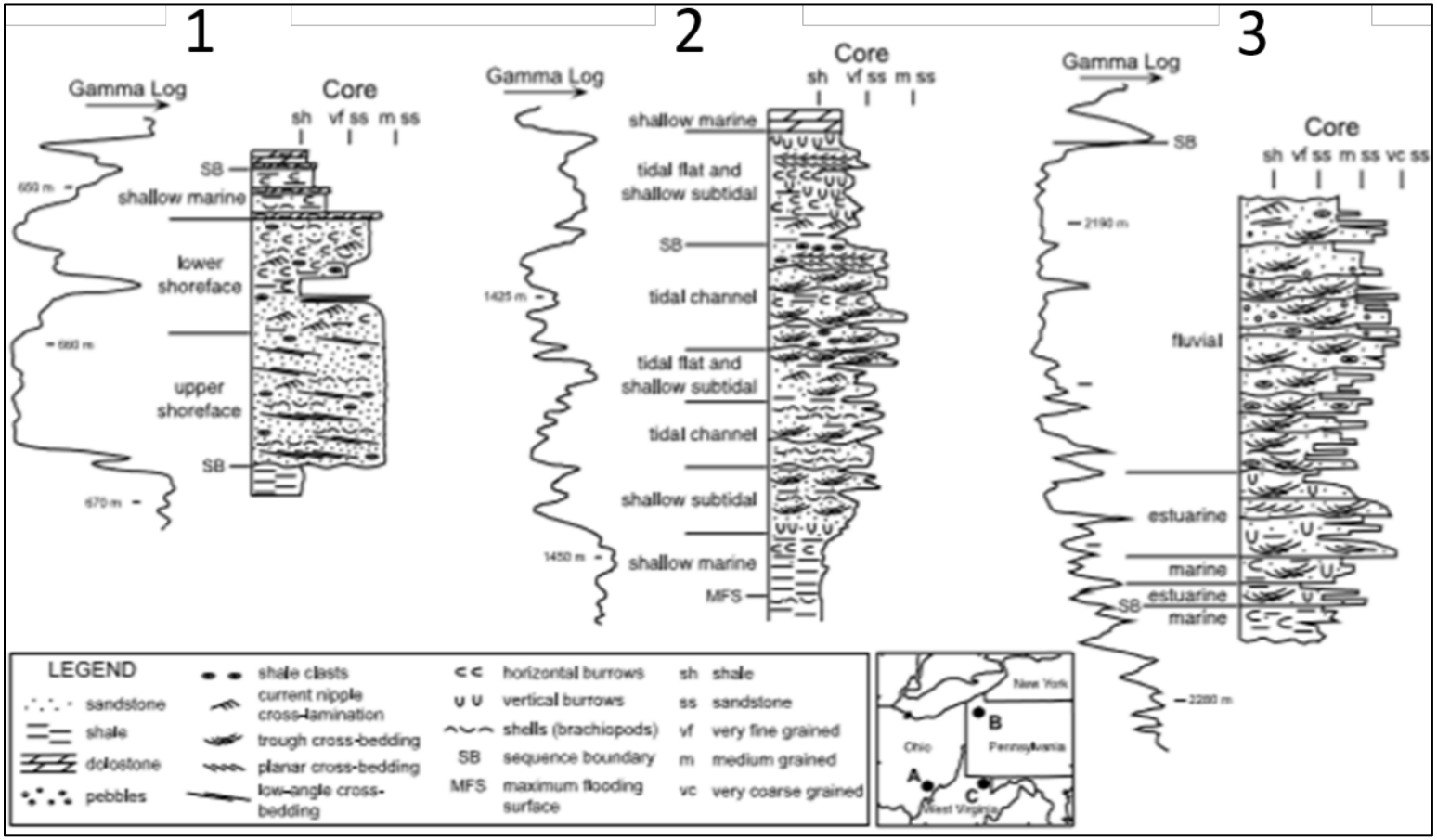

Figure 6: Digitization of all available geophysical logs that include the Tuscarora Sandstone allowed for statewide comparison of depositional stacking patterns and division into the three major types, following methodology of Castle and Byrnes (2005).

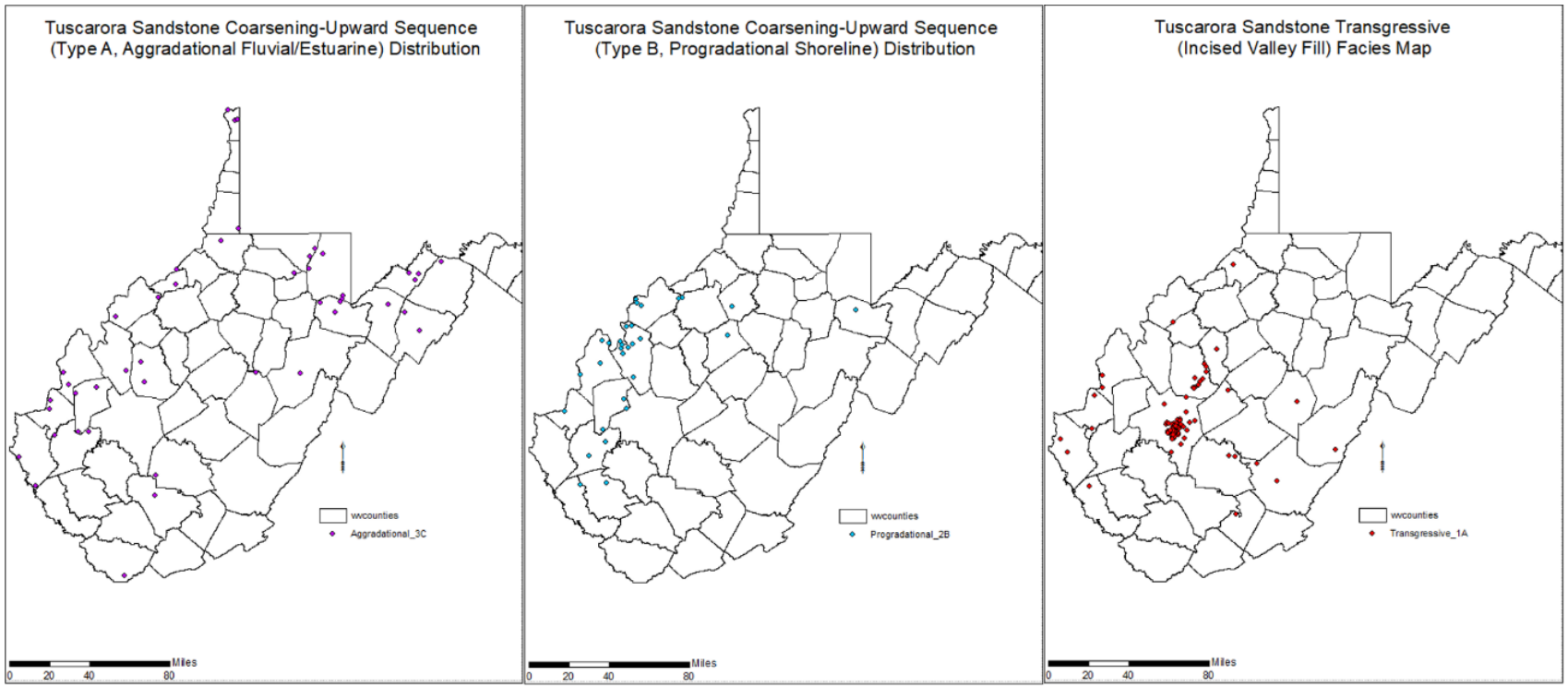

Figure 7: a) Coarsening-upward, aggradation fluvial/estuarine; Preston-119 core records this stacking pattern, but sediments are more characteristic of marine and estuarine deposition than of fluvial. b) Coarsening-upward, progradation shoreline; generally located in western portion of the study area. c) Fining-upward, incised valley fill; deposited as progressive infill of incised valleys during marine transgression.

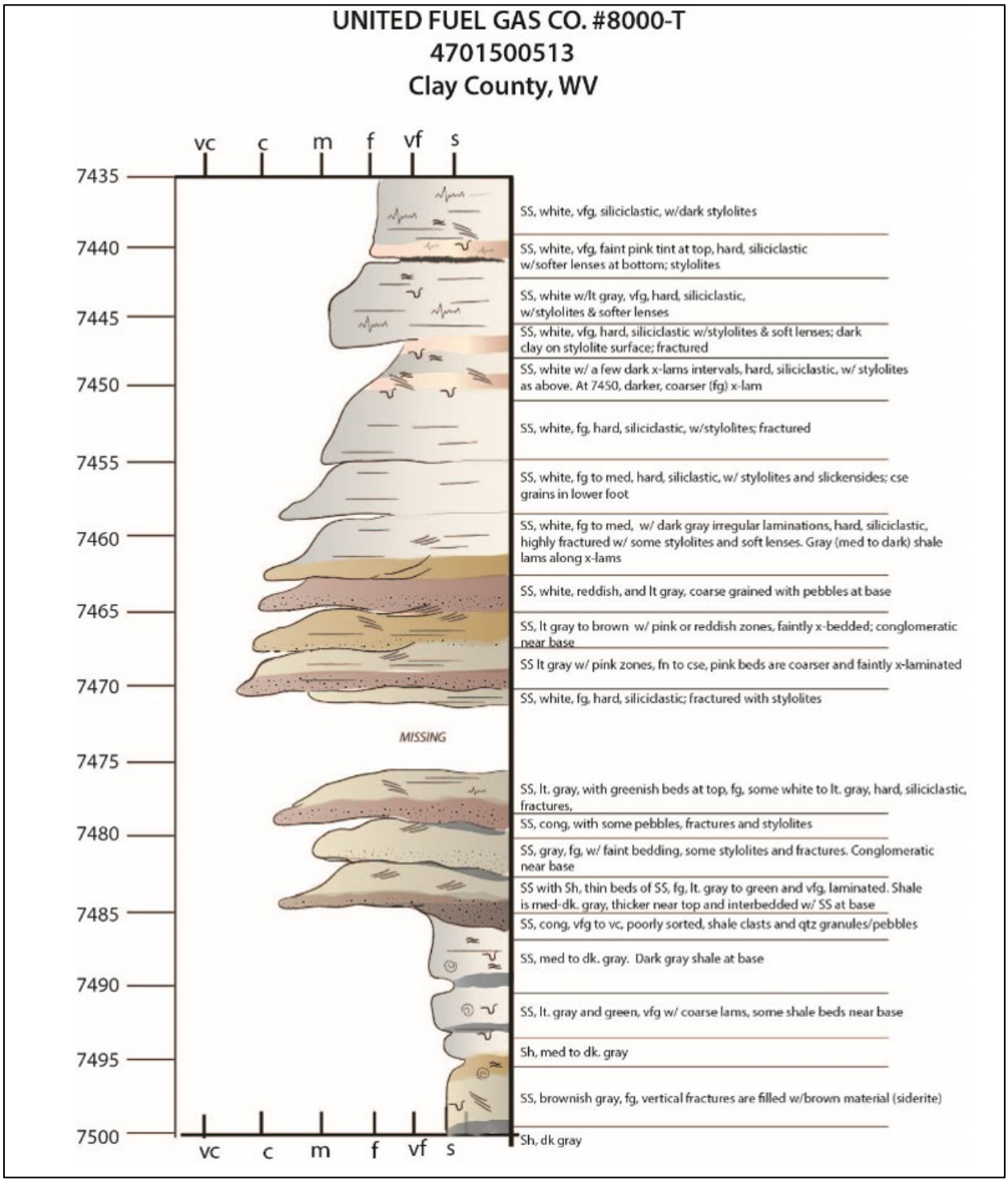

Figure 8: A graphic log constructed for the Clay 513 well closely corresponds to the coarsening-upward Type B sequence identified by Castle and Byrnes (2005). Deposited as progressive infill of incised valleys during marine transgression. Clay 513 is one example of stacked tidal channels that fine upward to marine sandstones.

Petrography

To further investigate the relationship between porosity and permeability in the Tuscarora Sandstone petrographic examination was performed on thin sections from two wells – Kanawha 2571 (19 slides) and Preston 119 (12 slides). Both sets of slides were impregnated with blue epoxy to emphasize porosity. The examination procedures were the same as described in the paper submitted previously to the GRC (McCleery et al., 2018). The emphasis of the examination was to look for any features that might enhance or effect permeability in the Tuscarora reservoir rock. Both sets of thin sections exhibited relatively large "visual" porosities, approaching, and exceeding 10% in Preston 119 and 25% in Kanawha 2571. Porosity appears to be primary in nature; thin sections from both wells contain relatively large pores (Figure 9) that contribute to the overall porosity. In addition, a type of "shelter" porosity was observed in thin sections from both wells where large grains appear to protect or shelter a cavity containing much smaller grains with associated uncemented pore space (Figure 10).

Illite clay and heavy quartz overgrowths (Figure 11**)** most commonly reduce porosity on both wells. Fracture porosity or porosity along stylolites was rarely observed. It is suspected that since the thin sections for both wells were taken from core plugs drilled at "high porosity" intervals, small-scale deformation features were selectively avoided.

Obviously, 3-dimensional connectedness between open pores cannot be assessed in thin section. However, the relatively high matrix permeabilities (≥ 3 mD) observed in the Preston 119 core might be partially explained by the relatively high porosities observed in thin section.

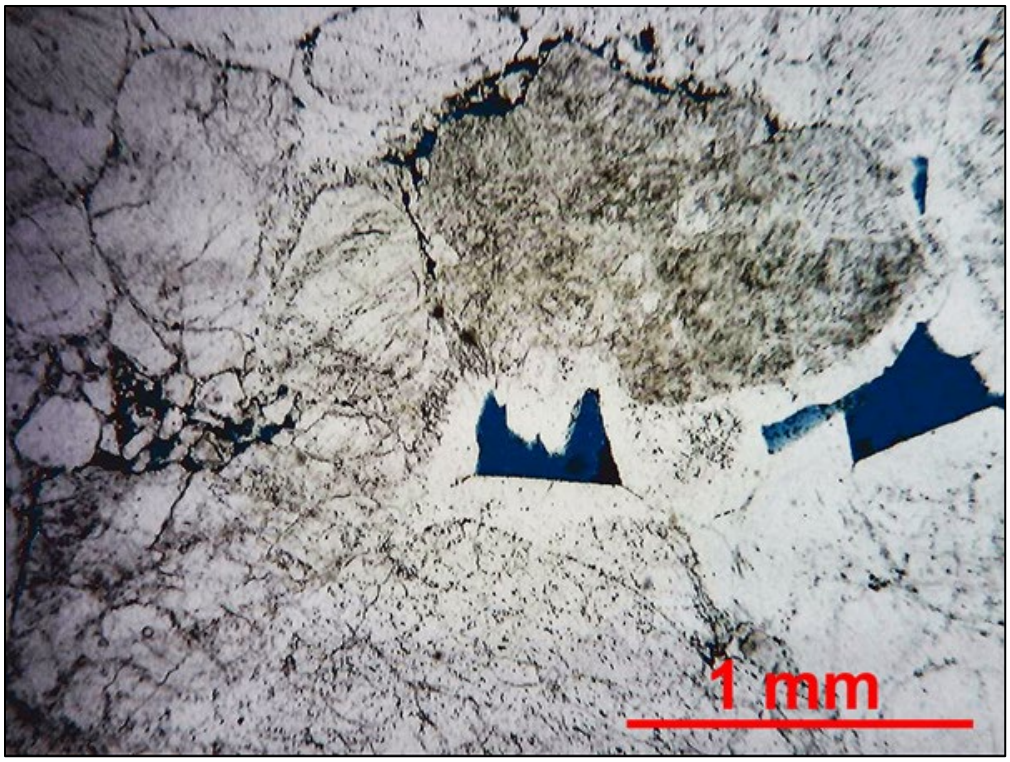

Figure 9: Large pores in the Silurian Tuscarora Sandstone. Blue epoxy fills the pore. Notice the euhedral quartz overgrowths protruding into the pores. Kanawha-2571: 6,805 feet below surface, 2.5x-plane light.

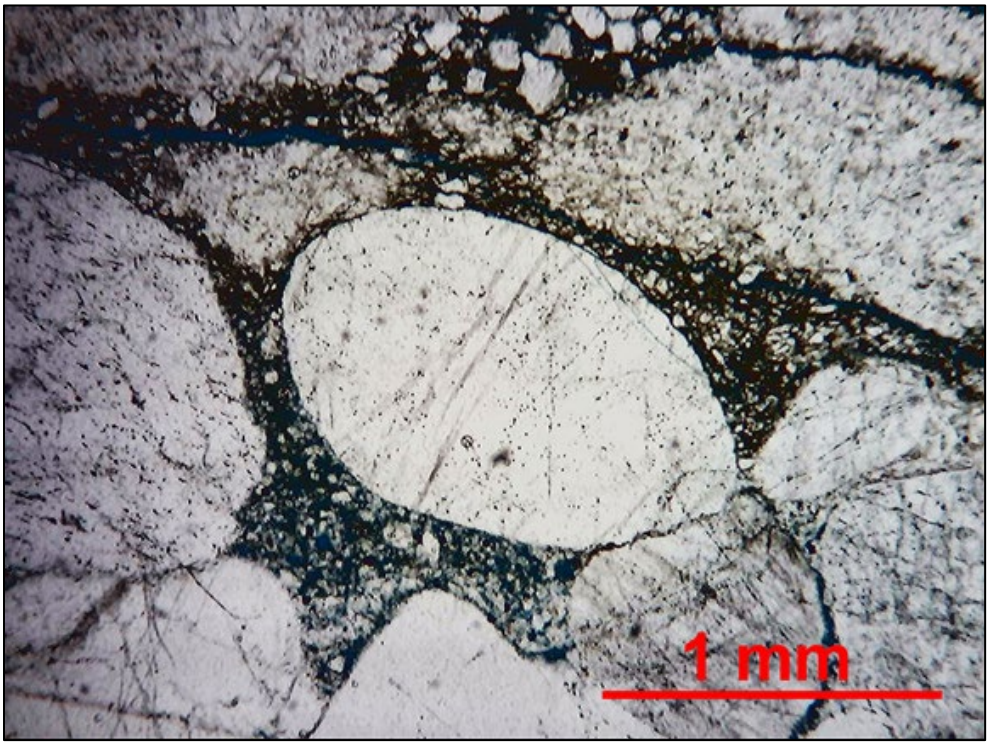

Figure 10: Large quartz grains overlying spaces containing numerous smaller grains in a partially open pore. This appears to be analogous to "shelter porosity" observed in carbonate rocks. Kanawha-2571: 6,805 feet below surface, 2.5x-plane light.

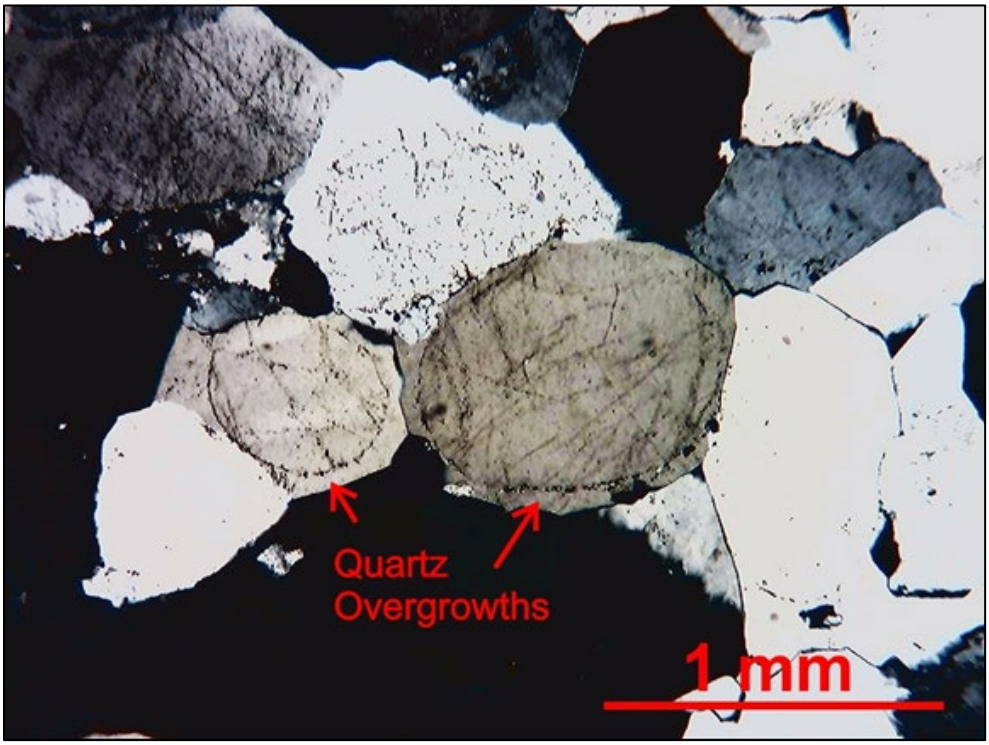

Figure 11: Thick quartz overgrowths on rounded quartz grains completely fill pore space. Kanawha-2571: 6,805 feet below surface, 2.5x-cross polars.

Task 1.2: Estimate Reservoir properties for modeling

Fracture investigation

An extensive literature search was conducted for published fracture studies of the Tuscarora sandstone, trying to evaluate the potential fracture trends, which might affect the proposed DDU well. No quantitative fracture evaluation studies were found for the Tuscarora sandstone. Fracture analysis data for the Marcellus shale from the nearby MSEEL site was compiled as potential proxy for regional stresses and potential fracture patterns affecting the DDU project (Figure 12). Figure 13 shows the location of MSEEL data used from the MIP-3H well.

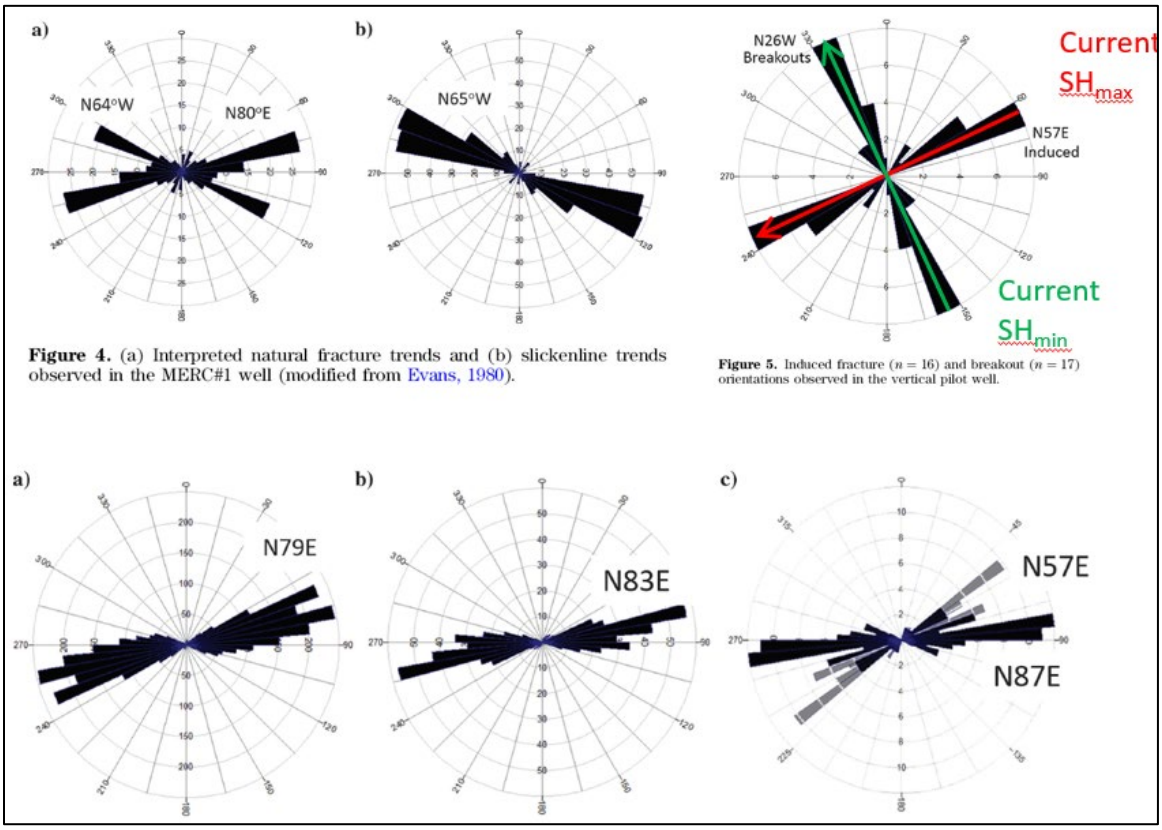

Figure 4. (a) Interpreted natural fracture trends and (b) slickenline trends observed in the MERC#1 well (modified from Evans, 1980).

Figure 5. Induced fracture ($n = 16$) and breakout ($n = 17$) orientations observed in the vertical pilot well.

Figure 12: Modified from Wilson, T. H., et al. 2018. Fracture azimuths displayed with black rosette diagrams. SH_{max} (red) is current maximum horizontal stress, SH_{min} (green) is current minimum horizontal stress. If this stress field is consistent with depth down to the Tuscarora, a geothermal well drilled in a direction parallel to SH_{min} should penetrate any open fractures, which should form parallel to SH_{max}.

Porosity and permeability evaluation from well log analysis

Additional well data was integrated, widening the evaluation area away from Morgantown, with the goal of developing a better understanding of reservoir properties for the Tuscarora sandstone, particularly the porosity derived from well log analysis. Eight additional wells were correlated, and three of these wells with digital well log data were processed to produce porosity estimations. In addition, historic state well documents for these wells were reviewed, looking for pertinent porosity, permeability, and well completion data. The original five Tuscarora (TUSC) wells used in the study are located inside the red dashed ellipse in Figure 13, located southeast of Morgantown.

Figure 13 also shows the location of the three wells processed for porosity, connected by the blue line of cross-section. The John Burley #1, located in the southeast corner of Marshall County WV, is approximately 30 mi (48 km) west-northwest of Morgantown, the James Messenger WTZ 3H, located in north-central Wetzel County WV, is about 38 mi (61 km) west of Morgantown, and the 07700119 USA #Q-1 (aka, USA #Q-1-119), located in southeastern Preston County WV, is approximately 36 mi (58 km) southeast of Morgantown.

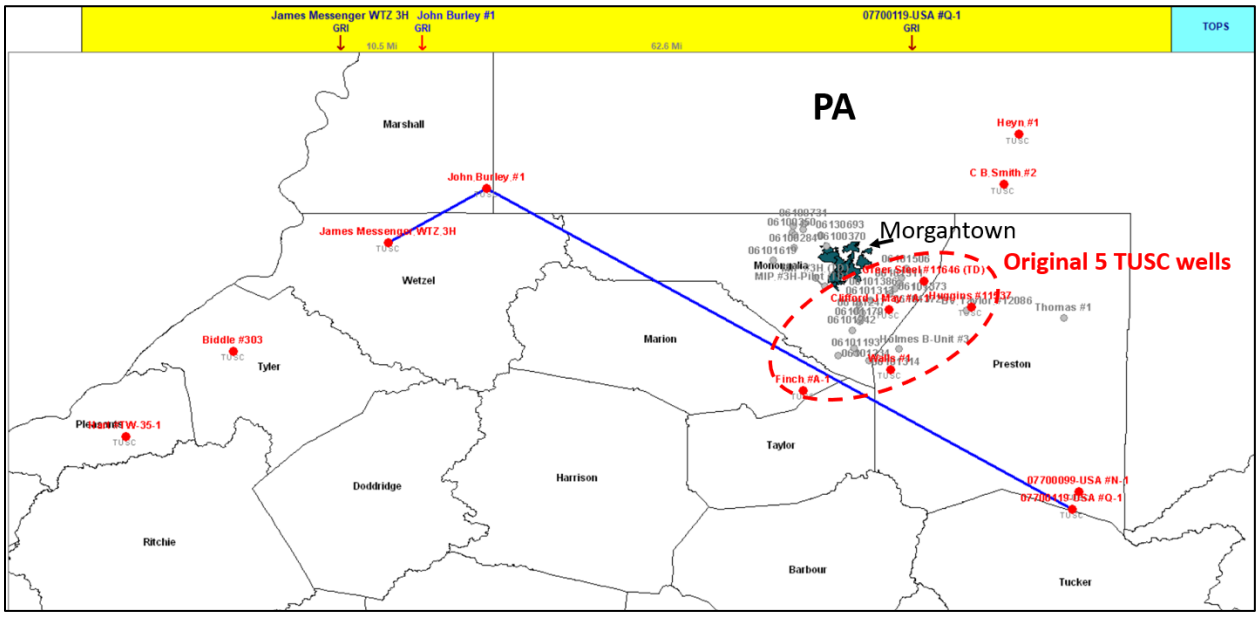

Figure 13: Location map of study wells. The original five (5) Tuscarora penetrating wells are shown with red dots inside the red dashed-line circle. Eight (8) additional correlated Tuscarora wells shown by red dots, outside the circle. Three (3) wells connected by the blue line were processed for porosity determination.

Geothermal Gradient (GTG) evaluation

An estimation of reservoir temperature in the Tuscarora sandstone was calculated for the five Tuscarora wells closest to the DDU study area (Figure 14). First, GTGs were calculated for wells, derived from bottom hole temperature information. At each logging point in a well, temperature measurements are made with thermometers run in the borehole along with electric logging tools. These temperatures are used to interpolate reservoir temperatures in potential hydrocarbon reservoirs. Figure 15 illustrates the data and how it is used.

Figure 15 contains data for the Clifford J May #A-1, located in Monongalia County, approximately 8 mi. southeast of the DDU project area. This well is the closest Tuscarora penetration to the study area. The first column of data, in the upper left of Figure 15, contains key depth measurements. Column 2, labeled "MudTemp", contains temperature measurements made at logging points. The third column, "TFT", contains adjusted temperature measurements from logging point temperatures, to compensate for cooling of the true formation temperatures caused by circulating mud. In this case, a +10% adjustment was made to recorded temperatures. Commonly, a +10%-to -15%, adjustment is made to correct logging measurements. These TFT (true formation temperature) values are then used to calculate segment GTG, and an overall well GTG. The graph in Figure 15 shows a plot of the data in depth vs. temperature. The approximate depth of the Tuscarora is shown on the plot in green. The temperature for the Tuscarora is interpolated from

the top and bottom values of the GTG segment in which it is contained. Temperature data and GTG plots for the other four Tuscarora wells can be found in Appendix A.

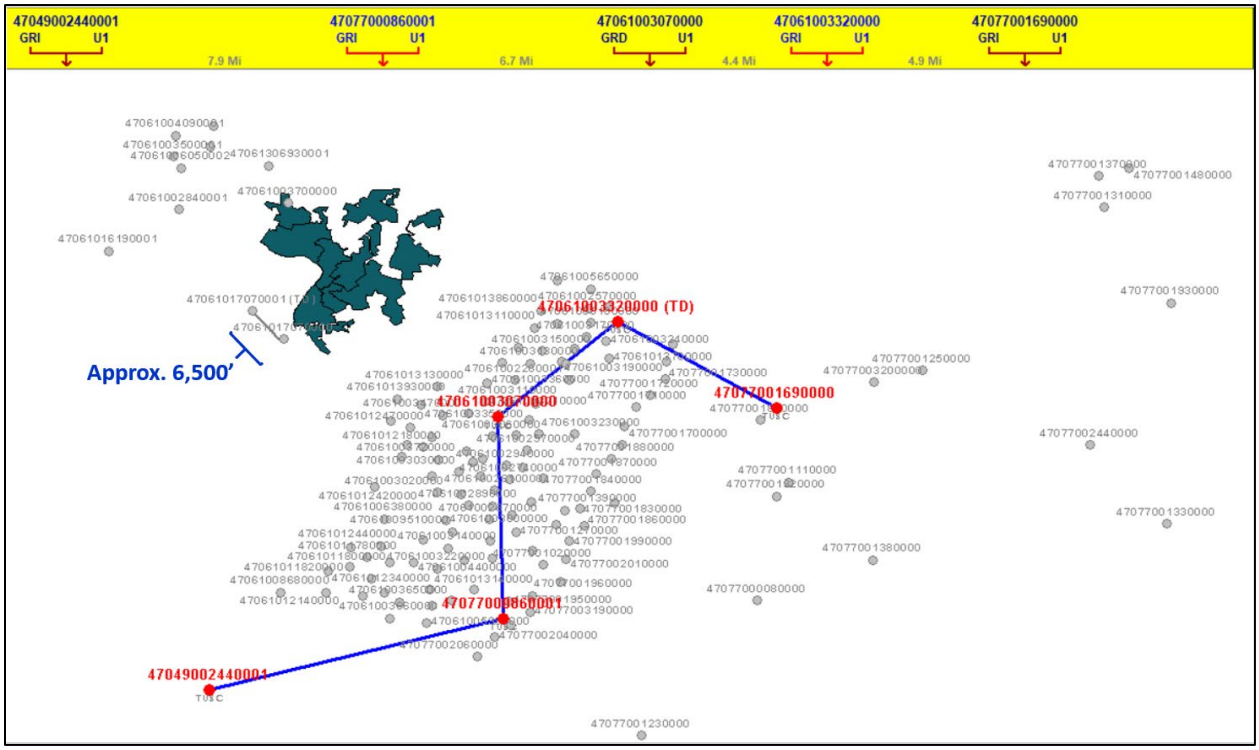

Figure 14: Map showing the location of the 5 closest Tuscarora penetrations. The city of Morgantown is shown with the teal-colored shapefile. The 5 wells are highlighted in red and identified at the top of the figure, along with distances between the wells along the blue line.

depth	MudTemp	TFT	Mud	Formation_TD	Grad_TFT	Age	AST
7646.5				ONDG		M_Dev	55.7
9135	145	159.5	Salt	SALINA	1.138	U_Sil	
10725	167	183.7	Salt	NIAGA	1.517	M_Sil	
10779				TUSC		L_Sil	
11047	185	203.5	Salt	JUNI	6.168	U_Ord	

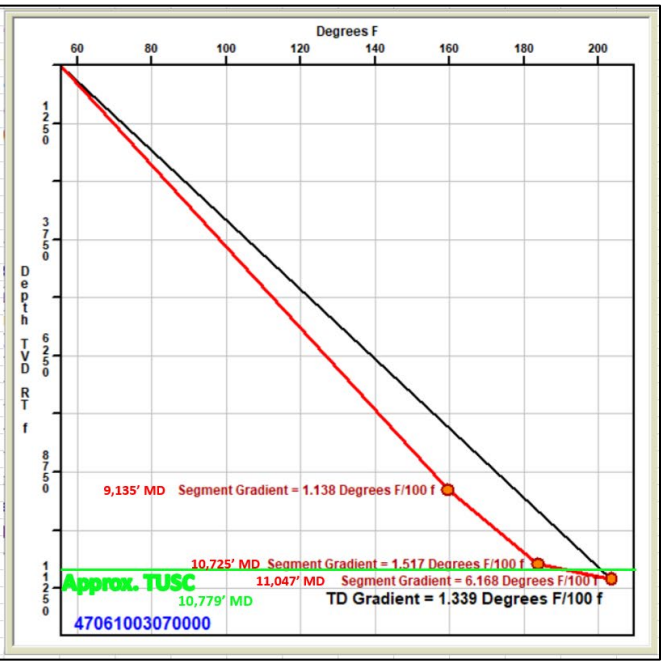

Figure 15: Temperature data and GTG plot for the Clifford J May #A-1, 47061003070000, in Monongalia, Co.

Task 1.3: Develop 3D Reservoir Model

To develop the 3D geological model, structural surfaces were constructed from subsurface well picks. First, oil and gas wells around the proposed geothermal site were identified with available electric logs, so that correlations between the wells could be made, and tops picked. Figure 16 shows a map of all oil and gas wells around the project area that have publicly available logs. The large cluster of wells, southeast of Morgantown, are wells drilled in the South Burns Chapel Field, an Onondaga-Oriskany natural gas field. (The black shapefile outlines represent the city of Morgantown).

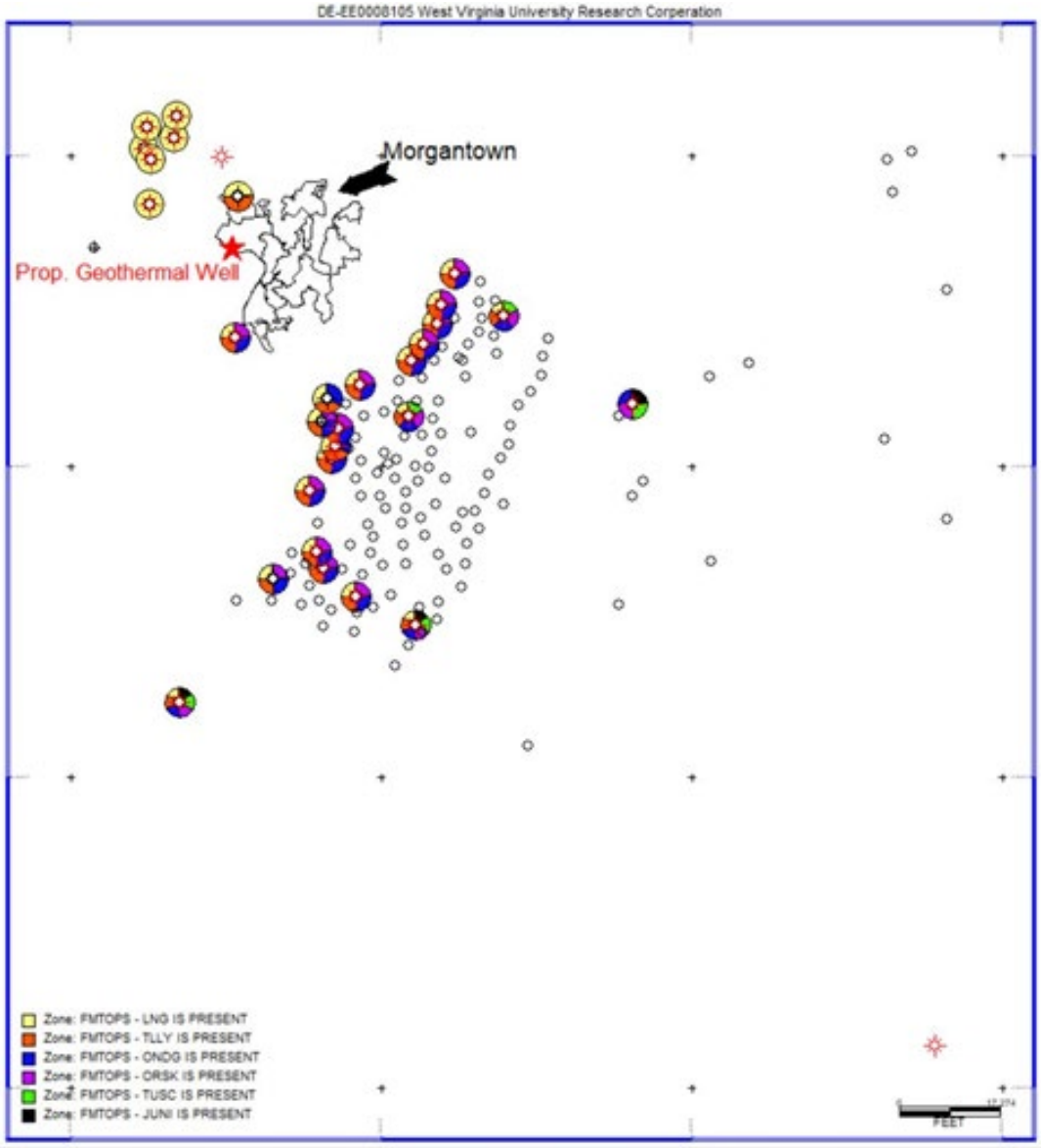

Figure 16: Map showing location of wells drilled around Morgantown, WV with available geophysical logs. Wells with tops picked are shown with color-filled doughnuts. Color-code for doughnut segments, located in the lower left-hand corner of the map, indicates tops available in each well. Stratigraphically, the shallowest top, LNG, is shown in yellow, and the deepest top, JUNI, is in black. Tuscarora (target) is represented by green. JUNI represents the base of Tuscarora pick. Tic marks on map are at 10-mile intervals.

There are several important aspects of the data availability shown on Figure 16:
1) in the 10 mi^2 (26 km^2) area surrounding the proposed geothermal wellsite, there are only 12 wells that have well logs,
2) most of the closest wells penetrate only the shallowest correlation top, indicated by the yellow circle segments,
3) only five wells in a 15 mi^2 (39 km^2) area around the proposed geothermal wellsite penetrate the top of the Tuscarora Sandstone (TUSC, in Figure 16; wells with green segments, and
4) only three wells in the area penetrate the base of the TUSC (top of Juniata).
These aspects create difficulty developing a structural model for the Tuscarora, around the proposed geothermal well.

Thirty wells surrounding the proposed geothermal wellsite were correlated to generate structural surfaces. Six key tops were identified for mapping, based primarily on the ability to confidently correlate them between wells; but they were also chosen to cover the depth range of the wells. The tops picked were LNG (unnamed marker-bed), TLLY (Tully Fm.), ONDG (Onondaga Fm.), ORISK (Oriskany Fm.), TUSC (Tuscarora Fm.), and JUNI (Juniata Fm.). The relative stratigraphic relationships between tops are displayed in Figure 16 and Table 1, from youngest to oldest. Table 1 shows the number of tops picked for each surface. The depth difference between the LNG and the TUSC surfaces is approx. 7,500 - 8,000 ft (2,286 – 2,438 m). Figure 17 illustrates the general stratigraphic column for WV, showing the stratigraphic ages and position of the marker tops (except LNG which is approximately basal Mississippian). The 2D-3D surface modeling was performed in GES modeling software (a product of GPT Reservoir Characterization Professionals).

Table 1: Number of Tops available for each surface.

Surface	No. of Tops
LNG–unnamed marker	28
TLLY–Tully limestone	22
ONDG–Onondaga limestone	22
ORSK–Oriskany sandstone	20
TUSC–Tuscarora sandstone	5
JUNI–Juniata Formation	3

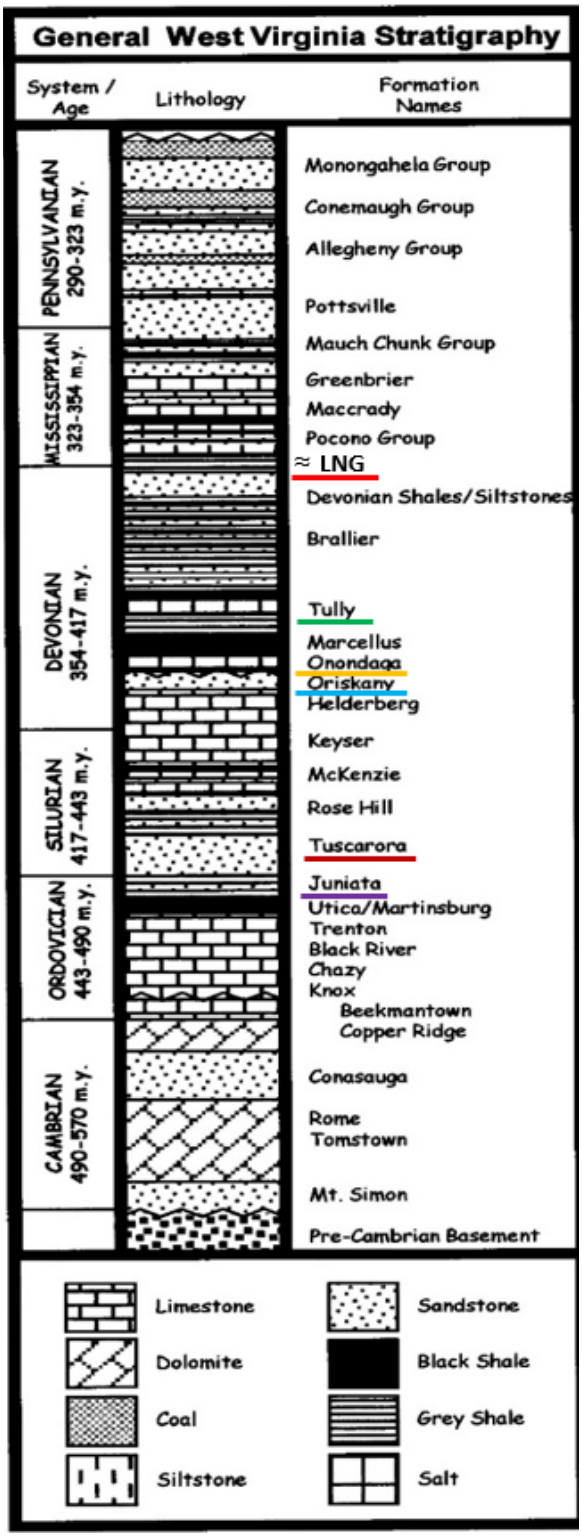

Figure 17: Generalized stratigraphic column of West Virginia.

Objective 2 – Characterize Existing Infrastructure

Task 2.1: Characterize Energy demand

The energy consumption data for the WVU campus is measured to characterize the energy demand. Five main energy distribution points across the campus are metered:

1. Medical Center: Health Sciences campus and Ruby Memorial Hospital
2. Towers: Residential area
3. Ag. Science: Engineering and Agriculture Science buildings
4. Life Sciences: Life Sciences building
5. Downtown: Majority of the campus buildings in downtown area.

Servers are installed at these five distribution meter points to record steam temperature, pressure, flow rate, and return condensate temperature and flow rate in 5-minute intervals. The data is downloaded monthly from the server to the desktop. The data is collected from January 2018 - September 2019. Steam temperature, pressure, and flow rate for the Engineering and Agriculture Sciences buildings (Ag. Science meter point) during September 2019 is shown in Figure 18. The data is also compared to the monthly invoice from Morgantown Energy Associates (MEA), the current steam supplier.

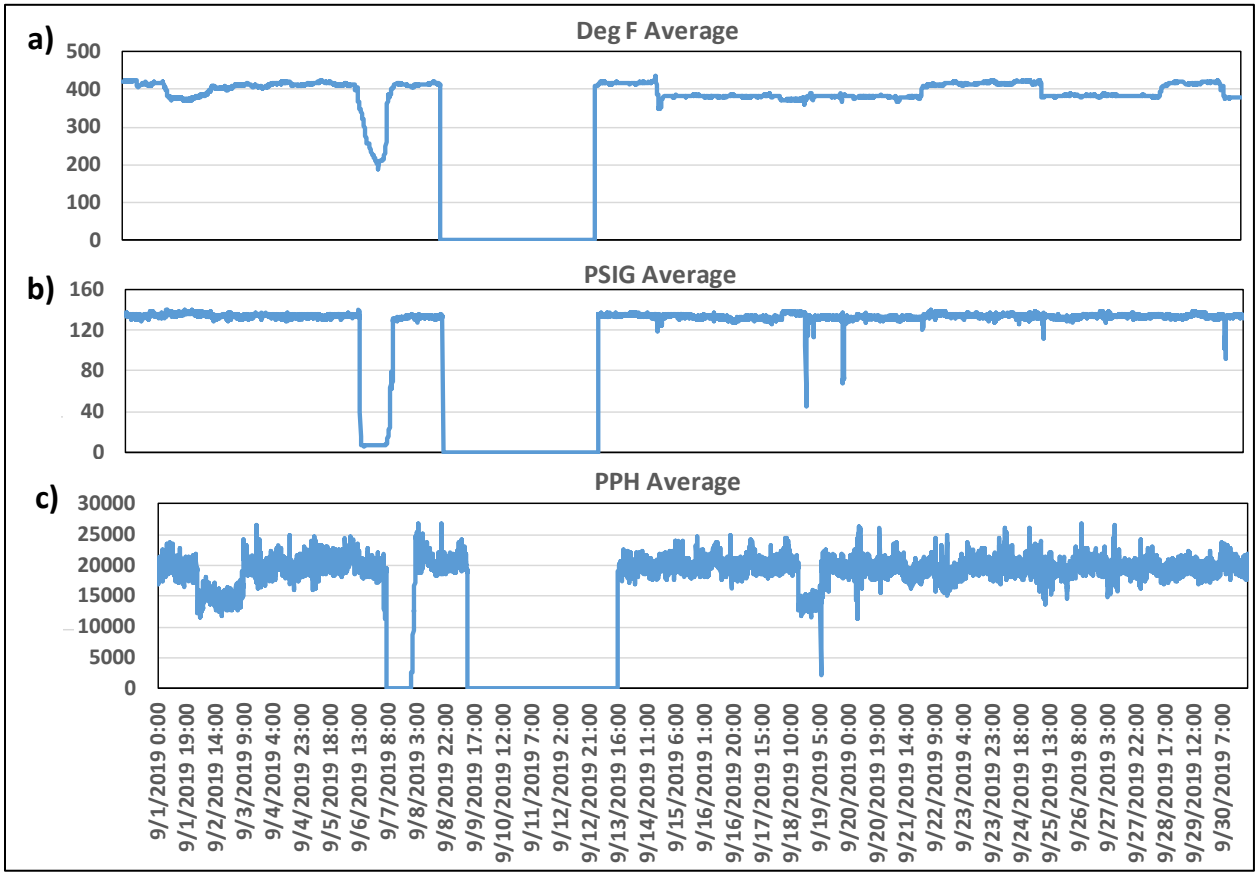

Figure 18: Steam temperature (a), pressure (b), and flow rate(c), for Evansdale campus (Ag. Science meter point) during September 2019.

Task 2.2: Perform Integration Assessment for Current District Heating System (DHS)

Geothermal site location

In response to surface landowner and lay down space concerns with the initially proposed WVU Arboretum site location, the team sought to investigate other possible locations on the WVU campus for the DDU project installation. In coordination with the WVU Real Estate Office, the team sought locations on campus to have:

1. reasonably close steam connections to campus,
2. enough "lay down" area for drilling rigs, casing, etc. (In consultation with industry experts, this equates to a roughly 200' x 200' (61m x 61m) area.),
3. clearance from overhead power lines, and
4. clear right of ways for heavy equipment to the site.

Additionally, clear chain of mineral rights is a critical piece of this project that was investigated. Three new sites were examined, and are shown in the overview map, along with the originally proposed site in Figure 19.

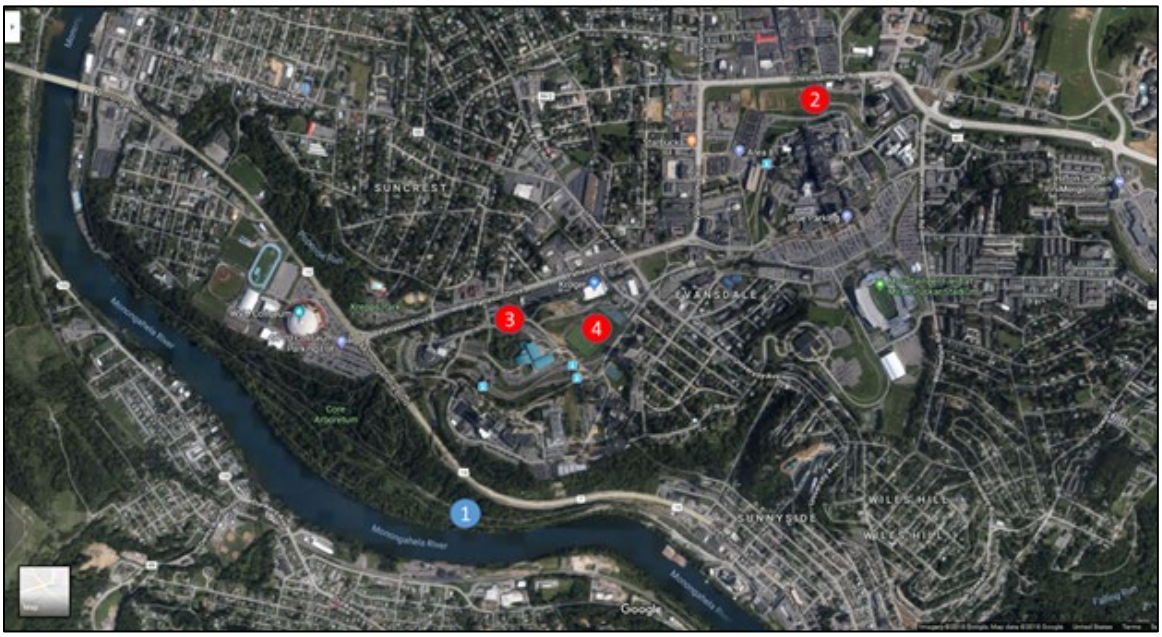

Figure 19: Aerial view of WVU Evansdale Campus. Original location #1, blue. Possible alternate locations #2, #3, #4, red.

Current steam-based DHS

The current district heating and cooling distribution system (Figure 20) will be used as is without any changes. To supply the required steam, a centralized hybrid GDHC system is proposed with natural gas fired boilers as a secondary heat source, integrated with the geothermal system. A one-line sketch of the piping information along with sizes and lengths from MEA distribution center to individual distribution point is shown in Figure 21. The pipeline elevations are calculated between the distribution points using Google Map estimations (see supporting document: Pipeline elevations_GoogleMaps). The water loss between steam and condensate return is assumed to be 10%, based on our current agreement with MEA. Currently, the return condensate flows freely due to gravity from the individual meter points to the MEA based on our current distribution lines (as shown in Figure 20). However, with change in the central plant location to the geothermal site,

pumps will be used at required meter points (D, H) to assist for return condensate flow to the central location. The return condensate is assumed to reach the distribution points at about 1.1 bara and pumps are used to return the condensate from distribution points to central plant at 1.0 bara.

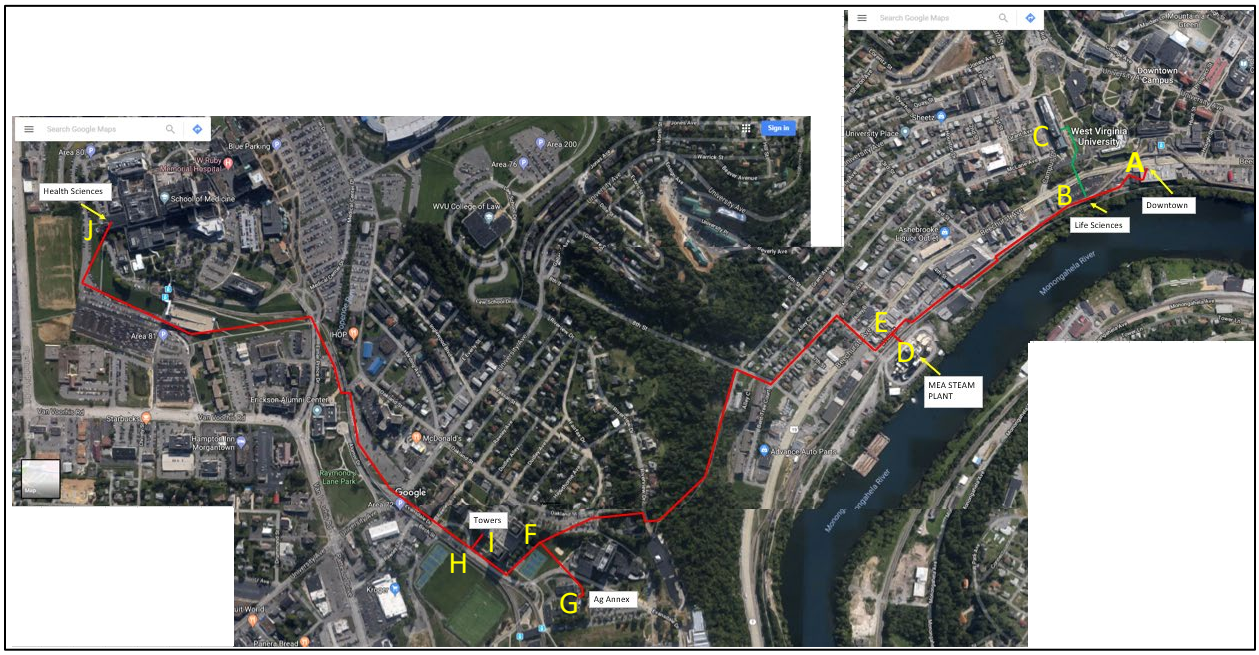

Figure 20: Google map showing the current locations of meter points and the distribution pipeline path, pipelines in red are owned by MEA and in green are owned by WVU. (Not to the scale).

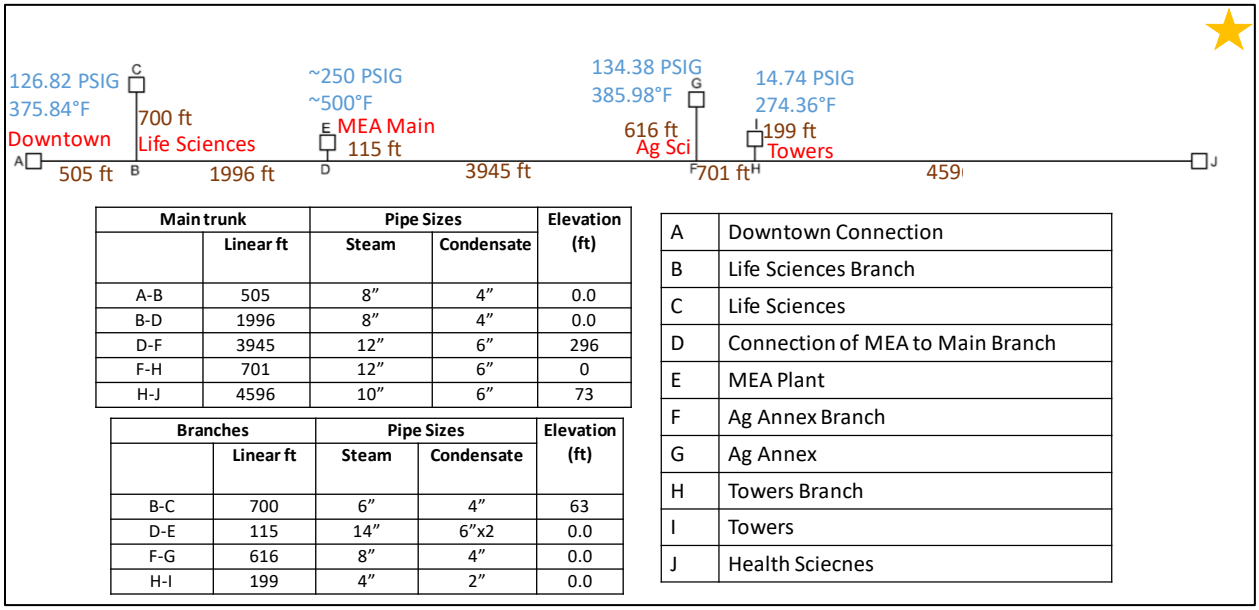

Main trunk		Pipe Sizes		Elevation (ft)
	Linear ft	Steam	Condensate	
A-B	505	8”	4”	0.0
B-D	1996	8”	4”	0.0
D-F	3945	12”	6”	296
F-H	701	12”	6”	0
H-J	4596	10”	6”	73

Branches		Pipe Sizes		Elevation (ft)
	Linear ft	Steam	Condensate	
B-C	700	6”	4”	63
D-E	115	14”	6”x2	0.0
F-G	616	8”	4”	0.0
H-I	199	4”	2”	0.0

A	Downtown Connection
B	Life Sciences Branch
C	Life Sciences
D	Connection of MEA to Main Branch
E	MEA Plant
F	Ag Annex Branch
G	Ag Annex
H	Towers Branch
I	Towers
J	Health Sciecnes

Figure 21: One-line drawing of MEA’s pipelines with distribution meter points along with linear pipe distances, elevations, and pipe sizes.

Geothermal hot-water system

We also considered changing the current existing steam infrastructure to a hot water-based system. Since we do not have access to exact details about the steam vs hot water usage at individual buildings, the best estimate of the total load to be maintained as hot water to steam (60/40 and 70/30 in summer and in winter, respectively) for the worst-case scenario is considered. In both cases, steam is used for heating domestic water through the existing steam – water heat exchangers. The temperature drop at the buildings is around 30°F (~16.7°C). If we included conversion of domestic hot water heat exchangers from steam – hot water to hot water – hot water exchangers, we would need approximately 30 heat exchangers for both the Ag. Science and Towers meter points (i.e., Evansdale Campus), and Health Sciences and Ruby Memorial Hospital (i.e., the Medical center meter point). Each heat exchanger costs about $10,000. In this case, 85% of the peak load would be hot water with the remainder being steam for equipment in winter.

The required amount of water flow rate is calculated based on the amount of steam used for heating purposes, latent heat (~ 850 BTU/lb) of steam and the temperature drop (30°F) at the buildings. Due to the large water flow rates needed for the system (as seen in Table 2), only the Evansdale campus (i.e., the Ag. Science and Towers meter points), Health Sciences and Ruby Memorial Hospital (Medical Center meter point) are considered for geothermal based system analysis, while it is assumed that the downtown campus steam requirement will be supplied through natural gas boilers.

Table 2: The required water flow rate estimated from the maximum steam flow rate during January and latent heat of steam.

Hot water/Steam→	**60/40**		**75/25**		**85/15**	
Meter point Location→	**Ag. Science + Towers**	**Medical Center**	**Ag. Science + Towers**	**Medical Center**	**Ag. Science + Towers**	**Medical Center**
Total amount of steam (lbs/hr)	70,000	75,000	70,000	75,000	70,000	75,000
Steam Converted to HW (lbs/hr)	42,000	45,000	52,500	56,250	59,500	63,750
Amount of water (lbs/hr)	1,190,000	1,275,000	1,487,500	1,593,750	1,685,833	1,806,250
Amount of water (kg/s)	**149.9**	**160.7**	**187.4**	**200.8**	**212.4**	**227.6**

Task 2.3: Develop Base Case Surface Facility Design

Based on the end-use requirement, a hybrid geothermal-natural gas boiler system was designed where geothermal fluid is used to preheat the water and then a natural gas boiler is used to further heat the hot water to provide steam at required conditions. A base case surface plant (Figure 22) facility is designed to deliver high-pressure steam at 250 psig (18.25 bar) and 500°F (260°C) centrally and is distributed to all the meter points using existing pipelines. The surface plant components consist of a geothermal heat exchanger, natural gas boiler, condensate receiver tank, pumps, and distribution pipeline units. The hot geothermal fluid (Geo-In) at a fixed temperature and a flow rate from the production well is first sent to the centralized geothermal plate heat exchanger (PHE) where heat from the geothermal fluid is transferred to the condensate entering the heat exchanger (Cold-In) and the spent geothermal fluid (Geo-Out) is reinjected back into the reservoir. The PHE in Figure 22 isolates geothermal fluid from the surface equipment and

distribution system to prevent scaling and corrosion. The preheated water (Hot water) is pumped into the natural gas fired boiler where it is further heated to produce steam at the required conditions. Steam produced is distributed to the campuses through the five main distribution points using existing network of pipelines. The condensate from the buildings is returned to the main five distribution points and it is finally recycled to the central plant through condensate pipelines by using pumps at the meter points.

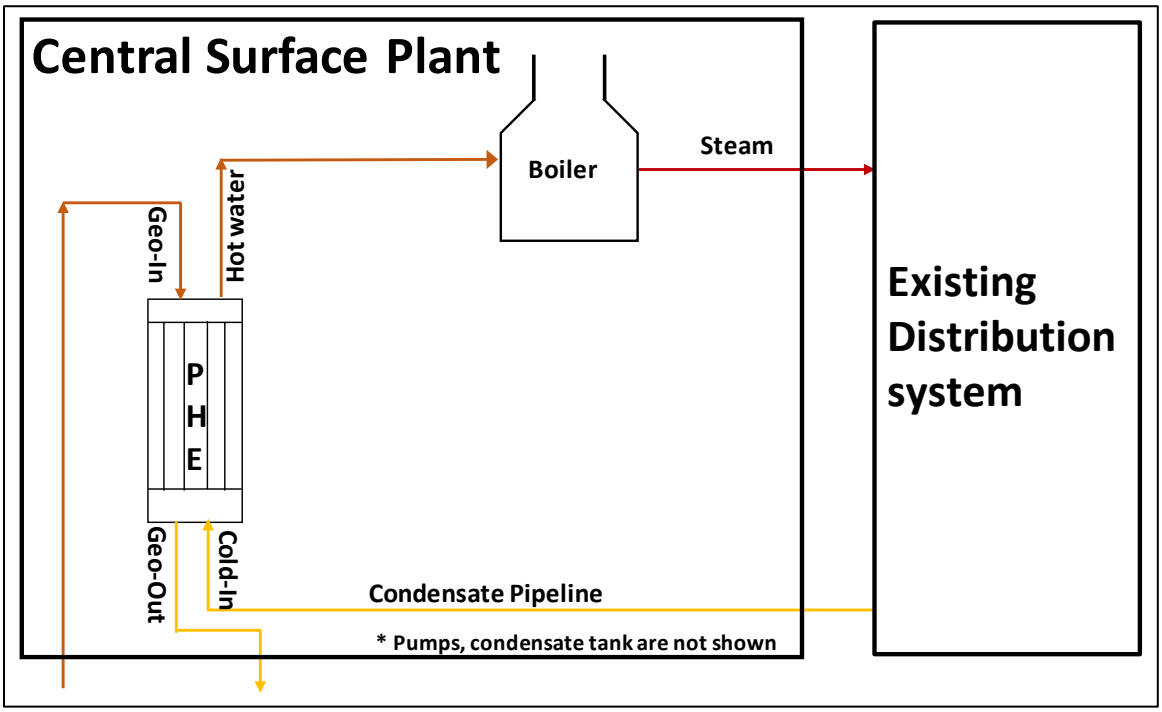

Figure 22: Schematic of the proposed hybrid geothermal-natural gas system to provide steam at required conditions for WVU campus.

We considered two scenarios based on geothermal site location:
Scenario 1: Supply steam at 18.25 bar (250 psig) and 260°C (500°F) to entire WVU campus (all five distribution meter points).
Scenario 2: Supply saturated steam at 12.5 bar (166 psig) to Evansdale campus (Ag. Science and Towers meter points) and Health Sciences campus and Ruby Memorial Hospital (Medical center meter point), while steam for the downtown campus will be provided by natural gas boilers.

The model along with the distribution pipelines and pumps is simulated using ASPEN HYSYS tool. The natural gas (95% methane, 2.5% ethane, 2.5% propane (Nasir et al., 2014)) at 65°C and 10% excess air at 25°C is supplied to boiler and the efficiency is fixed at 85%. New pipelines (one for steam and two for condensate return) are added to connect central plant to the existing distribution lines.

- New steam pipeline: transports steam from boiler outlet to the main MEA pipeline that connects to existing distribution pipeline at the Medical Center meter point.
- Two new condensate pipelines: 1) transports Evansdale and Downtown condensate return from current MEA line to the central plant site, and 2) transports Health Sciences condensate return to the central plant site.

Return condensate is assumed to reach the distribution points around 1.1 bar (1.2 psig) and pumps are used to overcome pressure losses in the pipes and due to elevations and is returned to central location at 1.0 bar (0 psig). The efficiency for all pumps is assumed to be 80%.

To carry out rigorous design of the PHE and make necessary correction for fouling and allowable pressure drop requirements, the process data in HYSYS are exported to Aspen Exchanger Design and Rating (EDR) where a detailed design is performed to determine the PHE area, plate configuration and number of plates. Fouling resistance of 0.0007 ft^2-h-°F/BTU (Hernandez-Galan & Alberto Plauchu, 1989) is used for geothermal fluid, to account for geothermal fouling in the heat exchanger, while for the condensate fluid a fouling resistance of 0.0001 ft^2-h-°F/BTU (K. Rafferty, 1998) is used.

Objective 3 – Create Subsurface Model and Design

Task 3.1: Simulate Base Case Vertical and Horizontal Well Configurations

The numerical simulator iTOUGH2 (Finsterle, 2016), which is based on TOUGH2 (Pruess et al., 1999, 2011), was used for the numerical simulations, using the equation of state package EOS1, designed for multiphase flow of water (liquid, vapor) and heat. iTOUGH2 and TOUGH2 employ the integral-finite-difference method (Edwards, 1972; Narasimhan and Witherspoon, 1976) for spatial discretization, which is a flexible method that can create accurate grids with variable resolution and provide convenient means to represent dual-continua (i.e., fractured and matrix) media (Pruess and Narasimhan, 1982; 1985).

The fact gas production has been successful from the unstimulated Tuscarora sandstone suggests a connective fracture network exists. Initially it was not clear how a geothermal reservoir model that assumed fracture permeability would compare to a simpler porous-medium continuum model with equivalent permeability values. As a result, three reservoir models were compared: a single permeability (K) model and two dual-K (fracture and matrix) models. The reservoir parameters for the single-K model are listed in Table 3.

Table 3: Reservoir physical parameters for the single permeability continuum model.

Reservoir Parameter/Condition	Value
Fluid	Pure Water
Thickness [m]	100
Porosity	0.08
Upper 2/3 reservoir permeability [m^2]	6.4×10^{-14}
Lower 1/3 reservoir permeability [m^2]	4.0×10^{-15}
Geothermal Gradient [°C/km]	26[1]
Thermal conductivity [W/m/ °C]	2.00
Rock specific heat [J/kg/ °C]	1000
Rock grain density [kg/m^3]	2500
Pore Compressibility [Pa^{-1}]	3.2×10^{-10}
Temperature of Injected fluid [°C]	21

[1] Average geothermal gradient estimated from the five drilled wells to Tuscarora Sandstone closest to the proposed Morgantown site. None of the wells are within five (5) miles of the proposed site. Also, though the number seems low, it is relatively higher compared to heat flow in other places in Eastern U.S

For the two dual-K models: The first model assumes that all fractures conduct flow, while the second model assumes only 10% of fractures conduct flow. For both models, a 2-D fracture network (i.e., only vertical fractures) is considered as the horizontal fractures are likely closed at the Tuscarora depth. The fracture properties are given in Table 4. Matrix permeability is 2.4×10^{-15} m^2 and porosity is 8%.

Table 4: Fracture specifications for Dual-K models.

Fracture Model Name	Porosity	Upper Layer Permeability [m^2]	Lower Layer Permeability [m^2]	Fracture Spacing [m]	Fracture Volume Fraction
Dual-K 1	0.99	6.4×10^{-14}	4.0×10^{-15}	0.3	1.5×10^{-3}
Dual-K 2	0.99	6.4×10^{-14}	4.0×10^{-15}	3.0	1.5×10^{-4}

With no samples available for geochemistry and gas analysis, pure water is considered in our simulations. The boundary conditions for all simulations are no fluid flow in all directions and no heat flow in lateral directions, while heat exchange at the top and bottom of the reservoir is calculated based on semi-analytic conductive heat exchange (Pruess et al., 1999). Initial temperature follows the geothermal gradient, while pressure is based on hydrostatic equilibrium.

Geothermal reservoir production simulations were carried out for two different injection-production well configurations: 1) two vertical wells, and 2) two horizontal wells for different well distances as explained in Garapati et al. (2019).

Task 3.2: Determine Well Configuration and Orientation/Economic Analysis

The performance of both horizontal and vertical configurations is compared based on production fluid temperatures, time to thermal breakthrough, and thermal drawdown. Based on the performance and cost, well configuration is selected for further uncertainty analysis.

Preliminary economic analysis of well-head LCOH (i.e., the capital costs for drilling wells and pumping costs for production and injection of fluid for different well configurations without surface plant capital cost), is performed using the software GEOPHIRES developed at Cornell University and maintained on Github by Beckers and McCabe (2018) (Beckers et al., 2013; 2014; 2016). We calculated well-head LCOH for a well spacing of 500 m. The well drilling costs are calculated using the default correlations and these values are considered as the upper bound. Horizontal wells with lateral length of 500 m are considered, and to consider high costs for horizontal well drilling, a cost adjustment factor of 1.5 is used. The technical parameters used are given in Table 5.

Table 5: GEOPHIRES input parameters to calculate well-head levelized cost for both vertical and horizontal well configurations.

Parameter	Vertical	Horizontal
Geothermal Fluid Flow Rate (kg/s)	16.5	17.0
Geothermal Gradient (°C/km)	26	26
Ambient Temperature (°C)	13.5	13.5
Well Depth (km)	2.9	2.9
Well Configuration (-)	Doublet	Doublet
Well Inner Diameter (inch)	8.0	8.0
Reservoir Impedance (GPa.s/m^3)	1.0	0.15
Production Wellbore Heat Transfer	Ramey's Model	Ramey's Model
Reinjection Temperature (°C)	20	20
Reservoir Model	User-provided TOUGH2 temperature data	User-provided TOUGH2 temperature data
Reservoir Water Loss Rate	0%	0%
Well drilling cost correlation	1 (vertical, small diameter)	1 (vertical, small diameter)
Well Drilling and Completion Capital Cost Adjustment Factor	1.0	1.5
Plant Lifetime (Years)	30	30
Economic Model	3 (Bicycle (Hardie,1981))	3 (Bicycle (Hardie,1981))
End-Use Option	2.0 (Direct-Use Heat)	2.0 (Direct-Use Heat)
Circulation Pump Efficiency	0.8	0.8
Utilization Factor	0.9	0.9
End-Use Efficiency Factor	0.9	0.9

Task 3.3: Perform Subsurface Uncertainty Analysis

Due to the potential lack of data and our incomplete knowledge of the proposed site, it is important to perform an uncertainty analysis to understand the potential range of model predictions (i.e., production temperature, reservoir productivity). It is also important to understand which parameters contribute most to the prediction uncertainty; thus, site characterization can be prioritized based on the parameters whose uncertainties contribute most to overall system performance uncertainty. Prediction uncertainty comes from two sources: 1) model uncertainty, and 2) parameter uncertainty. Work under Task 3.1 determined model predictions were not sensitive to the choice between a single-K versus dual-K models. In this section, effect of heterogeneity (which is not avoidable), as well as uncertain parameters on reservoir behavior is explored.

Impact of heterogeneity

There is very little information on the heterogeneity of the formation. Therefore, a heterogeneous permeability field is generated for the upper 2/3 formation using the Geostatistical Software Library, GSLIB (Deutsch and Journel, 1992) implemented in iTOUGH2. The effect of heterogeneity is studied in both vertical and horizontal well placements.

Uncertainty Quantification (UQ) Analysis using iTOUGH2:

Two types of uncertainty analysis are performed:

1. A First Order-Second Moment (FOSM) uncertainty propagation analysis to identify the most influential uncertainty parameter to model predictions, the results can be used to help prioritize site characterization effort, and

2. A formal Monte Carlo (MC) simulation that provides the potential uncertain range of the model predictions.

The uncertain parameters considered are average permeability (formation upper 2/3), porosity, rock compressibility, and seven geostatistical parameters from GSLIB including correlation length, sill, rotation angles and anisotropy ratios, which characterize the spatial correlation of the heterogeneous permeability distribution. The simulations are performed using a fixed flow rate of 15 kg/s. The model predictions (outputs) are production temperature and injection/production pressure difference as an indication of reservoir impedance (RI) for a fixed flow rate.

FOSM Analysis:
FOSM is the analysis of the mean and covariance of a random function (model output) based on its first order Taylor series expansion. It presumes the mean and covariance are enough to characterize the distribution of the dependent variables. FOSM analysis relies on two assumptions: 1) model outputs are normally distributed, and 2) perturbations about the mean can be approximated by linear functions. Because of the simplicity and low computational cost, FOSM can be used to provide preliminary uncertainty quantification and identify which parameter contributes more to the overall prediction uncertainty. The values of the parameters used for base case are given in Table 6

Table 6: The uncertain parameter values used for base case in FOSM analysis.

Parameter	Value
Permeability (m^2)	6.e-14
Porosity	0.03
Compressibility (Pa^{-1})	3.e-10
Correlation length (m)	100
Rotation angle 1	50º
Rotation angle 2	50º
Rotation angle 3	50º
Anisotropy 1	3.0
Anisotropy 2	1.0
Sill	1.0

Monte Carlo Simulations:
The FOSM analysis provided the first order model prediction uncertainty based on certain assumptions and identified influential parameters. MC simulations allow for higher order analyses but are more computationally intensive. Here a MC simulation is performed considering all ten uncertain parameters. Latin Hypercube Sampling (LHS) (McKay et. al., 1979; Zhang and Pinder, 2004) is used to ensure parameters are sampled within the parameter range and parameter distributions as listed in Table 7.

Table 7: The uncertain parameter range and distribution used in MC simulations.

Parameter	Range	Distribution
Permeability (m^2)	6.3e-15 - 1.0e-13	LogNormal
Porosity	0.01 - 0.1	Uniform
Compressibility (Pa^{-1})	1.e-10 - 1.e-9	LogUniform
Correlation length (m)	20 -200	Uniform
Rotation angle 1	0 - 90º	Normal
Rotation angle 2	0 - 90º	Normal
Rotation angle 3	0 - 90º	Normal
Anisotropy 1	1.0 - 10	Uniform
Anisotropy 2	1.0 - 10	Uniform
Sill	0.5 - 1.5	Uniform

Reservoir risk factor favorability for the Tuscarora sandstone near Morgantown, WV.

The methods described in Camp et al. (2018) and Jordan et al. (2016) are used to estimate geothermal reservoir productivity. Those methods and reservoir productivity metrics, along with any additional assumptions and modifications made for this analysis, are summarized in this section.

Reservoir Productivity Metrics

The permeability of the Tuscarora is expected to be fracture dominated (Avary, 1996), the most appropriate metric to evaluate reservoir productivity from Camp et al. (2018) and Jordan et al. (2016) is the reservoir flow capacity (RFC). The RFC considers the (average) permeability over the thickness of the reservoir, which may have several permeable zones, and is therefore indifferent to the cause of the permeability (e.g., matrix, fracture, stylolite). A limitation of the RFC is that the importance of vertical permeability is not adequately captured.

Despite evidence suggesting the Tuscarora has fracture-dominated permeability, there is a chance the Tuscarora near Morgantown has few fractures and instead provides essentially matrix flow. Matrix flow is a worst-case scenario if matrix permeability is too low for economic extraction of heat; but matrix flow could be beneficial if it allows for greater heat sweep of a reservoir compared to fracture flow. The reservoir productivity index (RPI) is the metric used for matrix flow, which assumes a homogeneous and isotropic porous medium with a single fluid (i.e., water) produced from two vertical wells in a doublet arrangement (e.g., Craft and Hawkins, 1959; Dietz, 1965; Gringarten, 1978).

Equation 1 and Equation 2 provide the RFC and the RPI metrics, respectively, with units

$$\mathrm{RFC} = \mathrm{k_w H}\ [\ \mathrm{mD\ m}\ ] \qquad [1]$$

$$\mathrm{RPI_w} = \frac{2\pi\, \mathrm{k_w H}}{\mu \ln\left(\frac{\mathrm{d}}{\mathrm{r_{well}}}\right)} \rho_w \left[\ \frac{\mathrm{kg}}{\mathrm{Pa{\cdot}s}}\ \right] \qquad [2]$$

where k_w is the water permeability (mD for RFC, m^2 for RPI_w), H is the thickness of the reservoir (m), μ is the dynamic viscosity of water at the temperature of the reservoir (Pa - s), ρ_w is the density of water at the temperature and pressure of the reservoir (kg/m^3), d is the distance between

wells (m), and r_{well} is the inner radius of the well (m). The density of water is needed to convert the RPI_w metric to units of kg/Pa-s. A constant value of 988 kg/m^3 is used, which is the same as used in Camp et al. (2018). Further details about these metrics are provided in Camp et al. (2018) and Jordan et al. (2016).

Klinkenberg Permeability Correction

The RFC and RPI_w metrics require the rock permeability for water. Permeability was measured using air in the dataset for this analysis; therefore, a Klinkenberg correction to the air permeability is needed to convert to an effective water permeability. The Klinkenberg correction used in this study is provided in Jones (1987) (equation developed for sandstones with permeability range [0.01 mD to 2,000 mD]). All air permeability measurements in the dataset used in this analysis are greater than 0.01 mD; thus, Klinkenberg corrections developed for tighter sandstones (e.g., Jones and Owens, 1980) are not necessary. Some air permeability measurements are greater than 2000 mD; but applying the correction to these high permeability values reduces their values only slightly. The maximum correction above 2,000 mD is for the maximum permeability observed in the dataset, 9,184 mD, which is reduced to 9,165 mD. Thus, applying the Klinkenberg correction to all air measured permeabilities can be considered as a conservative estimate of effective water permeability. The true water permeability could be even smaller because of differences in air and water as fluids (Jones and Owens, 1980).

Equation 3 provides the general form of the Klinkenberg correction, and Equation 4 provides the parameter specification for b

$$k_w = \frac{k_g}{1+\frac{b}{p}} \text{ [mD]} \qquad [3]$$

$$b = 15.61\left(\frac{k_g}{\phi}\right)^{-0.447} \text{ [psig]}, \ 0.01 \text{ mD} < k_g < 2000 \text{ mD} \qquad [4]$$

where k_g is the gas (air) permeability (mD), ϕ is the rock porosity (-), b is the "fractional increase in apparent permeability which would be observed when measuring k_g [with air] at atmospheric pressure" (Jones and Owens, 1980) (psig), and p is the mean flowing gauge pressure of the equipment used to measure k_g (psig). In this study, p = 26 psig using a Core Labs PPP-250 minipermeameter with air.

The rock porosity in this study is estimated from core samples, as discussed below, and provided in more detail within McCleery et al. (2018). The average porosity is assigned to all values of permeability because enough porosity and permeability measurements in the same core sample locations are not available to develop a porosity-permeability relationship. Even so, deviations in porosity from the average for the smallest k_g measured in this dataset, 0.4 mD, will affect the correction to k_w by less than a factor of 1.2 (Appendix B). The factor is smaller for higher values of permeability. Therefore, the average porosity for all k_g will not have a significant impact on the resulting k_w values.

Well Specifications for the RPI_w Metric

The RPI_w requires a well separation distance and a wellbore radius. The distance between injection and production wells is being optimized within the geothermal reservoir thermal-hydraulic models

used in this project. The wellbore distance is expected to be about 400 m – 1,000 m. For consistency with the GPFA-AB project, a 1,000 m distance will be assumed to compare the productivity among other reservoirs within the Appalachian Basin. The impact of well separation distance on the RPI_w metric is also evaluated for well separations from 400 m to 1,000 m in increments of 200 m. The assumed inner radius of the well at production depth is 0.1 m (3.93”), which is the same value used in the GPFA-AB study. This is slightly larger than the 6.2” inner diameter value used for “small diameter” geothermal wells in the well cost correlation study by Lowry et al. (2017).

Uncertainty Analysis for RFC and RPI_w

To provide estimates of uncertainty in the RPI_w and RFC, a Monte Carlo analysis of the uncertain reservoir and fluid properties within these equations is implemented, as described within Camp et al. (2018) and Jordan et al. (2016). The uncertain properties considered for analysis are the reservoir thickness, reservoir permeability, and fluid viscosity. Selection of values for the mean, uncertainty, and probability distribution for each of these properties are described in the following sections.

Spatial Extent of the Tuscarora near Morgantown, WV

To update the GPFA-AB Reservoir Risk Factor analysis, the spatial extent of the Tuscarora that could serve as a geothermal reservoir is needed. Because Morgantown and surrounding cities that would utilize any heat extracted from the reservoir for this project, the spatial extent of the Tuscarora was selected based on reasonable pumping distances from the production well to users. In the GPFA-AB report, a 5 km pumping distance was assumed as a maximum distance in the utilization risk factor analysis (Jordan et al., 2016). Therefore, a 5 km buffer around Morgantown was used to set the spatial extent of the Tuscarora to not limit the analysis of combined risk of a geothermal project. The true useful extent of the Tuscarora is likely larger in area.

Another consideration for defining the spatial extent of the Tuscarora is structural features that may provide significantly different reservoir flow properties within the 5 km buffered area. As stated in Avary (1996), the permeability of the Tuscarora is thought to be structurally controlled. A fold southeast of Morgantown, visible on the surface, is of concern because folded rock could provide greater fractures than limbs of the fold. The extent of the Tuscarora for Morgantown was clipped to be north and west of this fold, as shown in Figure 23. Further extension or narrowing of the spatial extent of the Tuscarora may be made after more detailed local analyses are completed.

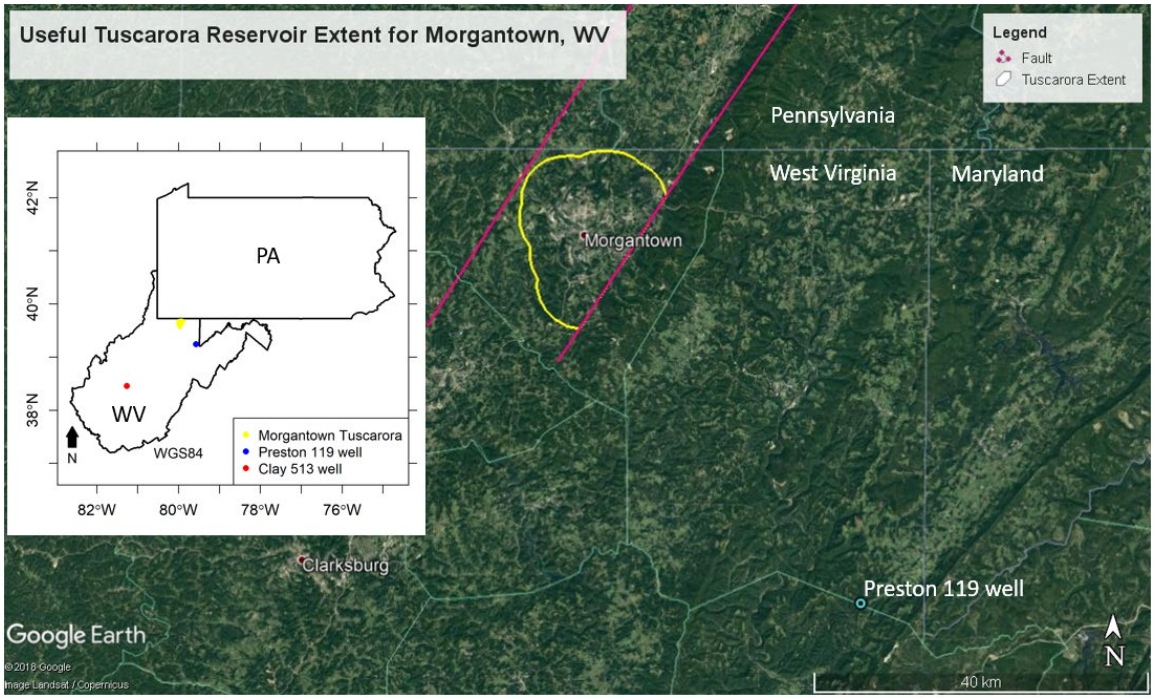

Figure 23: Estimated spatial extent (yellow) of the Tuscarora Sandstone as a geothermal reservoir near Morgantown, WV. The yellow outline provides a 5 km buffer around Morgantown as defined in the 2010 Census Incorporated Places (West Virginia GIS Technical Centers, 2010). The buffer is limited on the eastern side because of a fault (magenta).Location of other data used for this analysis are provided as points on the inset map.

Tuscarora Depth and Thickness near Morgantown, WV

The depth and thickness of the Tuscarora is not expected to vary greatly within the spatial extent of the Tuscarora provided in Figure 1. Based on a local well analysis provided in McCleery et al. (2018), the thickness of the Tuscarora near Morgantown is expected to be on average 400 ft (122 m), with a TVD of about 10,030 ft. (3,058 m) below ground surface. It is unclear if this entire thickness would be productive as a geothermal reservoir; yet permeability measurements described below indicate it is possible.

The depth and thickness estimates are uncertain because only five wells within 15 km provided information on the depth of the top of the Tuscarora, and three wells provided thickness information (McCleery et al., 2018). All wells are located south and southeast of Morgantown. Thus, depth control of the Tuscarora for other directions from Morgantown is poorly constrained and could only be obtained using correlations of shallower formations, as described in McCleery et al. (2018).

For this project, following the Uncertainty Index Method of Camp et al. (2018) and Jordan et al. (2016), the uncertainty assigned to the Tuscarora thickness is 1, stating a ±20% of the mean thickness defines the lower and upper bounds of a symmetric triangular distribution of reservoir thickness. Using 122 m as the mean reservoir thickness, the bounds of reservoir thickness are 97 m, and 147 m, respectively. Two of the three thicknesses measured from local wells fall within this interval, and the third well is only 4 m thinner.

In Camp et al. (2018) and Jordan et al. (2016), the reservoir depth was known because only existing oil and gas plays were used to assess the Reservoir Risk Factor. For consistency with that analysis, depth of the Tuscarora will be assumed constant at the predicted mean from McCleery et al. (2018). Depth will only affect the RPI_w metric through the value assigned to water viscosity, which is dependent on temperature. Viscosity is the least sensitive parameter in the RPI_w equation (Camp et al., 2018). At the temperatures considered in this analysis, even a relatively large uncertainty of ±100 m depth would result in only a 3% change in RPI_w metric.

Tuscarora Porosity for the Klinkenberg Permeability Correction

McDowell (2018) collected visual porosity estimates for 29 thin sections spanning 19 m (62.3 ft.) of the Clay 513 well (API 4701500513) in Clay County WV (visual porosity chart in Appendix C). A thickness of 19 m is a smaller scale than the thickness of the Tuscarora, and over this thickness there are a variety of features that induce localized porosity contrasts, including stylolites, "irregular blobs" or burrows, and fractures. This small sample of Tuscarora porosity is likely insufficient to fully characterize the distribution of porosity; however, this dataset is the largest available with which to estimate an average porosity for use in the Klinkenberg permeability correction equations. As stated above, the correction is relatively insensitive to changes in porosity, a best-available porosity estimate that this dataset provides is enough for this analysis. A summary of the visual porosity estimates from the Clay 513 well is provided in Table 8.

Based on data from the Clay 513 well, the most likely value of porosity is less than 1%. There are zones of porosity greater than 10% that occur because of "irregular blobs" and from coarse or very coarse local grain size distributions. Fractures seem to have less impact on porosity than the blobs and grain size for this well. The minimum and maximum visual porosity estimates for all core sample depths are provided in Figure 24. The porosity can vary by as much as 10% within a 5 ft interval.

Table 8: Number of samples or parts of samples within estimated visual porosity classes for 29 thin sections of the Tuscarora sandstone in the Clay 513 well. Parts of samples means that some (4) samples had zonal porosity differences (e.g., matrix vs. "irregular blob").

Count	Estimated Porosity (%)
17	≤1
5	1 to 2
4	2 to 5
5	5 to 10
1	10 to 15
1	15 to 25

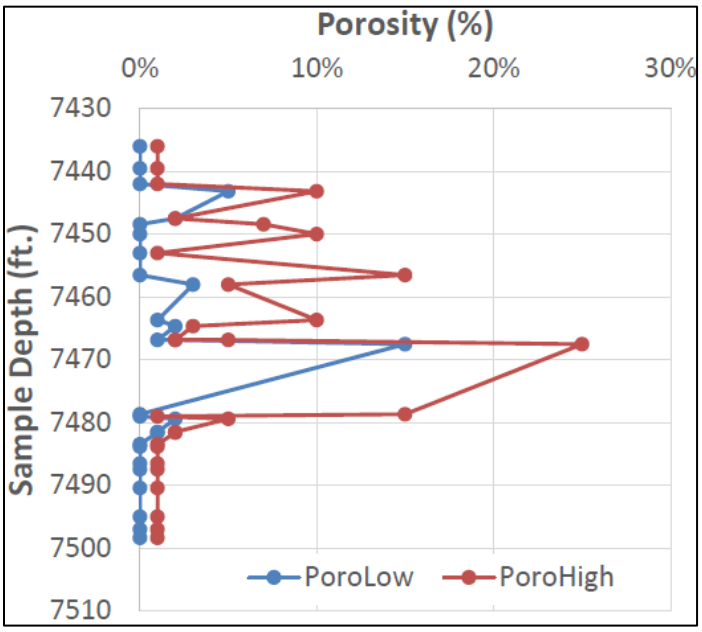

Figure 24: Porosity range (low to high) based on visual porosity estimates taken at the listed sample depths in well Clay 513. Straight lines connect sample points for visual reference but should not be used to infer geologic trends with depth.

Using this dataset, the average low porosity is about 1.3%, and the average high porosity is about 4.7%, with an overall average of about 3%. A second dataset with eight 8 porosity measurements from the more local-to-Morgantown Preston 119 well (API: 4707700119) had an average porosity of about 3.8%. Despite being closer to Morgantown, the Preston 119 well is in a different structural setting than Morgantown, while the Clay 513 well is in a similar setting (McCleery et al., 2018). Therefore, considering the variability in the data and structural setting, 3% porosity is assumed in the Klinkenberg correction.

Tuscarora Permeability

McDowell, Lewis, and Daft (2018) collected permeability measurements for 753 unique locations on 279 different core samples spanning a 273 ft (83 m) thickness of the Tuscarora sandstone in the Preston 119 well, located in Preston County, West Virginia. Three measurements were taken in each location to estimate measurement errors resulting from the data collection method. Generally, errors increase in magnitude for higher permeabilities. For this analysis, the average of the three measurements are used, after converting to Klinkenberg effective water permeability. Measurements taken on fractures listed as horizontal or subhorizontal with dip angles less than 20° were excluded because these fractures are likely to be closed at the depths of the Tuscarora.
The effective water permeability with depth for Preston 119 well is plotted in Figure 25.
Permeable zones greater than 1 D are found throughout the Tuscarora thickness. Calcite fill is present in some fractures in the deeper depths of the Tuscarora; however, the calcite fill does not appear to affect the frequency of highly permeable zones.

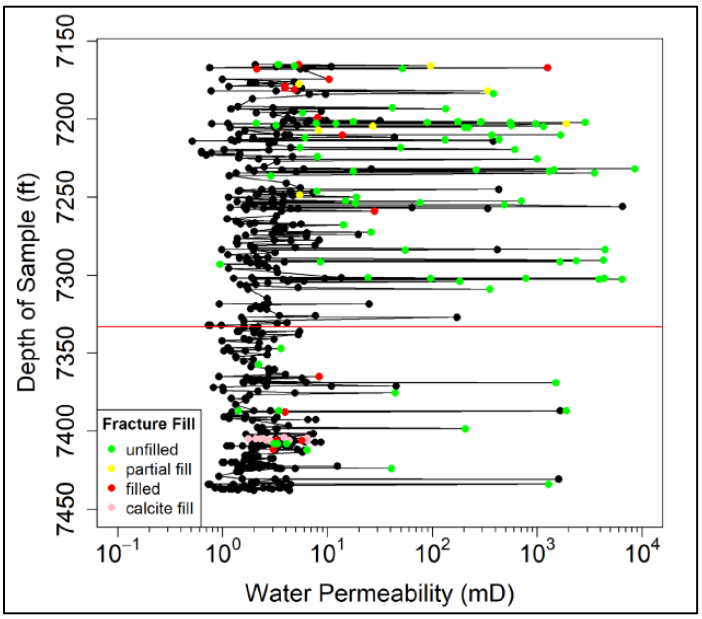

Figure 25: Tuscarora effective water permeability (mD) based on core samples from the Preston 119 well in Preston County, WV. Horizontal and subhorizontal fractures with dip angles less than 20° are not plotted. Lines connecting measurements are for visual aid and should not be used to suggest geologic trends in permeability with depth. The depth of an estimated changepoint in effective water permeability is shown as a horizontal red line.

The shallower portion of the Tuscarora seems to have more frequent permeable zones than the deeper portion. A nonparametric at-most-one changepoint (AMOC) analysis (cumulative sum test [CUSUM] as implemented in Killick and Eckley (2014); described on Page 1954) on the change in mean effective water permeability assuming a constant variance, and another AMOC analysis on the change in variance of the effective water permeability assuming a constant mean is performed. Both the analysis detected a changepoint at essentially the same depth: 7,332 ft. or 7,334 ft. (2,234.8 m or 2,235.4 m). If there is a smaller mean and/or variance of the effective water permeability deeper than about 7,333 ft., then the shallower portion of the Tuscarora could be treated as the productive geothermal reservoir thickness, while the deeper portion could be treated as less productive or not productive. Productive thickness based on this changepoint analysis is not explored in this study; however, multiple mean thicknesses of the Tuscarora are evaluated within the Monte Carlo analyses to test the effect of thickness on the reservoir productivity metrics.

Permeability measurements were taken on several structural features known to affect permeability. The effective water permeability distribution categorized by the type of feature is provided in Figure 26. Permeabilities less than 10 mD are found primarily in the matrix rock. The following features were grouped into a Matrix Rock category to calculate the permeability in the RPI_w metric: matrix, matrix with stylolites, coarse grain with and without stylolites or voids, granular, and burrow. Matrix permeability was measured on every core sample; thus, the resulting distribution should be representative of the population Tuscarora matrix permeability over this depth range. For the fracture permeability, note the Preston 119 well is located about 0.7 miles from the crest of the Eglon Anticline (Preston County Geologic Map, 1914). Based on early observations from the core (McDowell, personal communication), this limb of the anticline seems highly fractured. Therefore, the effective water permeability for fractures in Figure 26 should be considered as an upper bound estimate of Tuscarora fracture permeability.

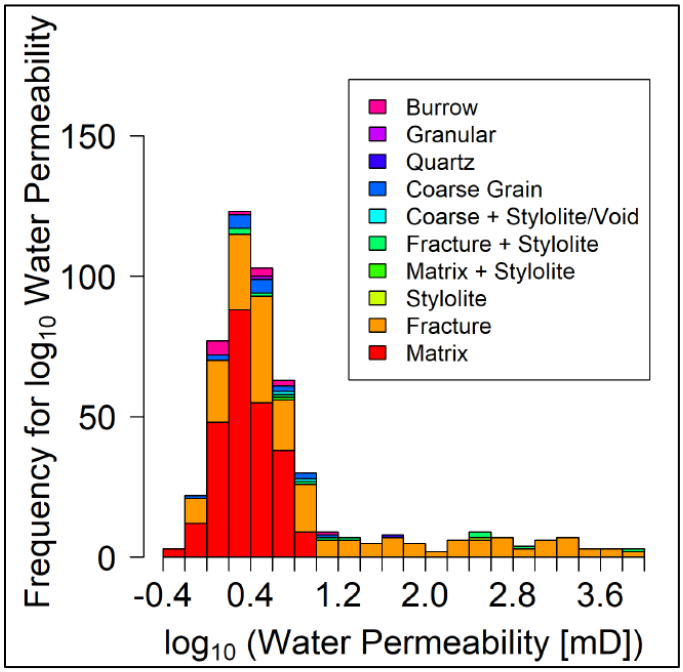

Figure 26: Stacked bar plot showing the contribution to the observed log10 (water permeability [mD]) by the type of structural feature measured. The aggregate distribution is the effective water permeability histogram for the samples collected. Horizontal and subhorizontal fractures with dips less than 20° are not plotted.

Matrix-based permeability

For the RPI_w, using the above assumptions for matrix rock results in a real space mean of 2.67 mD and real space standard deviation of 1.56 mD (CV = 58%). The histogram of observed Matrix Rock data (Figure 27) does not clearly resemble an analytic distribution. The lognormal distribution is commonly used to model permeability, it was also used in Camp et al. (2018), and it is also used in this study. Based on the data, the uncertainty index for Matrix Rock permeability was assigned as three (3), which corresponds to a lognormal distribution coefficient of variation of 50%. The resulting lognormal distribution fit to the data is displayed in Figure 27. Using a smaller CV than the data results in the tails of the distribution being thinner in density than were observed.

Fracture-based permeability

For the RFC, the entire distribution shown in Figure 26 was used to fit an analytic permeability distribution. Interpretation of Figure 26 for this analysis relies on every important feature being sampled, or a statistical random sampling scheme. Such methods would allow for the assumption the collected data reflect the population of rock features, rather than a preferential sampling to collect contrasting information about permeability from the different features. Every important feature was sampled on these cores (R. McDowell, 2018, personal communication), the distribution of water permeability is assumed representative of the population.

The RFC metric assumes a mean water permeability is specified for the reservoir. Assuming this reservoir is representative of all Tuscarora reservoirs, a bootstrapping approach is appropriate to estimate the distribution of the mean effective water permeability for Tuscarora reservoirs. A 1D

spatial autocorrelation of the calculated effective water permeability was estimated using a variogram cloud to inform if block bootstrapping methods would be necessary to capture autocorrelation (Appendix D). Vertical autocorrelation did not appear to change over a 100 ft. separation distance for samples; thus, block bootstrapping was not used in this study.

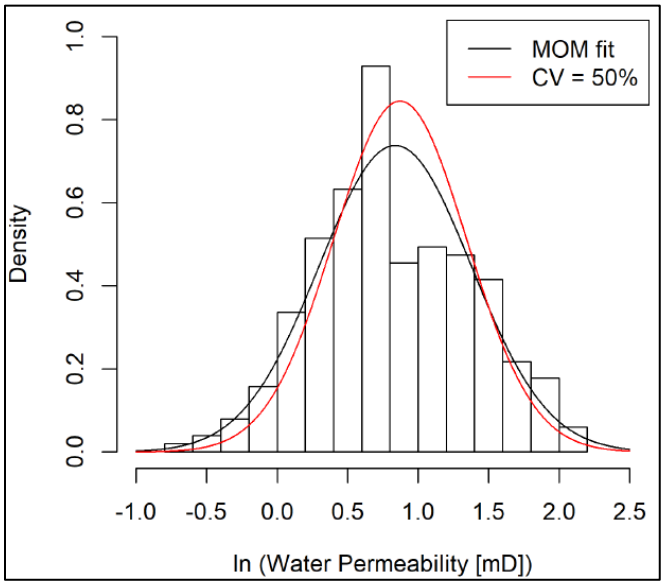

Figure 27: Lognormal distribution fit to Matrix Rock effective water permeability using the method of moments (black) and fit assuming an uncertainty index of three (3), corresponding to a CV of 50% (red).

100,000 bootstrapped random samples of size 753 were used, selected with replacement from the original sample, which had 753 measurements. The mean of each 753-element sample was computed as an estimate of the mean effective water permeability for Tuscarora reservoirs. The resulting distribution of the mean effective water permeability computed from 100,000 random samples is provided as a histogram in Figure 28. The bootstrapped real-space mean of the effective water permeability is 164 mD, and the bootstrapped real-space standard deviation is 27 mD for a CV of about 17%. A lognormal distribution fit using the Method of Moments is provided in Figure 28, along with lognormal distribution fits corresponding to uncertainty indices of one and two for CVs of 12.5% and 25%, respectively. Neither of the uncertainty index choices for CV provide good fits to this bootstrapped distribution. To provide a wider range of possible values for the mean reservoir permeability, the CV of 25% is selected. Several choices of CV are evaluated in the Monte Carlo analyses to test the impact of permeability uncertainty on the RFC metric.

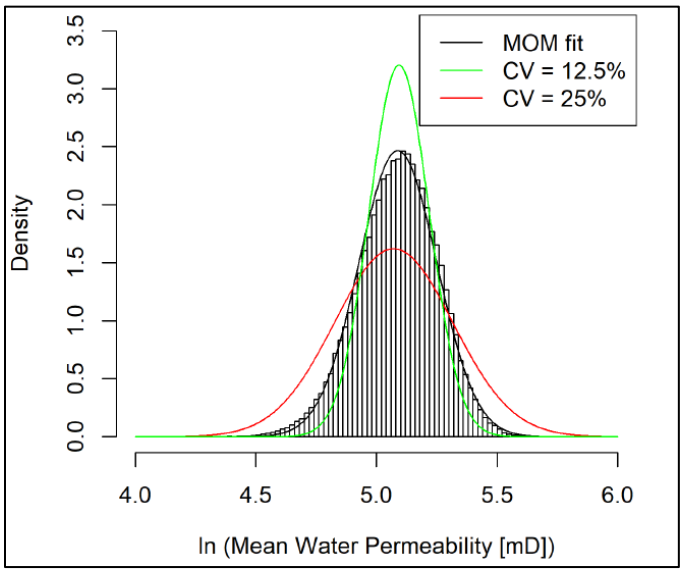

Figure 28: Lognormal distribution fit to a histogram of bootstrapped random samples of the mean effective water permeability using the method of moments (black), fit assuming an uncertainty index of one, corresponding to a CV of 12.5% (green), and fit assuming an uncertainty index of two, corresponding to a CV of 25% (red).

Fluid viscosity

At the temperatures considered for this analysis, which are greater than 75°C, the viscosity of water is primarily a function of temperature and not a function of pressure. Water is assumed to be pure water (due to lack of samples for geochemistry and gas analyses[2]) for the purposes of having well-defined thermodynamic equations to use, as is consistent with the GPFA-AB project since the main objective of this task is to compare favorability of Morgantown Tuscarora reservoir relative to other GPFA-AB reservoirs.

The temperatures at depths for Morgantown considering uncertainties in the estimated surface heat flow, geologic and thermal properties of rocks, and spatial interpolation uncertainties is provided in Figure 29 (analysis from Smith, 2019). Figure 29 consists of violin plots (kernel density plots / smoothed histograms with boxplots in the center) of temperatures at depths in 0.5 km intervals based on 10,000 Monte Carlo replicates of uncertain geologic and thermal properties. The top of the Tuscarora is expected to be at an approximate depth of 3 km, which corresponds to a mean of 88 °C and 5th and 95th percentiles of 72.5°C and 104°C, respectively.

The temperatures are used to estimate the viscosity at depths using Equation 5

$$\mu = 2.414E^{-5} * 10^{\left[\frac{247.8}{T+273.15-140}\right]} \qquad [5]$$

where T is the water temperature (°C) and μ is the dynamic viscosity (Pa - s). The corresponding distribution of viscosity at depth is provided in Figure 30. The change in viscosity with increasing temperature is progressively smaller; therefore, the uncertainty in viscosity decreases with increasing depth, despite increasing uncertainty in the temperature with increasing depth. The mean of the dynamic viscosity at 3 km depth is 3.22x10^{-4} Pa-s and the standard deviation is

[2] In our next phase, fluid samples will be collected from an exploratory well for geochemistry analysis and both subsurface and surface analysis will be updated to include geochemistry.

$3.35x10^{-5}$ Pa-s. This standard deviation maps to an uncertainty index of four (4) for a normal distribution, which is an adequate distribution approximation for this data.

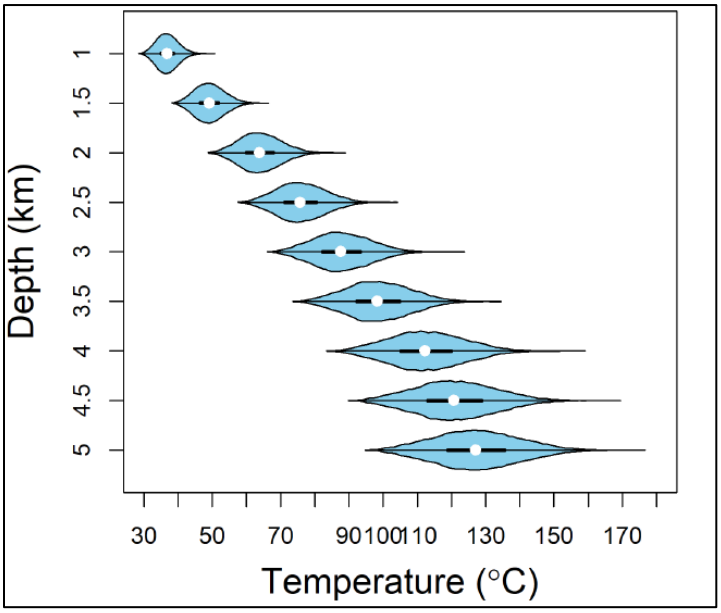

Figure 29: Estimated temperatures at depth for Morgantown, WV provided in 0.5 km depth increments. Violin plots (smoothed histogram plots) have white dots at the median value of the temperature at depth, and a black box in the center that spans the 25th to the 75th percentile estimates.

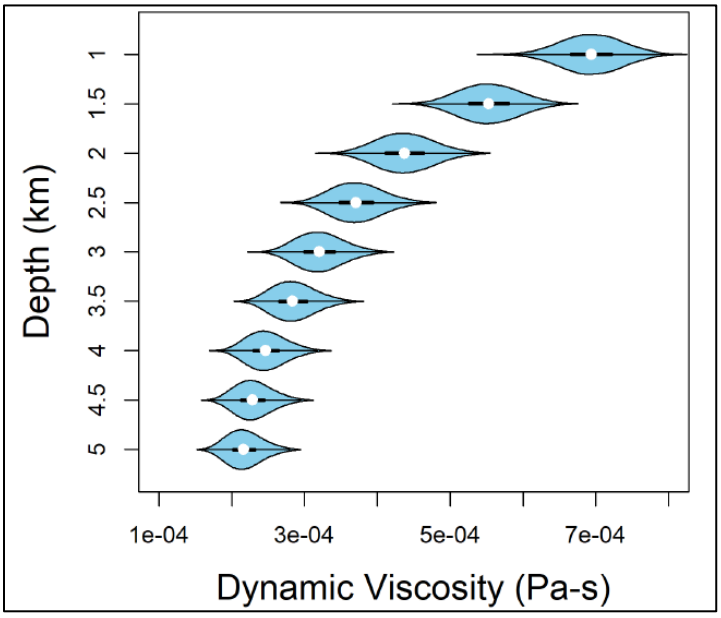

Figure 30: Dynamic viscosity of pure water with depth in Morgantown.

Monte Carlo analysis for RPI_w and RFC

A Monte Carlo analysis using 100,000 replicates of the uncertain parameters within the RFC and RPI_w equations was run to estimate the RFC and RPI_w for the Tuscarora reservoir near

Morgantown. Table 9 provides a summary of the values and distributions selected for each parameter. Water permeability is provided for matrix rock only, which is used for computing the RPI_w metric, and for fracture-based, which is used for computing the RFC metric. Results of this analysis are provided in the Discussion of Results section.

Table 9: Values and probability distributions selected for the Monte Carlo analysis.

Parameter	Distribution	Mean	Uncertainty Index
Water Permeability	Lognormal	Matrix Rock: 2.67 mD Fracture-based: 164 mD	3 2
Reservoir Thickness	Triangular	122 m	1
Dynamic Viscosity	Normal	3.22×10^{-4} Pa-s	4
Water Density	Constant	988 kg/m^3	NA

Objective 4 – Develop and Optimize Integrated Geothermal District Heating and Cooling (GDHC) System

Task 4.1: Estimate Base Case Levelized Cost of Heat (LCOH)

Capital cost for the centralized surface plant:

The total capital investment is the sum of fixed and working capital investment.

$$C_{cap} = C_{fixed} + C_{working} \quad [6]$$

The working capital is the additional cost, apart from fixed capital investment, needed for start-up of the project and keep the surface plant in operation. The working capital is assumed to be 20% of the total capital investment for the project (Timmerhaus et al., 2003). Therefore, the total capital investment is given as:

$$C_{cap} = 1.25\, C_{fixed} \quad [7]$$

The fixed capital investment is the sum of direct and indirect costs.

$$C_{fixed} = C_{direct} + C_{indirect} \quad [8]$$

The direct costs for the major equipment (including heat exchanger, boiler, heat pump, and new pipelines connecting to existing distribution pipelines) of the surface plant for all scenarios are calculated using ASPEN economic analyzer and quotes from vendors for boiler and heat pump. For new pipelines, the material is considered carbon steel with a polyurethane insulation to prevent piping corrosion (Rafferty 1989; 1998), while for PHE, the material considered is stainless steel (SS-304).

The indirect costs including construction expenses, contingency, contractor fees and engineering expenses, are assumed to be 35% of the fixed capital investment (Timmerhaus et al., 2003). Therefore, the fixed capital investment is given as:

$$C_{fixed} = 1.54\, C_{direct} \quad [9]$$

Hence, the total surface plant capital investment is approximately twice the direct cost.

$$C_{cap} = 1.93\ C_{direct} \approx 2.0\ \ C_{direct} \qquad [10]$$

Distribution pipelines:
To determine the cost of purchasing existing steam distribution pipelines (owned by MEA), three scenarios are considered: 1) MEA donates the pipelines to WVU, 2) WVU purchases pipelines from MEA for $15M, and 3) $25 M for installations of new distribution pipelines across the campus.

Economic analysis:
An economic analysis for the GDHC is performed using GEOPHIRES and BICYCLE levelized cost model is used to evaluate LCOH. The current version of GEOPHIRES is open-source code, written in python and does not include analysis for hybrid system. Therefore, the code is edited to account for a natural gas boiler, its heating duty, and yearly cost for natural gas. The natural gas costs are assumed to be ~$4.12/MCF ($3.702/MCF plus monthly add-ons), the electricity price is considered as $0.067/kWh, and the heat price is estimated based on our current MEA price $15/MMBTU ($0.05/kWh).

Task 4.2 – Optimize Integrated GDHC System
As per DOE review, we considered conversion of the current steam infrastructure to a hot water system and use geothermal as the sole energy source.

Steam-based hybrid system:
To improve the utilization of heat, a heat pump (Figure 31) is used to extract heat from the low temperature return condensate and is used to heat the geothermally preheated hot water before sending to the boiler, thereby enhancing the utilization of heat, and improving the geothermal heat extraction.

The standard components of a heat pump system include condenser, compressor, evaporator, and an expansion valve. The heat is extracted from the low temperature heat source in evaporator, where refrigerant is evaporated, and the refrigerant condenses and rejects heat to produce high temperature water. The compressor efficiency is 75% (default value). Multiple refrigerant options were considered, and ammonia (NH_3) water source heat pump is considered based on our requirements. However, commercial NH_3 water source heat pumps can only produce hot water at a maximum temperature of 90°C. Aspen HYSYS simulations are repeated for both scenarios and PHE is redesigned for new conditions in EDR using a fouling resistance of 0.0007 ft^2-h-°F/BTU (Hernandez-Galan & Alberto Plauchu, 1989) for geothermal fluid, to account for geothermal fouling in the heat exchanger, and 0.0001 ft^2-h-°F/BTU (K. Rafferty, 1998) for the condensate fluid.

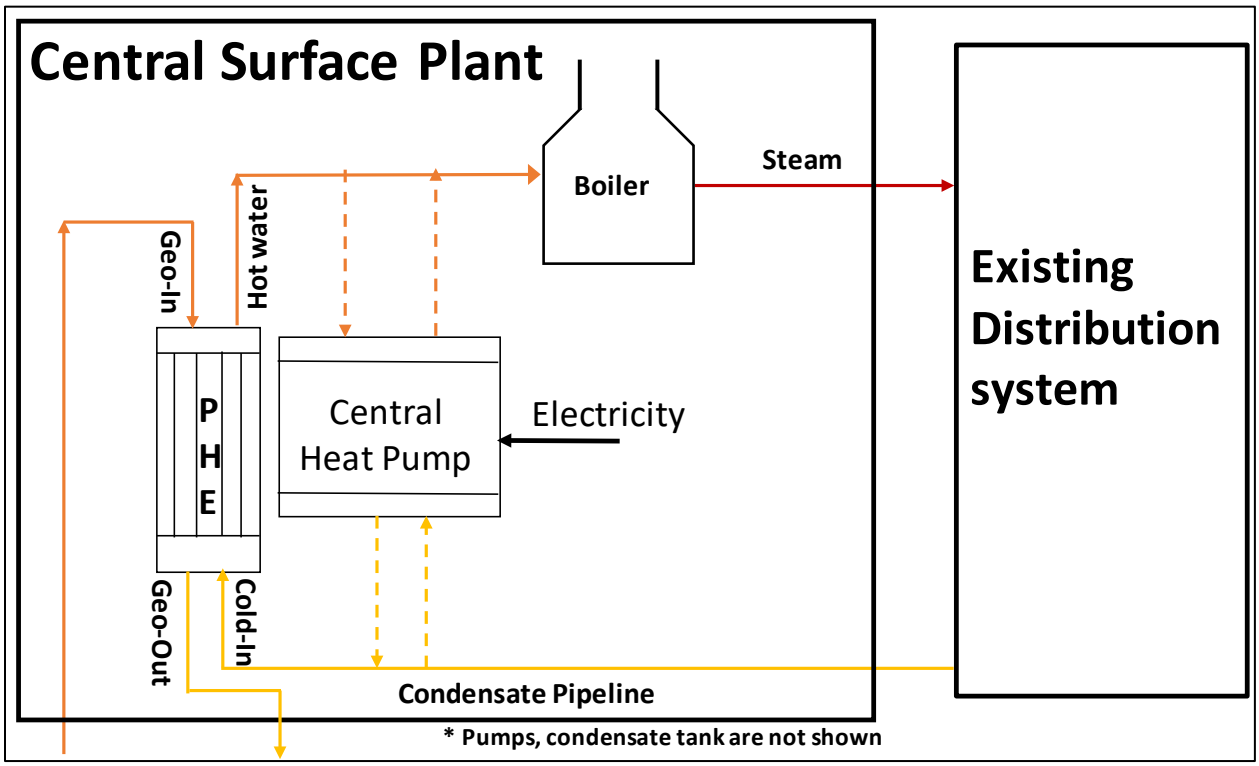

Figure 31: Schematic of the improved hybrid geothermal-natural gas system with heat pump to provide steam at required conditions for WVU campus.

Hot water-based system:
The supply temperature at the buildings is around 200°F (93.3°C) and since the geothermal production temperatures are around 187-210°F (86°C-99°F), a heat pump (max. temperature 90°C) is installed close to the buildings (instead of at the central surface plant) to further heat the geothermally heated water and extract the heat from the return condensate and thereby, improve the performance of the system. A "new pre-insulated piping system" will be considered to reduce the heat loss during distribution.

A schematic of the hot water-based system is shown in Figure 32 and is modeled using ChemCAD. A 5°C temperature drop is considered between the heat pump and the PHE to account for distribution losses and a temperature drop at the buildings and the distribution losses between buildings and heat pump is 17°C. PHE design is performed using the CCTHERM program. The number of heat pumps required is calculated based on the hot water flow rate and rating of the commercially available heat pump.

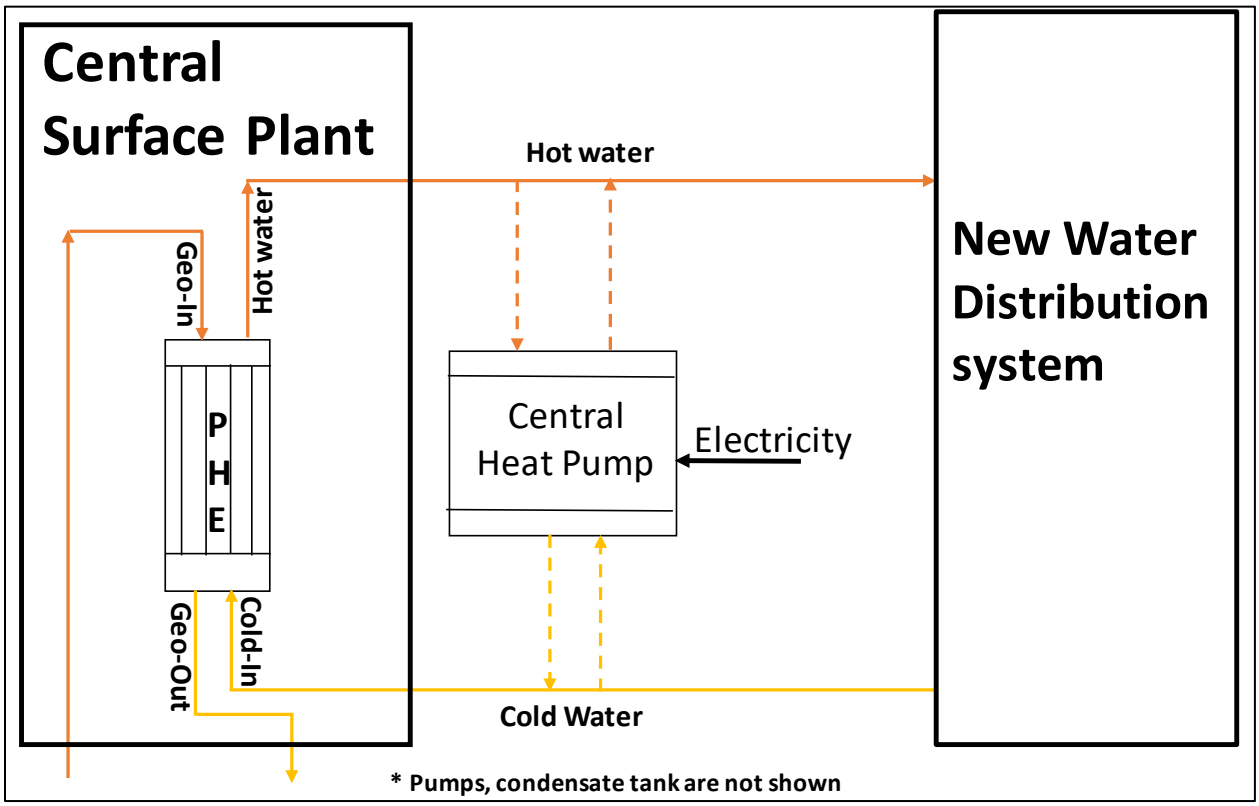

Figure 32: Schematic of the proposed geothermal hot water –based system with heat pump for WVU campus.

Task 4.3 – Quantify Minimized System Uncertainties &Development Risks

Economic analysis based on uncertainty quantification results from Task 3.3 are performed for steam-based system for scenario 1 (entire campus supply).

Objective 5.0 Maintain & Update Market Transformation Plan:

Task 5.1 – Maintain & Update Market Transformation Plan

The reservoir characteristics results from Objective 1, end-use load assessment in Objective 2, uncertainty analysis in Objective 3, and economic analysis in Objective 4, are unified and reported as appropriate through normal quarterly technical reports.

DISCUSSION OF RESULTS

Objective 1 – Characterize the Geothermal Site

Task 1.1: Perform Core Analysis and estimate temperatures

Detailed analyses of geophysical well logs, cores and thin sections has greatly increased our knowledge of the physical properties of the Tuscarora Sandstone, including information about permeability, porosity, fracture characteristics, formation thickness and facies architecture, and its potential to be a target reservoir for this geothermal energy project.

Task 1.2: Estimate Reservoir properties for modeling

Permeability and fracture porosity measurements display several general trends. As expected, the matrix (range of 0.6 to 11.3 mD, average of 2.94 mD) is less permeable than the fractures (range of 0.82 to 8587.7 mD, average of 264.8 mD). Some of the lower values recorded in the fracture measurements is likely due to those being filled fractures as opposed to open. Fracture porosities calculated from CT images are in general agreement with horizontal and vertical porosities measured by industry (Cities Services data); the fracture porosities range from 0% to 7.7% with an average of 2.2%. There is remaining porosity within the Tuscarora as well as a partially open fracture network, despite the presence of pressure solution features and the remobilization of silica in the previously thought low-permeability formation.

Depositional patterns and facies associations help characterize primary porosity and permeability in the Tuscarora. Three major types were identified:
a) as fining-upward, incised valley fill which was deposited as progressive infill of incised valleys during marine transgression and generally located in southern WV and seen in stacking patterns of Clay 513; our examination found that these incised valley deposits may be narrower and more localized than what is described in Castle and Byrnes (2005).
b) coarsening-upward, progradation shoreline, generally located in western portion of the study area with a potential unidentified uplift/source area supplying sediment; no core samples in WVGES collection record this stacking pattern; and
c) coarsening-upward, aggradation fluvial/estuarine deposited in relative proximity to source area; high rates of sedimentation kept pace with accommodation space created by basin subsidence that resulted in thick accumulations of sandstone with sandstone beds exhibiting the highest permeability for a given porosity; Preston-119 core records this stacking pattern, yet sediments are more characteristic of marine and estuarine deposition than of fluvial.

Our prediction is that this fracture network could provide pathways for removal and reinjection of formation fluids; however, observations of the Tuscarora in closer proximity to the proposed site is advised.

Porosity and permeability evaluation from well log analysis

The results from the porosity analysis for the Tuscarora sandstone in the three analyzed wells are shown in Table 10. A search of historic well documents for the USA #Q-1-119, revealed core plug porosity analyses which fit well with the interpretations of porosity from the electric log data. Maximum porosities values for the three wells were between about 9% to 20% and average porosity values ranged from about 2% to 4%.

Table 10: Tuscarora porosity analysis based on three wells. Year values represent the year the well was drilled. Porosity values are in decimal percent. USA #Q-1-119 has porosity from logs, and from core plugs.

Well	Location	Year	Min Φ (v/v)	Max Φ (v/v)	Avg Φ (v/v)	Porosity Logs	Notes
Messenger WTZ 3H	Wetzel Co. WV	2014	0.001	0.116	0.021	Density-Neutron-Sonic	
John Burley #1	Marshall Co. WV	1969	0.001	0.197	0.042	Density-Sonic	
USA #Q-1-119	Preston Co. WV	1964	0.001	0.109	0.018	Old-style Neutron	Generated Sonic from ILM and converted neutron to porosity
USA #Q-1-119	Preston Co. WV	1964	0.01	0.089	0.038	Core Plugs	8 core plugs, 7164-7425 ft. Avg. grain density 2.65 (well file)

Table 11 illustrates permeability data measured on the core plugs for the USA #Q-1-119 (left half of table) and completion details (right half of table.) Horizontal and vertical permeability was measured on eight core plugs. The column "Perf feet" represents the net perforated interval. "Perf mD-ft" represents the average horizontal permeability, measured in mD, from the core plugs multiplied by the net perforated interval, in feet (ft).

The relatively high-test rate of 16.3 million cubic feet of gas per day (16.3 MMCFGD), shown in Table 11, is not consistent with the low number calculated for Perf mD-ft, suggesting that fracture porosity and permeability are significant factors in this well's test rate. The bottom of the perforated interval (gross) corresponds to the top of the cored interval in the USA #Q-1-119; 7,165 ft-measured depth (md). Figure 33 is a core photo from a whole core taken from the bottom of the well test interval. The core photo reveals abundant fractures which would likely extend up into the perforated interval. Note the large vertical fracture on the right side of the photo, largely filled by mineralization and/or cataclastic material, but having visible, vugular porosity. This photo is consistent with this idea of enhanced fracture porosity and permeability for the Tuscarora in the USA #Q-1-119.

Table 11: Core permeability measurements and well test data.

USA #Q-1-119	Min mD	Max mD	Avg mD	Perf. Feet	Perf. md-ft	Test Rate	Notes
k_h (core plugs)	0	10.7	1.5625	23.8	37.2	16.3 MMCFGD	Not acidized, Not fractured. (well File)
kv (core plugs)	0	12.2	1.675				Perforated interval 7115-7165 ft-md (gross)

Figure 33: Whole cored interval taken from the bottom of the Tuscarora well test in the USA #Q-1-119. Core shows abundant fractures with visible porosity, likely extending up into the production-test interval.

Geothermal gradient evaluation

The temperature data derived for the five wells is shown in Table 12. The depth of the Tuscarora formation in the DDU study area is anticipated to fall within the range of depths shown in Table 12.

Table 12: Temperature data calculated for the Tuscarora formation in the five closest wells to the DDU study area. Depths to the Tuscarora are shown in subsea-true-vertical depth (SSTVD) and measured depth (MD). The GTG values are in degrees F/100 ft. The reservoir temperature calculated for the Tuscarora is shown in degrees F (TUSC_tmp_F) and in degrees C (TUSC_tmp_C).

Well Name	API	Distance from proposed site (miles)	SSTVD (ft)	MD (ft)	GTG_F (°F/100 ft)	TUSC_tmp_F (°F)	TUSC_tmp_C (°C)
Clifford J May #A-1	47061003070000	~8.0	-8583.0	10779.0	1.22	187.02	86.12
Finch #A-1	47049002440001	~16.0	-8695.5	10062.5	1.40	196.26	91.26
Greer Steel #11646	47061003320000	~8.5	-9086.1	11176.5	1.32	203.22	95.12
Huggins #11537	47077001690000	~13.0	-8833.0	10886.0	1.59	229.18	109.54
Walls #1	47077000860001	~14.0	-8623.0	10472.0	1.47	209.53	98.62

Task 1.3: Develop 3D Reservoir Model

The structure and depth relationship of four (LNG, TLLY, ORSK, and TUSC) of the six surfaces, Tuscarora being the deepest surface is shown in Figure 34. Apart from the shallowest surface, which had the most data points, the five deeper surfaces were gridded using the trend of the surface above it as a control, beginning with the shallowest (LNG surface). This conformable gridding methodology was key to developing a meaningful structural interpretation for the Tuscarora because there are so few Tuscarora data points (well penetrations).

Figure 35 shows a 2D structure map of the Tuscarora surface. Figure 36 is a cross-section through four wells, in a general NW-SE direction, including the proposed geothermal well and two Tuscarora penetrations. The cross section shows all six mapped surfaces. The location of the cross section is indicated by a green line on Figure 35. The cross-section displays, from left-to-right (NW-SE), a gently southeast dipping Tuscarora surface, into a syncline separating the proposed geothermal site from the South Burns Chapel Field (a NE-SW trending anticline).

Due to the lack of subsurface data in proximity to the site available for this study, the results of the structural modeling have a significant amount of uncertainty. While the final structural interpretation of the Tuscarora is reasonable, in the context of regional structural trends, it lacks the data density to precisely constrain the structure under the site of the geothermal project.

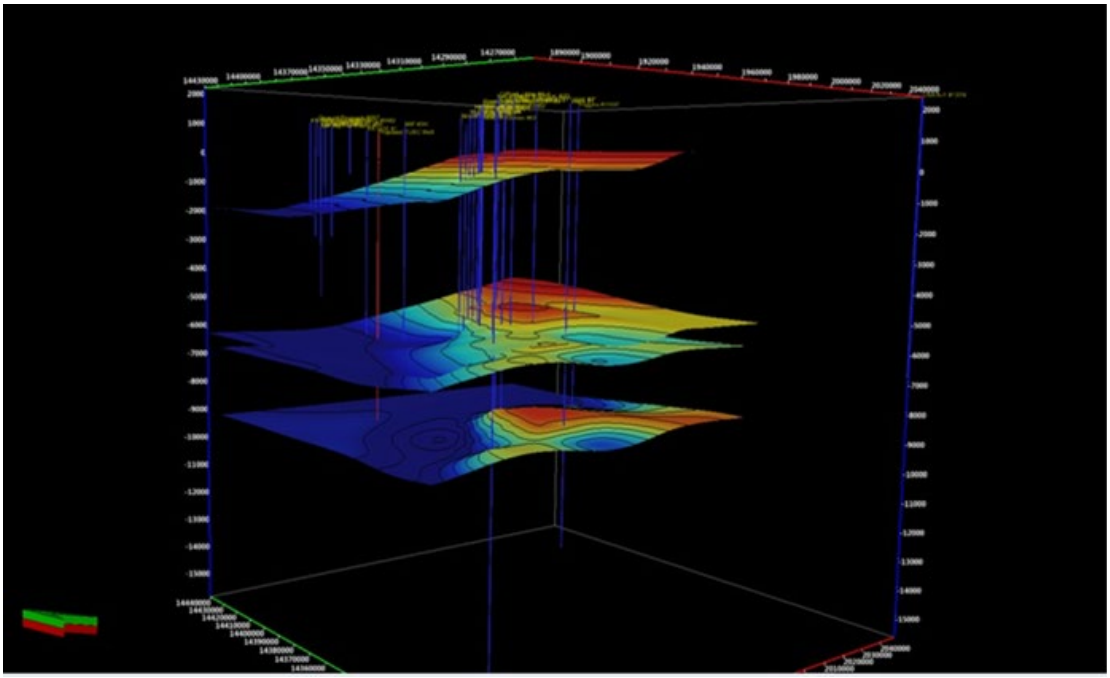

Figure 34: View of the 3D model, looking northeast. 4 of the 6 surfaces are shown. From shallowest to deepest: LNG, TLLY (Tully Ls.), ORSK (Oriskany Ss.), and TUSC (Tuscarora Ss.). Wells with tops are drawn with blue lines, the proposed geothermal well is represented with the red line. Depth axis runs from +2,000 ft. SSSTVD to -15,000 ft. SSTVD, labels at 1,000 ft. intervals. Map extents are approximately 30 mi^2 (78 km^2).

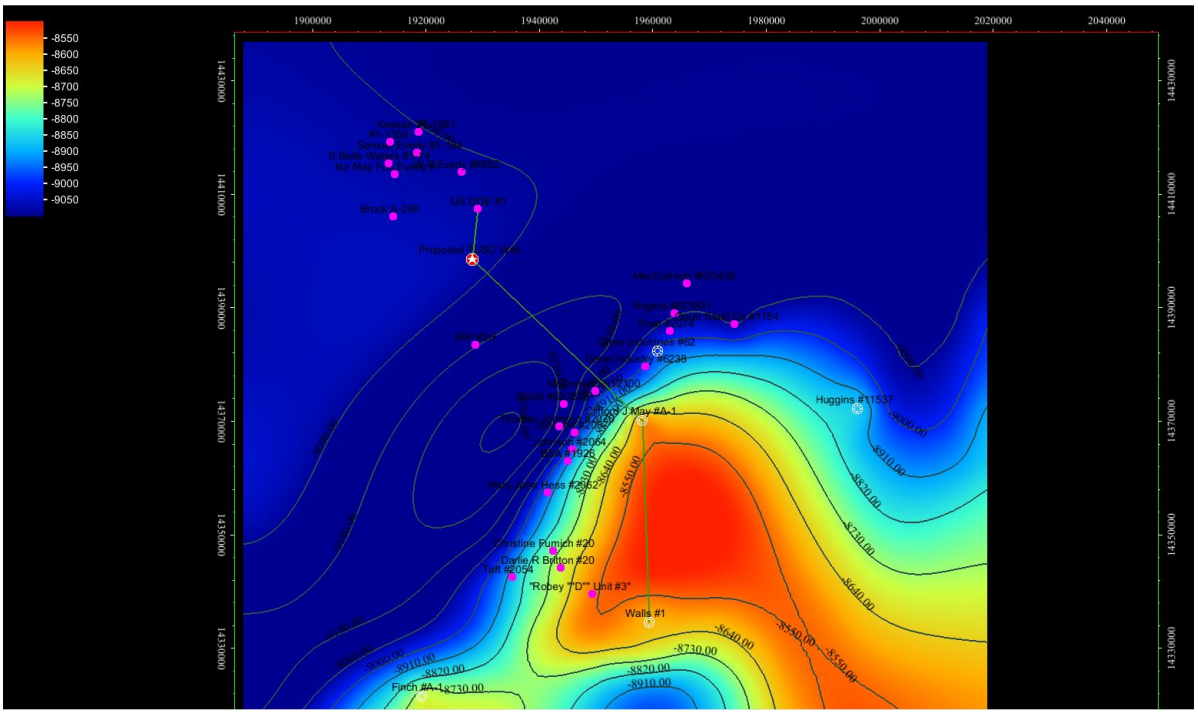

Figure 35: 2D structure map of the target Tuscarora Ss. Wells penetrating the Tuscarora are shown with white well symbols, the proposed geothermal well is shown with a white star on a red background. Contour interval is 90 ft. Axes are labeled every 20,000 ft (6.1 km). The top of the Tuscarora in the proposed geothermal well is at a depth of approximately -9,072 ft. SSTVD. Location of a line of cross section is shown with a green line.

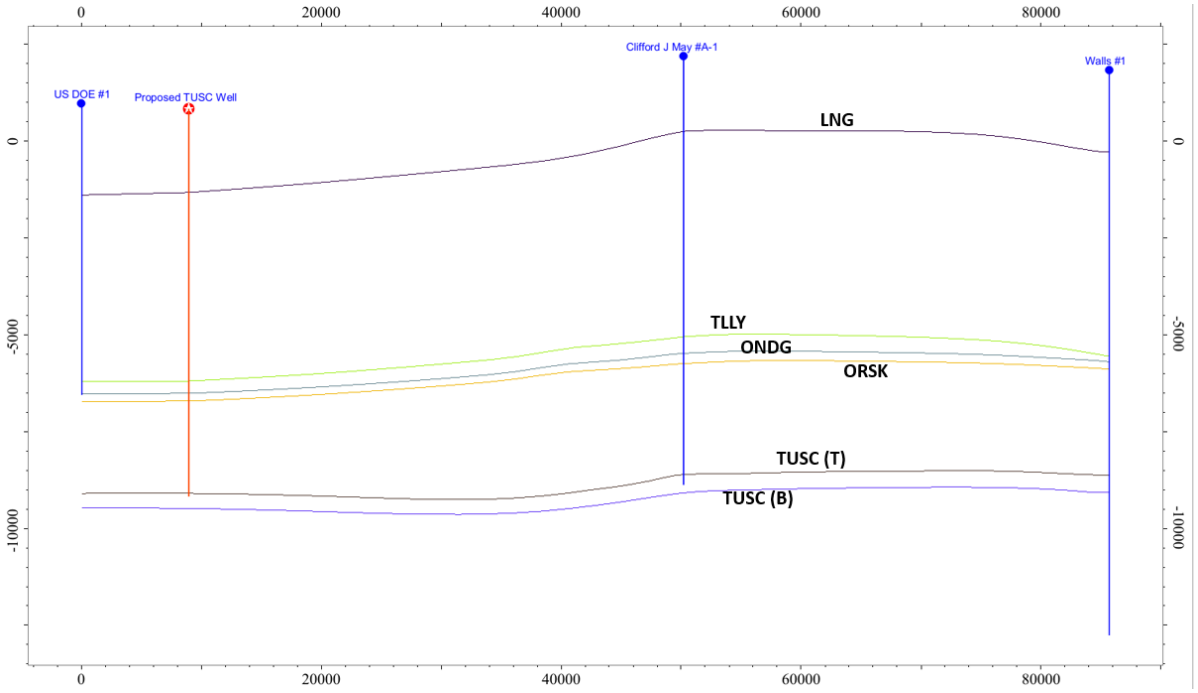

Figure 36: Line of cross section shown on Figure 35. Line of section runs generally NW-SE. The 6 mapped surfaces are labeled. The horizontal scale is 20,000 ft (6.1 km) between labeled tick marks. The vertical scale is 5,000 ft (1,524 m) between labeled tick marks.

Four proprietary 2D seismic lines were provided for review through industry contacts. Figure 13 indicates the location of the seismic lines (green, red, orange, and blue lines). A good well-tie (time to depth) could not be made due to the lack of availability of good quality well log data proximal to the seismic lines. Additionally, no wells penetrating the Tuscarora are located near the seismic data or have good quality sonic log data available. However, an evaluation of the blue seismic line, located about a mile to the northeast of the revised proposed DDU well location, reveals a very flat-to-very low angle, northwest dipping seismic reflectors in the proposed DDU well, like the interpretation shown in the cross section Figure 36. The cross section and seismic line are roughly parallel to one another. This provided credibility to the results from the structural modeling described previously.

A 3-D geological model (Figure 37) centered on the proposed well location was constructed with the 3-D GeoModeller GMS (Aquaveo, LLC in Provo, Utah; 2013) based on three geological studies: (1) through the Appalachian Basin (Ryder et. al., (2009), cross sections C-C', D–D' and E-E'; (2) on the Trenton-Black River reservoirs in West Virginia (Patchen, 2006); and (3) on the Tuscarora sandstone at the Morgantown region (McCleery et al., 2018).

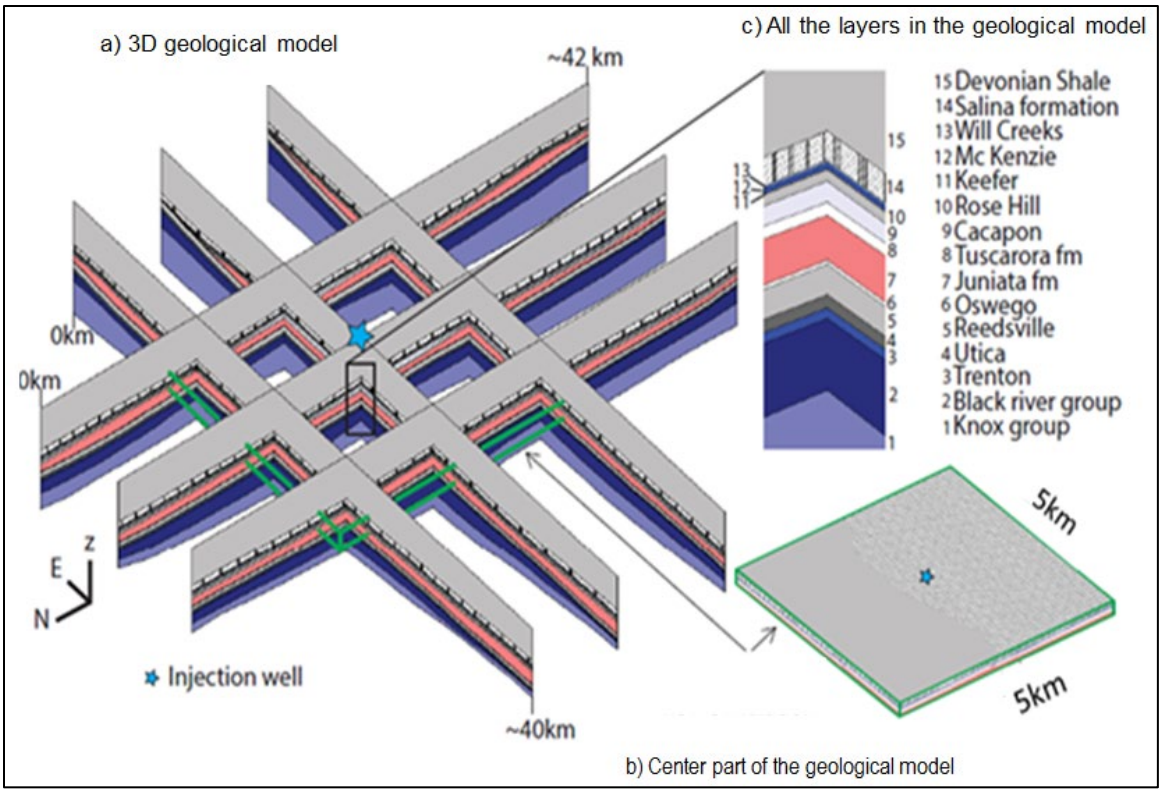

Figure 37: a) 3D geological model centered on the proposed well location as the basis for a 3-D numerical model; b) the horizontal domain used for the reservoir model, including all the geological layers shown in c). Notice the Tuscarora formation in c) is included in the reservoir model.

Only the Tuscarora formation is included in the numerical model for two reasons: (1) The permeabilities above and below the Tuscarora formation are so low that it is assumed there is no fluid flow into or out of the Tuscarora formation; and (2) the heat exchange at the top/bottom of

the Tuscarora formation can be modeled using a semi-analytical solution (Pruess et al., 1999). After some initial simulations using a model with a horizontal extent of 17 km in each direction, and a pair of vertical wells 500 m apart, it was determined the model domain can be reduced to 5 km x 5 km horizontally (horizontal domain is shown in Figure 1b), as the pressure change at 2.5 km away from the wells is negligible. The vertical extension of the model is between -2,600 m and -2,940 m, although the reservoir thickness is only about 100 m. This is due to the vertical depth variation of the target formation Tuscarora.

Objective 2 – Characterize Existing Infrastructure

Task 2.1: Characterize Energy demand

The steam temperature, pressure, and flow rate, and return condensate temperature and flow rate are recorded every month and are compared to the steam invoices generated by MEA. The steam usage for the entire campus for fiscal year of 2017-2018 is shown in Figure 38. Most of steam usage comes from the Medical Center (Health Sciences campus and Ruby Memorial Hospital), Ag. Science, and Downtown meter points. The peak usage was observed in the month of January, the minimum usage is in July, and the average flow rates for January and July are 15.2 kg/s and 6.4 kg/s, respectively. Therefore, a geothermal flow rates of 15.2 kg/s and 10.1 kg/s are used for further subsurface and surface modeling for scenario1 (entire WVU campus, all five distribution points) and Scenario 2 [Evansdale (Ag. Sciences and Towers), Health Sciences and Ruby Memorial Hospital (Med Center)], respectively.

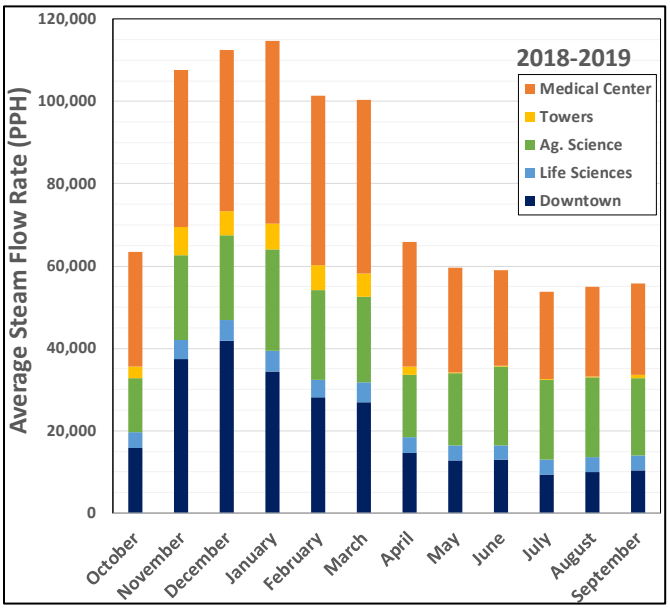

Figure 38: The average steam flow rate in pounds per hour (PPH) for 2018-2019.

Task 2.2: Perform Integration Assessment for Current District Heating System (DHS) Geothermal Site Location:

Site #2

Site #2 is commonly referred to as the "HSC" (Health Sciences Center) site. This location provides short-run connections to the WVU Hospitals Complex, a 690-bed academic medical center of roughly 500,000 square feet. Figure 39 provides a more detailed view of this site. This site has

existent high-pressure steam and natural gas lines parallel to Chestnut Ridge Road and connect to a retired steam plant. Right of ways/conduit for historical steam lines connect from this site to HSC, and the modern (in-use) steam line is in the vicinity. The recreation field in the upper left corner of this site, has no major utility lines buried in this space, and overall, the site provides good access to a major highway (WV Route 705 – 5-lanes adjacent) and adequate laydown room.

Site #3

Site #3 is commonly referred to as the "ST1" (Short Term Parking Area #1) site (Figure 40). This location would provide possible connections to the Evansdale Campus booster station, and would allow for support of the Engineering, Towers Dormitory, and possibly the HSC campuses. A 6" diameter gas line runs in the near vicinity. There is a significant distance to the trunk steam line, over 1,000 ft (+300 m). While it appears there are no major utilities that would interfere with construction, there is a stream and other storm water facilities in the area. The site provides good access to a major highway (WV Route 705 – 5-lanes adjacent) and adequate laydown room.

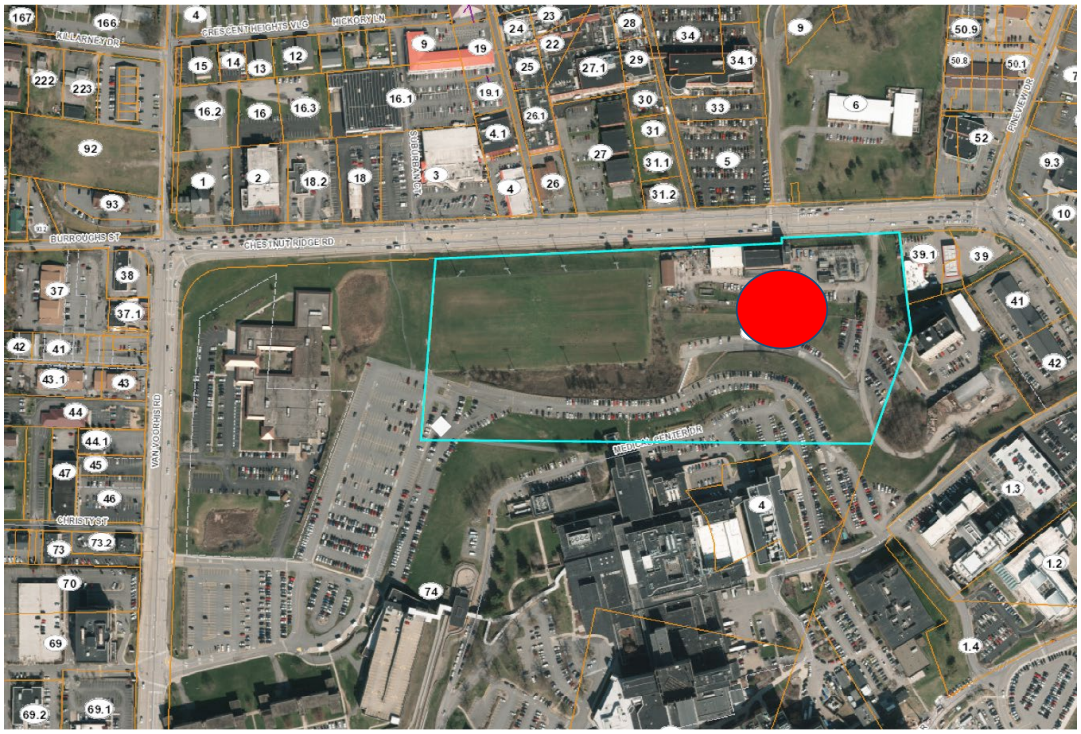

Figure 39: Aerial view of Site#2 (HSC) on Health Sciences campus.

Site #4

Site #4 is commonly referred to as the "Rec Field" site (Figure 40). This location would provide possible connections to the Evansdale Campus booster station, and would allow for support of the Engineering, Towers Dormitory, and possibly the HSC campuses. Both an 8" gas line and steam line are within 200 ft (60m) of the site, there would be some construction involved in crossing the PRT (WVU Personal Rapid Transit) infrastructure. The site has an extensive drainage system, no other major utilities would be impacted. Highway access is more challenging for Site #4; but infrastructure interconnections for steam and natural gas are simplified.

For all sites, WVU has clear chain of surface title, and for sites #3 and #4 clear chain of minerals title. For site #2, there is an old, non-producing gas well on site (circa 1946) that is owned by Monongalia County, and language appears to sever natural gas ownership for the utilization by this well. If other factors lead to this being a site of primary interest, WVU has a good relationship with leadership in Monongalia County, and it is expected that the proposed project would not negatively interfere with the gas rights/production of this well. The project team would seek an agreement to either transfer the mineral rights or acquire a written waiver from the county for execution of this project.

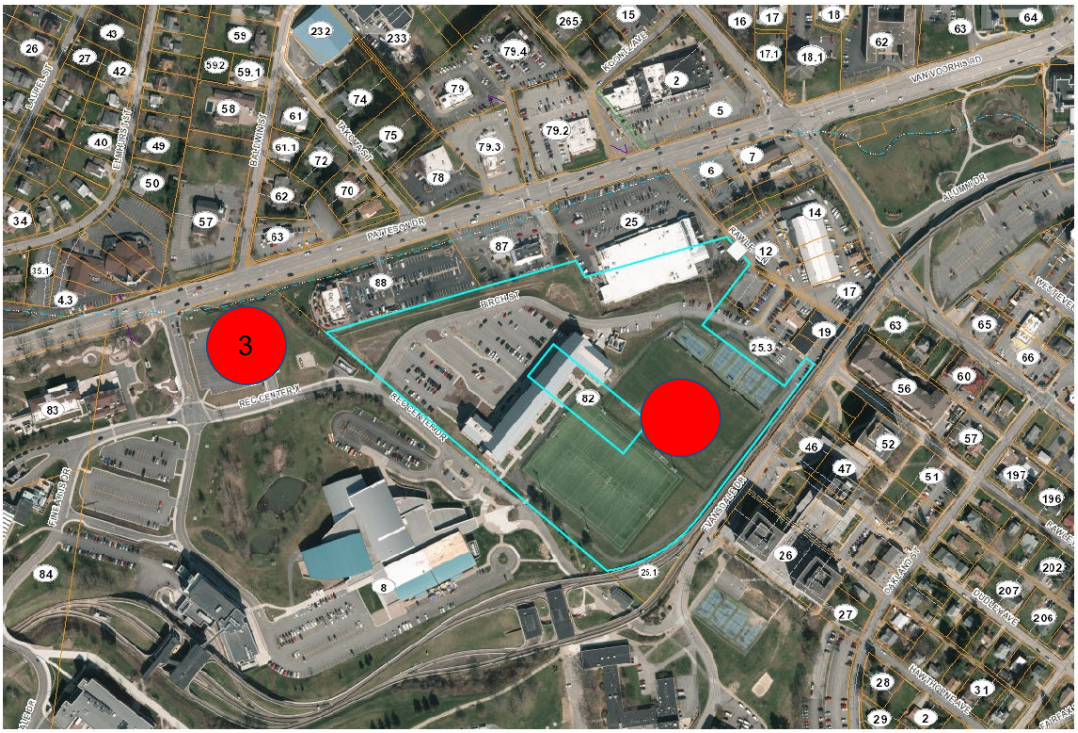

Figure 40: Aerial view of Site#3 (ST1) and Site#4 (Rec Field) on Evansdale campus.

Task 2.3 – Develop Base Case Surface Facility Design

Steam-based GDHC

The equipment design and costs are calculated using the flow rate in January (i.e., 15.2 kg/s for Scenario 1 and 10.1 kg/s for Scenario 2). The heat duty from PHE and boiler are given in Table 13 and the geothermal contribution to the proposed hybrid GDHC system was calculated using Equation [11]. The pumping power required for hot water and condensate pumps along with the pressure head is tabulated in Table 14.

$$\%Geo = \frac{Q_{Geo}}{Q_{Geo} + Q_{Boiler}} \qquad [11]$$

Table 13: The thermal contribution through different units to production of steam at required conditions for scenario 1 and 2.

Unit	Scenario 1	Scenario 2
PHE (Q_{Geo})	1.03 MW_{th}	0.71 MW_{th}
Boiler(Q_{Boiler})	40.33 MW_{th}	25.04 MW_{th}
Total (Q_{Geo}+Q_{boiler})	41.36 MWth	25.75 MWth
%Geo	2.49	2.76

Table 14: The pumping capacity of hot water pump at central location and return condensate pumps at distribution points D and H for scenario 1 and 2.

Pump Type	Mass Flow (kg/s)		Pressure Head (ft)		Power (kW)	
	Scenario 1	Scenario 2	Scenario 1	Scenario 2	Scenario 1	Scenario 2
Hot water Pump	15.20	10.10	595.9	397.30	33.84	14.99
D	4.13	-	296.6	-	4.578	-
H	7.98	3.70	82.39	75.32	2.349	0.9375

Plate heat exchanger design:
PHE is modeled with a temperature difference of 5°C. The PHE geometry obtained for both scenarios from rigorous heat exchanger design along with inlet and outlet temperatures for the geothermal fluid and condensate water is shown in Figure 41 and the parameters are detailed in Table 15.

The geothermal contribution is extremely low due to the high latent heat needed for conversion of hot water to steam. Therefore, a heat pump is used to improve heat utilization and thereby geothermal contribution. In addition, preliminary analysis for conversion of the existing steam-based system to a hot water-based system is also performed.

Table 15: PHE design details obtained through EDR for scenario 1 and 2.

Parameter	Scenario 1	Scenario 2
Heat Duty (kW)	1,031.0	707.5
PHE Area (m^2)	180.7	105.5
Number of Plates	199	117
Plate length (mm)	2023.22	2023.22
Plate width (mm)	495	495
Overall heat transfer coefficient U (W/m^2-K)	1353.4	1445.5
PHE Cost ($)	168,500	149,200

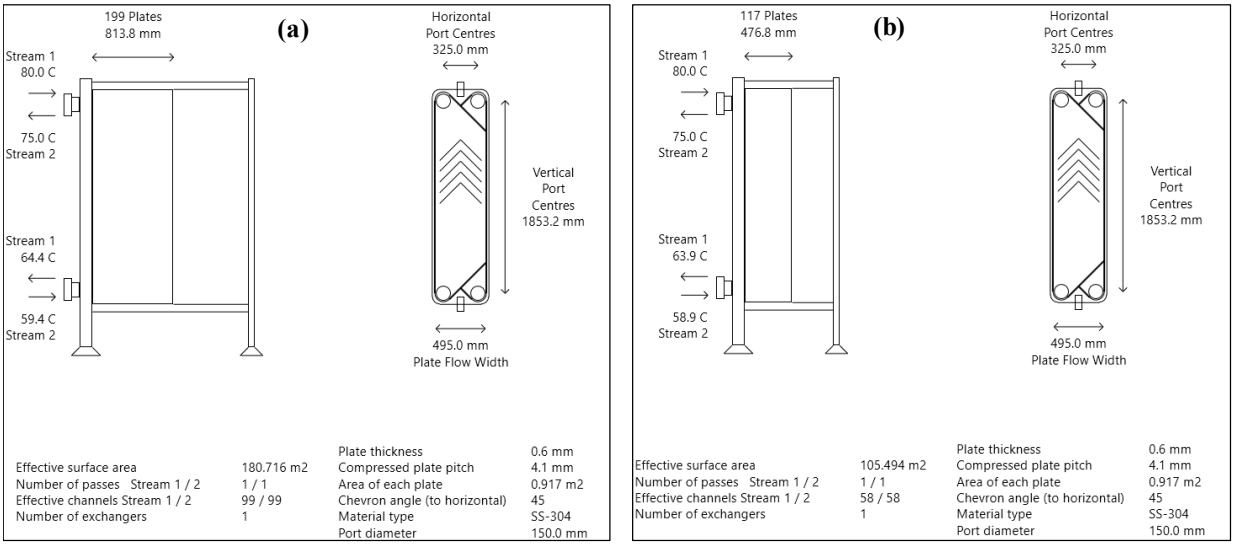

Figure 41: PHE geometry configuration for scenario 1 and 2.

Objective 3 – Create Subsurface Model and Design

Task 3.1: Simulate Base Case Vertical and Horizontal Well Configurations

Vertical well layout

Simulations with vertical injection and production wells on single-K and dual-K models are performed for different well spacing. The mesh around the injection well is locally radial with a wellbore radius of 0.1 m. Injection well flow rate is specified as 15 kg/s. The production well is specified using a deliverability model against a fixed bottom hole pressure (P_{wb}) of 18 MPa. The production fluid temperature with respect to time with a well distance of 500 m for all three permeability models described in Methods section under Task 3.1 is shown in Figure 42, and the thermal breakthrough happens after 20 years of operation, in all three models. There is hardly any difference in the two dual-K models; and the difference between the single-K model and the dual-K model is very minimal considering the time scale. Temperature distribution at different times as shown in Figure 43 also shows no visual difference among the models.

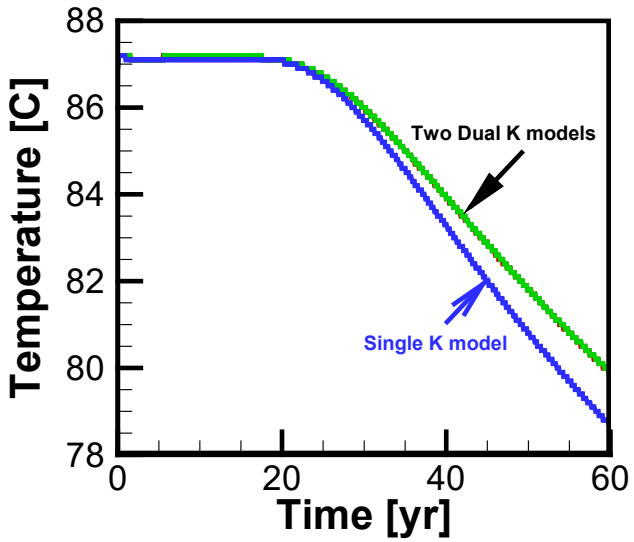

Figure 42: Thermal breakthrough curve at the production well for the case with two vertical wells, 500 m apart layout.

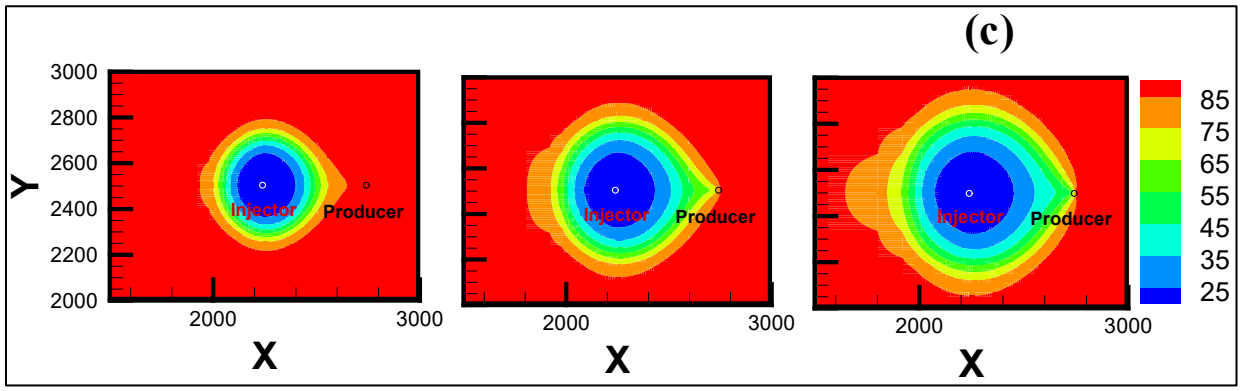

Figure 43: Temperature distribution on a XY plane at an elevation where injection/production wells are perforated at (a) 20 years; (b) 40 years; and (c) 60 years for the single-K model. Results from the two dual-K models are very similar, with no visual difference, therefore, are not shown here.

To examine why the temperatures in the formation and at the production wells are not sensitive to the model choice, the following investigation is performed:

1. In the dual-K model, the difference between matrix permeability and the fracture permeability is not significant (i.e., only about one order of magnitude). As a contrast, the fracture volume is only on the order of 0.015~0.15% of the entire rock mass. Therefore, matrix carries a significant amount of flow. Initial hypothesis is the heat transfer regime in the dual-K becomes convection dominates, which is like a single-K model, hence dual-K model had very similar results as single-K model. To test the hypothesis, the matrix permeability is decreased to 2.4e-20 m^2 for the dual-K model and examined the flow between matrix blocks and flow between matrix and fracture blocks. Any flow involving matrix blocks is negligible compared to the flow between fracture blocks. However, the thermal breakthrough curves (BTCs) are still very similar between the single-K model and dual-K models. This means the hypothesis of a heat transfer regime dominated by convection cannot explain the similarity in the BTC predictions from the three models.

2. From the previous investigation, it is clear the heat conduction is still very effective in the dual-K model. Re-examining the fracture parameter sets for both dual-K models, it is postulated the similar thermal breakthrough between single-K and dual-K model could be due to the fracture spacing choice in the two dual-K models. To investigate this phenomenon, the diffusive length with three matrix thermal conductivities is calculated and is shown in Table 16. The matrix thermal conductivity in our model is 2 W/(m °c), corresponding to a thermal penetration of 10 m at one year, which is much larger than the fracture spacing used in both of dual-K models (i.e., 0.3 m and 3 m). Hence, the dual-K model results are very similar given the time scale considered in our simulations.

Table 16: Thermal penetration for different thermal conductivities K_c

(W/ m °C)	K_c=1	K_c=2	K_c=3
Time (yr)	Length (m)	Length (m)	Length (m)
1	7.1	10.0	12.3
5	15.9	22.5	27.5
10	22.5	31.8	38.9
20	31.8	44.9	55.0
30	38.9	55.0	67.4
40	44.9	63.6	77.8
50	50.2	71.1	87.0
60	55.0	77.8	95.3

To further confirm our hypothesis, the temperature distributions for both fractures and matrix in dual-K model 2 are examined and it is observed there is no difference between the temperature in fracture elements and corresponding matrix elements.

Lastly, a new dual-K model (M_{test}) with fracture spacing of 100 m is built. The purpose of this model is not to represent the WVU geothermal site but to confirm our hypothesis and help to understand the model choice. The goal of using this large fracture spacing is to simulate large sparse fractures that can have dual-K effects, and to compare with our previous models to see if the choice of model has any effect on the results.

The temperature in fractures is much colder than in the matrix around the injection well after one year for the M_{test} model, as shown in Figure 44 (notice only the model domain around injection well, i.e., 100 m in each direction is shown). The temperature difference between matrix and fractures is seen only in early years, then it gradually diminishes as the heat in matrix blocks is exhausted, as shown in Figure 45. Figure 45 shows temperature in both continua after 20 years, 40 years and 60 years, with large difference observed at 20 years, which gradually reduced and almost diminished at the end of 60 years.

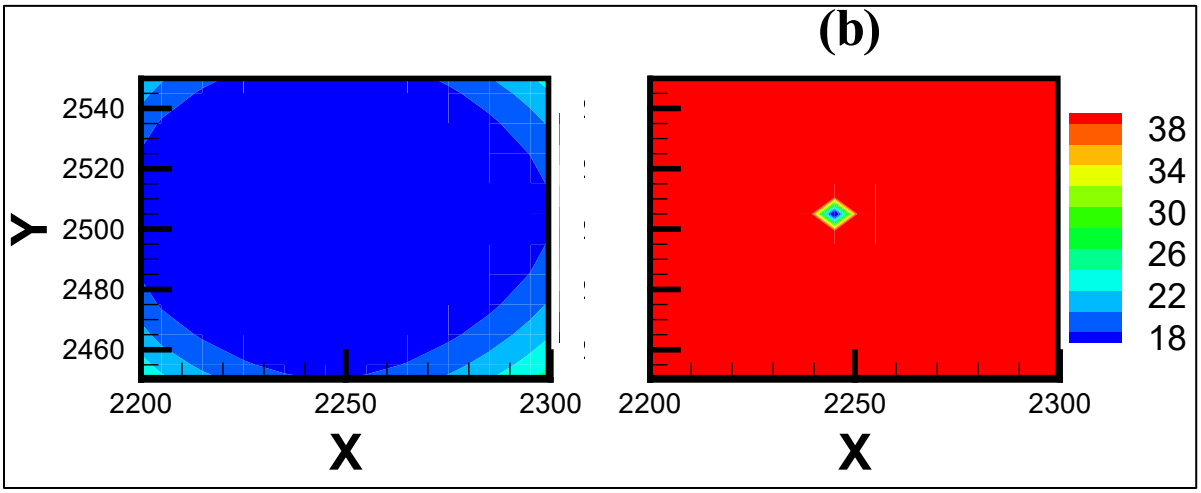

Figure 44: Temperature in (a) fracture and (b) matrix at the end of first year for the M_{test} model.

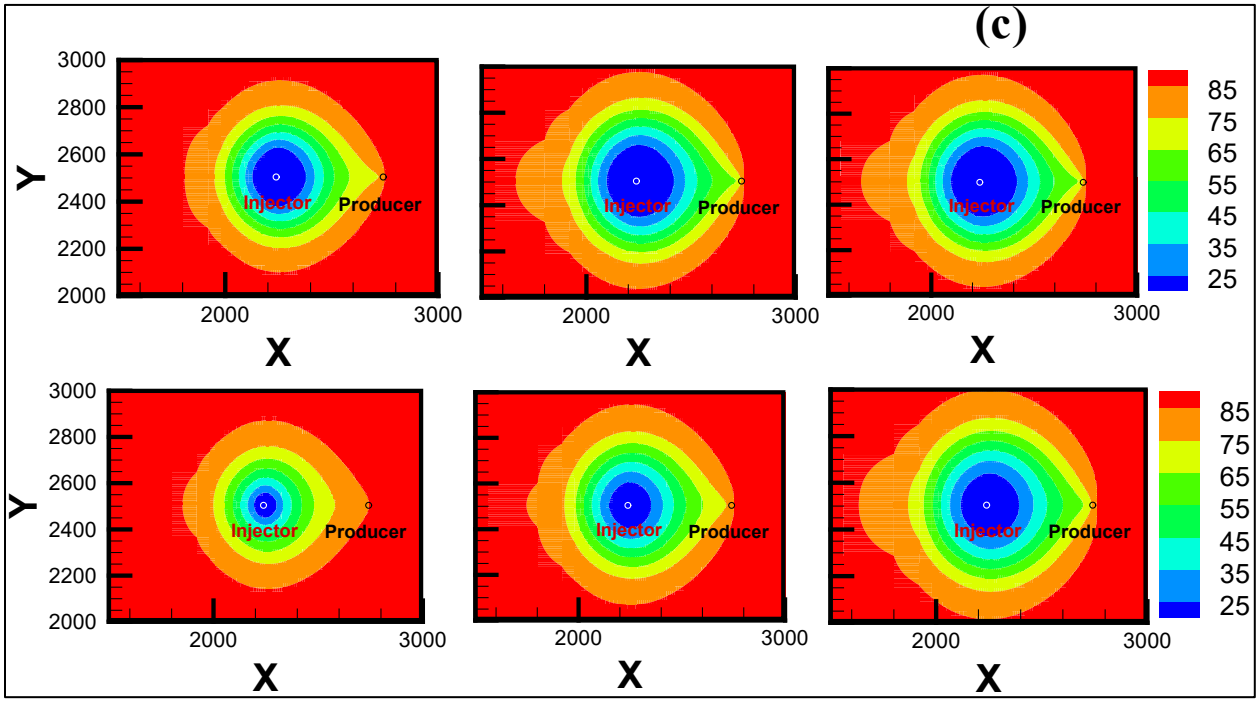

Figure 45: Temperature distribution at the end of (a) 20 years; (b) 40 years; and (c) 60 years for the M_{test} model. The upper panel shows temperature in fractures and lower panel shows temperature in matrix.

Summarizing the analysis, the large distance between the injection/production wells (in all potential scenarios) and radial geometry of an injected cold-water plume led to a large volume of matrix to be accessed by flow. Given the long residence time and relatively small fracture spacing even in a more conservative scenario, the heat exchange between fracture and matrix is dominated by the matrix volume rather than heat exchange area between fracture and matrix (Zhou, et. al., 2019); therefore, dual-K models behaved like the porous media.

The above analysis leads to the conclusion for this analysis, the thermal behavior at the production well is not sensitive to the model choices (i.e., between a single-K and a dual-K model, or two dual-K models with different parameters). Given the interest in the long–term thermal behavior, and that there are no known large fractures, we only considered single-K models for further analysis.

The above discussion focuses on the temperature results for the vertical well layout. Another factor to be considered for the feasibility analysis is the reservoir impedance (RI), which is defined in this study as the pressure difference between the injection and production wells divided by the flow rate. Relative to initial hydrostatic reservoir pressure, the pressure increase at the injection well is about 11~14 MPa; and the pressure drop at the production well is about 9 MPa, leading to a RI between 1.00~1.53 MPa•s/kg.

With increase in well spacing, the time for thermal breakthrough increased as shown in our paper submitted to 43rd Stanford Geothermal workshop (Garapati et al., 2019).

Horizontal well layout

Simulations for horizontal well configurations (lateral length = 300 m and 500 m) in the single continuum model were completed for various well spacing. The injection and production wells are represented using locally radial meshes with a wellbore radius of 0.1 m. Injection flow rate is 15 kg/s, while the production well is modeled as a sink with a constant pressure of 25 MPa. The production fluid temperature and reservoir impedance (RI) are compared with results from vertical well configurations in Figure 46 and Figure 47, respectively. With an increase in the horizontal lateral length, the time until thermal breakthrough increased, and the reservoir impedance decreased. For the well spacing evaluated, the reservoir impedance for horizontal wells is much less compared to vertical wells.

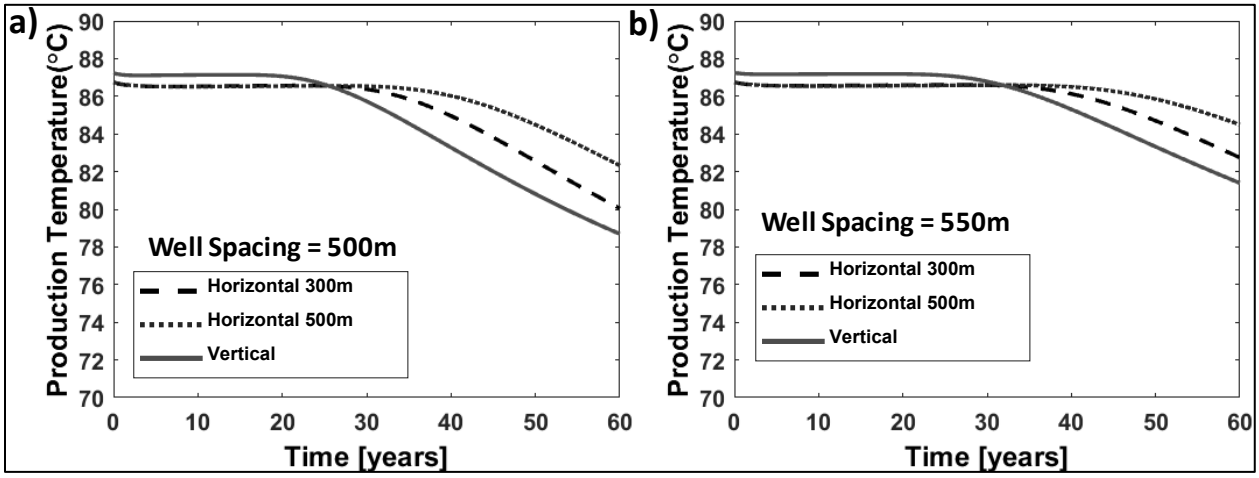

Figure 46: Produced fluid temperature over time for well spacing of 500 m (a) and 550 m (b) for vertical and horizontal well configurations.

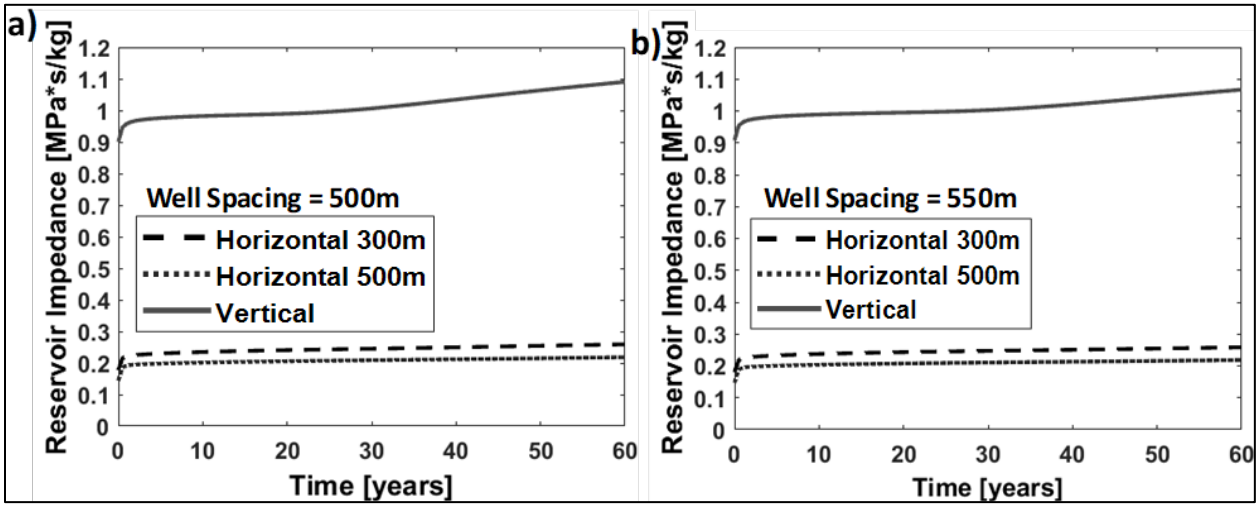

Figure 47: Reservoir Impedance over time for well spacing of 500 m (a) and 550 m (b) for vertical and horizontal well configurations.

The reservoir fluid swept between the two horizontal wells is much more than in the two vertical wells, as shown in Figure 48. As a result, thermal breakthrough happens much later (i.e., around 40 years as shown in Figure 53c homogeneous case, vs. 20 years for vertical wells for a well spacing of 500 m). At the end of the 60 years, the production temperature is still above 82ºC.

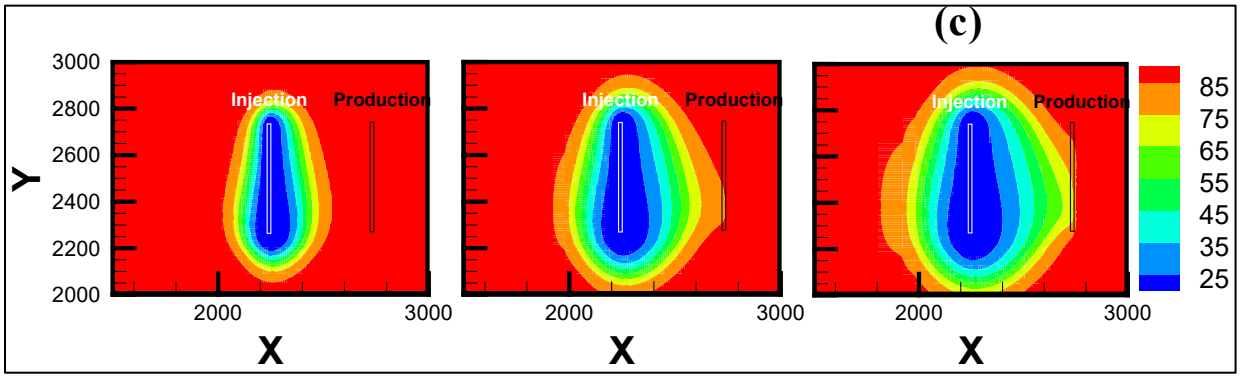

Figure 48: Temperature distribution on a XY plane at an elevation where injection/production wells are perforated at end of (a) 20 years; (b) 40 years; and (c) 60 years.

Effect of reinjection temperature and flow rates:

The effect of reinjection temperature and production flow rate was investigated using horizontal wells with a lateral length of 500 m. The reinjection temperature is varied between 15°C – 60°C for different flowrates (10 kg/s – 50kg/s). Comparison plots of production fluid temperature and reservoir impedance for different reinjection temperatures at different flowrates are shown in Figure 49 and Figure 50, respectively. From Figure 49, it is observed time for thermal breakthrough decreased with increase in production rate and remained constant for different reinjection temperatures. However, the rate of temperature drop decreased with increase in reinjection temperature. While reservoir impedance (Figure 50) remained constant for different flowrates and decreased slightly with increase in reinjection temperature.

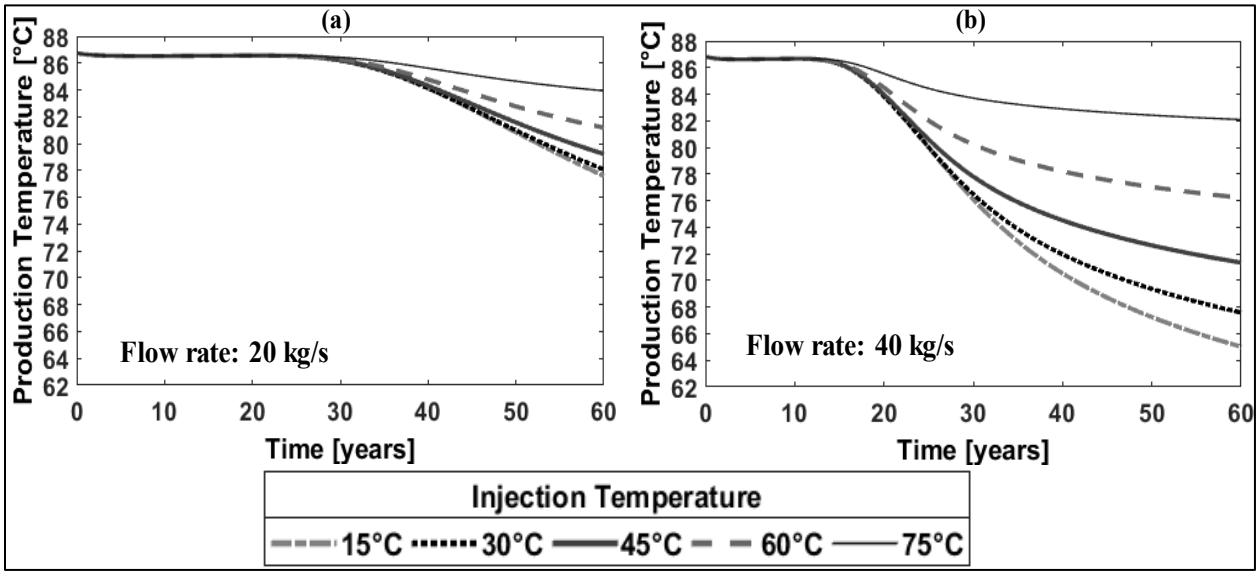

Figure 49: Production temperatures at varying injection temperatures for a horizontal well with lateral length of 500 m well at production flow rates of 20 kg/s (a) and 40 kg/s (b).

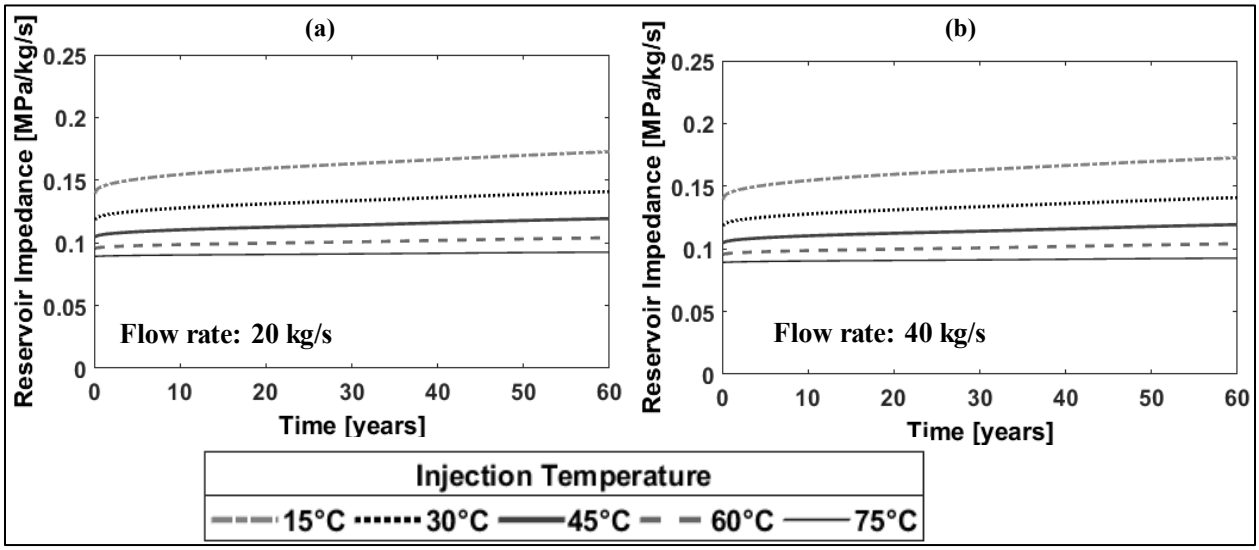

Figure 50: Reservoir Impedance at varying injection temperatures for a horizontal well with lateral length of 500 m well at production flow rates of 20 kg/s (a) and 40 kg/s (b).

Multiple well Configurations:

Simulations are also performed with two horizontal production wells and one horizontal injection well, all with a lateral length of 500 m. The production wells are equidistant from the injection well and the well distance considered is 460 m and 480 m. The production fluid temperature for two production wells configuration with single production wells for different flow rates at a reinjection temperature of 45°C are shown in Figure 51. The pressure change in the formation is shown in Figure 52 and pressure changes observed in the formation are higher in single production well compared to double production wells.

Task 3.2: Determine Well Configuration and Orientation/Economic Analysis

Compared to the vertical well placement, horizontal well placement clearly has an advantage: the thermal breakthrough is later due to the much larger sweep distance along the y-direction. The increase in pressure at the injection well bottom is much less (i.e., ~1 MPa vs. 14 MPa) in the vertical well placement scenario, and the pressure drawdown needed at the production well is ~ 1 MPa vs. 9 MPa in the vertical well placement scenario, thereby reducing the RI. The well-head levelized costs for both scenarios are calculated based on the parameters given in Table 5. The well-head LCOH for vertical and horizontal well configurations are $16.15/MMBTU and $18.13/MMBTU, respectively. The quotes for drilling costs are also obtained from Northeast Natural Energy (NNE) as 2.1 M$/well and 3.8M$/well for vertical and horizontal configuration respectively. The LCOH is reevaluated using these costs and LCOH is found to be $9.13/MMBTU and $9.59/MMBTU, for vertical and horizontal configuration, respectively. Since the horizontal well has less reservoir impedance values, which implies the pressure maintenance is much easier than in vertical well, and the economics are comparable, we considered horizontal well configuration for further analysis.

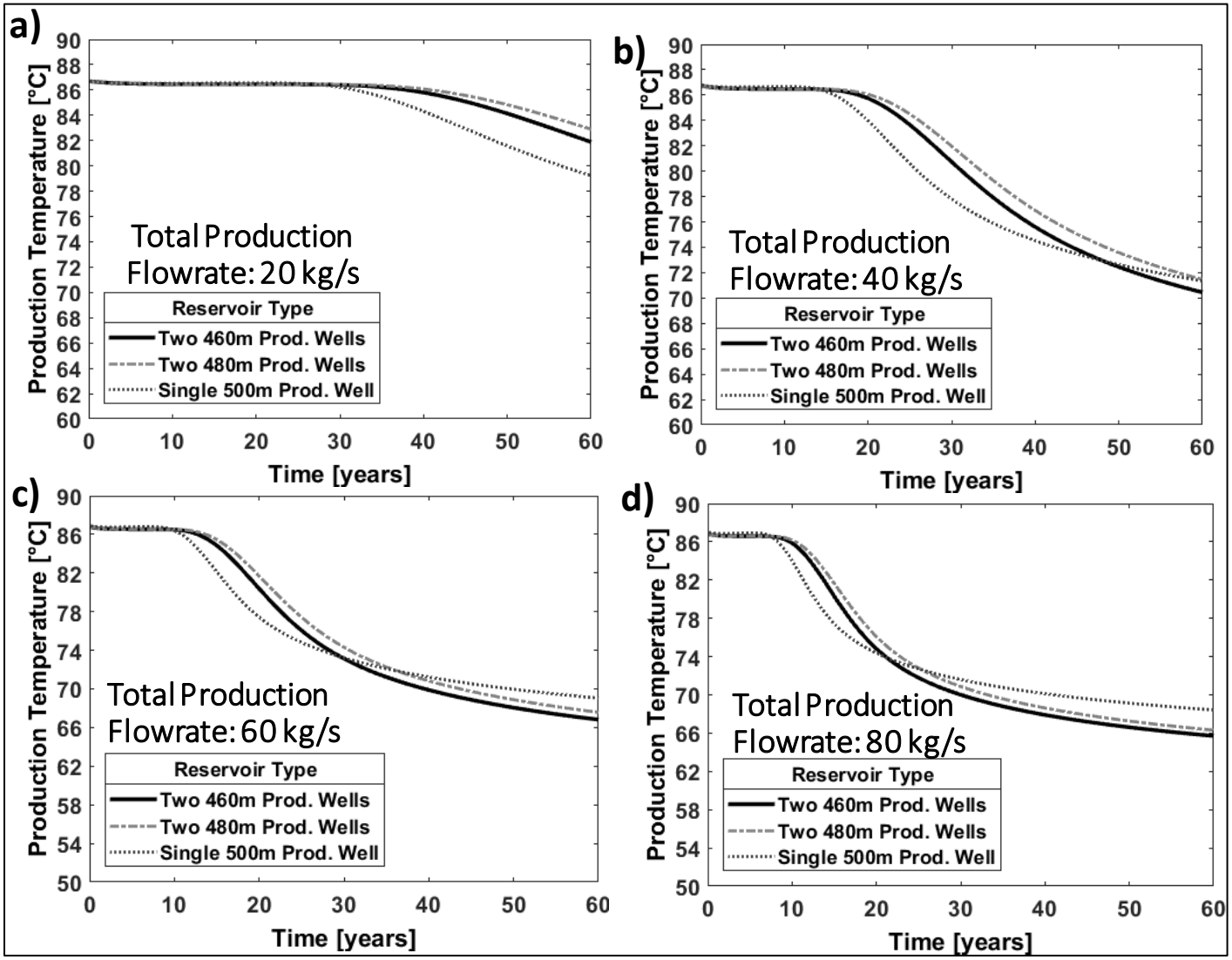

Figure 51: Production fluid temperature over time using single production and two production wells for different production flowrates at a reinjection temperature of 45°C.

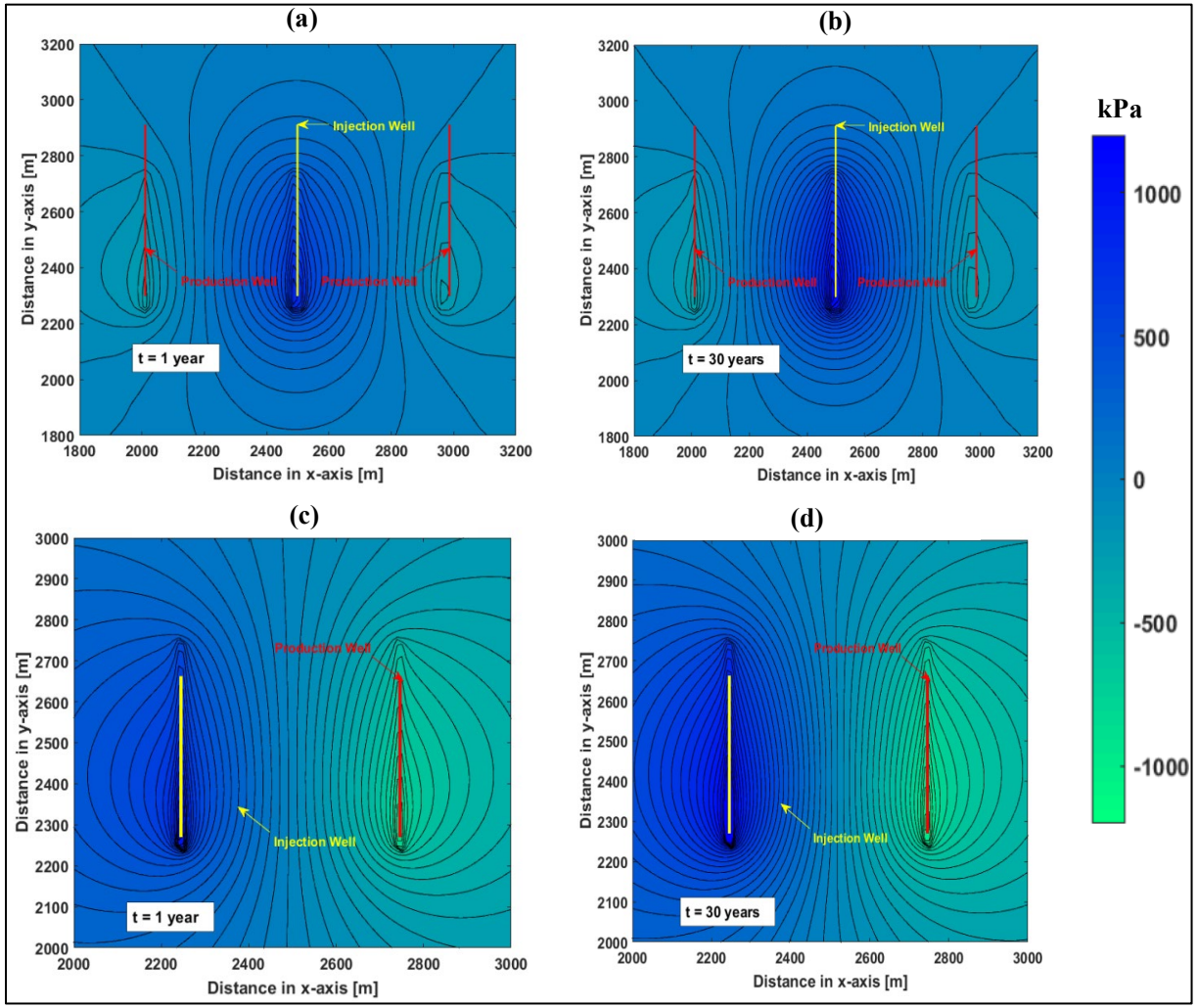

Figure 52: Change in reservoir pressure for double production wells and single production well at end of 1 year (a & c) and 30 years (b & d) at a total flowrate of 40 kg/s and reinjection temperature of 45°C.

Task 3.3: Perform Subsurface Uncertainty Analysis

In this section, impact of heterogeneity as well as uncertainty of reservoir parameters on the geothermal production is studied. The reservoir data set developed in Objective 1 is also used to calculate the risk factors for Tuscarora sandstone in Morgantown and update 2016/2017 Reservoir Risk Factor favorability and uncertainty maps made for the Geothermal Play Fairway Analysis of the Appalachian Basin project.

Impact of heterogeneity

Simulations are performed for both vertical and horizontal well configuration using heterogeneous field. Results showed the heterogeneity has a huge impact on thermal breakthrough curves and reservoir injectivity for both configurations.

Based on few forward simulations using heterogeneous field for vertical well placement, it is observed the smallest overpressure possible is around ~30 MPa, which is greater than hydrostatic pressure. Injecting with this overpressure could cause hydraulic fracture, which makes vertical well pairs a non-option. For this reason, and based on Task 3.2, horizontal well is optimum configuration and the rest of the investigation only focuses on horizontal wells.

For horizontal wells, the thermal breakthrough curve for a heterogeneous permeability field (shown in Figure 53a) is very different from the homogeneous field (model discussed in Task 3.1), as demonstrated in Figure 53c. The reason is heterogeneity could provide preferential flow paths, as shown in Figure 53b, therefore, leading to earlier thermal breakthrough (i.e., ~ 10 year for this permeability field, as compared to 40 years for a homogeneous case). Therefore, it is very important to incorporate heterogeneity in our UQ analysis.

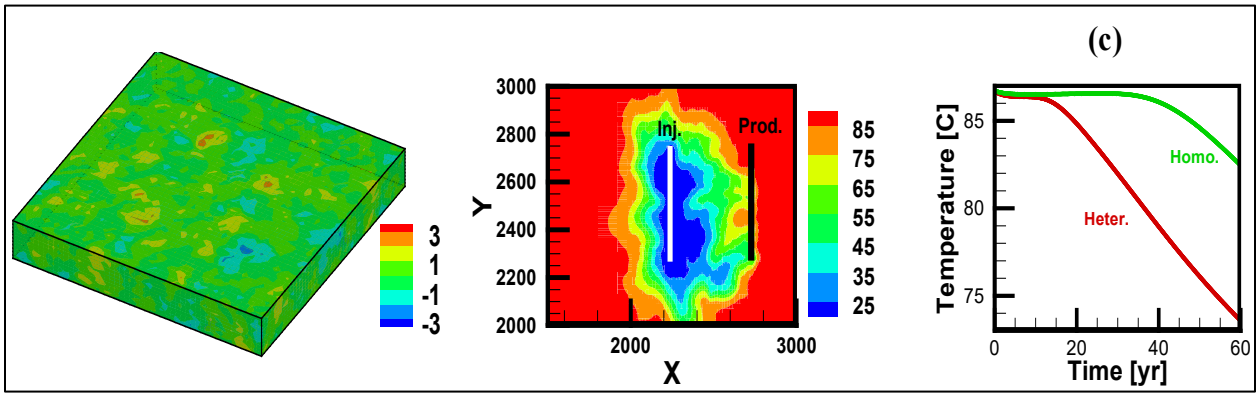

Figure 53: (a) one example of permeability field (the center 1 km x 1 km) generated using the Sequential Gaussian Simulation (SGS) model with a correlation length of 100 m; (b) the temperature distribution at 60 yr for the horizontal well layout from that permeability field; and (c) temperature BTC at the production well from this permeability field in red, as compared to the one from previous homogeneous permeability field in green.

Uncertainty Quantification analysis

Heterogeneous model is used for UQ analysis, as heterogeneity has substantial impact on reservoir performance. The uncertain parameters considered are average permeability (upper 2/3rd formation), porosity, rock compressibility and seven parameters from GSLIB including correlation length, sill, rotation angles and anisotropy ratios. The flow rate of 15 kg/s and reinjection temperature at 20°C is used in both analyses.

FOSM analysis

Table 17 shows the average contribution of each uncertainty parameter to reservoir performance (production temperature and pressure drop between injection and production wells). This result clearly showed that the correlation length contributes most (~ 2/5) to the uncertainty in both production temperature and pressure difference predictions. The other three parameters that have notable uncertainty contributions are permeability, porosity, and sill (representing variance). This result further confirms that heterogeneous features have a large impact on production temperature and RI.

Table 17: Uncertainty parameters used in FOSM and their average contribution to model prediction uncertainty.

Parameter	Production temperature	Injection/production pressure difference
Permeability	12.40	25.87
Porosity	11.48	9.79
Compressibility	3.03	2.45
Correlation length	43.14	42.95
Rotation angle 1	1.41	2.83
Rotation angle 2	6.91	2.12
Rotation angle 3	2.10	2.52
Anisotropy 1	0.93	0.6
Anisotropy 2	0.51	0.87
Sill	19.94	10.01

MC simulations

MC simulation results (Figure 50) show that the average thermal breakthrough happened around 15 years for a heterogeneous field, although it could happen as early as 8 years, or as late as 30 plus years. The injection/production pressure difference is about 4 MPa on average, ranging from 2~8 MPa. Further characterization of the four influential parameters identified by FOSM analysis (Table 17) would help reduce this uncertainty in the prediction.

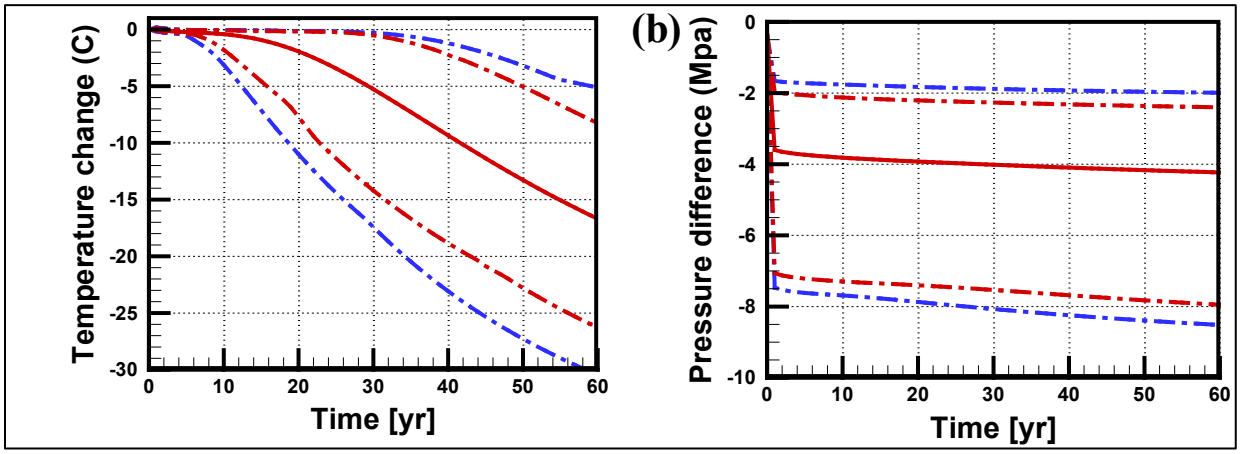

Figure 54: Statistical estimate of (a) production temperature change and (b) production/injection pressure difference from the MC simulations. Red solid line indicates the mean prediction, red dashed lines indicate 95 and 5 percentiles and dashed blues lines are upper/lower bounds.

Uncertainty due to initial reservoir temperature

All previous simulations were performed using a geothermal gradient of 26°C/km (Base case). To understand how initial reservoir temperature, affect production temperature decline, two additional scenarios using a higher geothermal gradient (HighG) of 30°C/km, and a lower geothermal gradient (LowG) of 22°C/km were simulated with a production rate of 15 kg/s and reinjection temperature of 20°C. As shown in Figure 55, the thermal breakthrough curves are more or less shifted up and down, in parallel for the three cases, although the final temperature drop (at 60 year) is a little more in the HighG case and a little less in the LowG case. These results demonstrate that once the initial reservoir temperature is obtained after wells are drilled in the field, if the actual reservoir temperature is not too off from the scenarios considered in this study, the thermal predictions can be shifted accordingly.

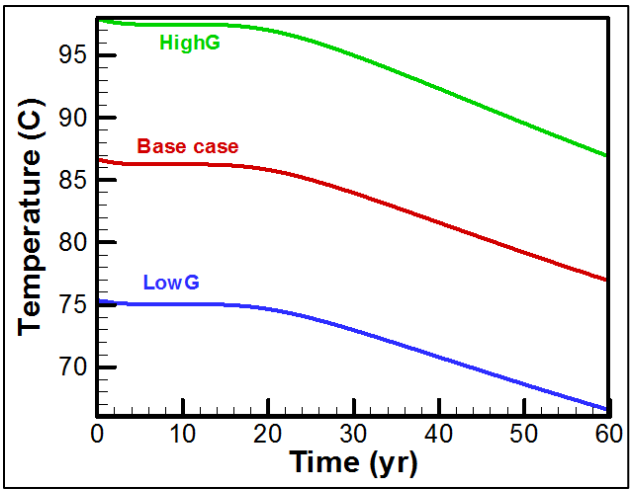

Figure 55: Thermal breakthrough curves for a heterogeneous model with two horizontal well layouts, using a high geothermal gradient 30°C/km (HighG), base case geothermal gradient 26°C/km, and a low geothermal gradient 22°C/km (LowG).

Reservoir risk factor favorability for the Tuscarora sandstone near Morgantown, WV.
Matrix reservoir productivity

The distribution of Monte Carlo replicates for the RPI_w is provided in Figure 56. 9.2% of the RPI_w estimates are in the "Favorable" range, and the rest are in the "Okay" range, where these ranges are defined in the GPFA-AB project. The RPI_w metric provides a low-end estimate of reservoir productivity because only matrix permeability is considered in this analysis. An alternative measure of favorability for matrix rock permeability using the RFC rates the Tuscarora as "Favorable" using the GPFA-AB ranking scheme (Figure 57). Only 1.4% of the replicates are "Okay", and about 0.5% of the replicates are "Very Favorable."

Thus, there is a difference in favorability using the different reservoir productivity metrics. For the same permeability and thickness, the RFC provides a more favorable outlook on reservoir productivity than the RPI_w metric, using the favorability threshold assumptions in Camp et al. (2018). Overall, considering a worst-case permeability scenario in which no fractures are encountered, the Tuscarora near Morgantown is estimated to have favorable or okay productivity, on average, and there is a small chance that productivity will be very favorable.

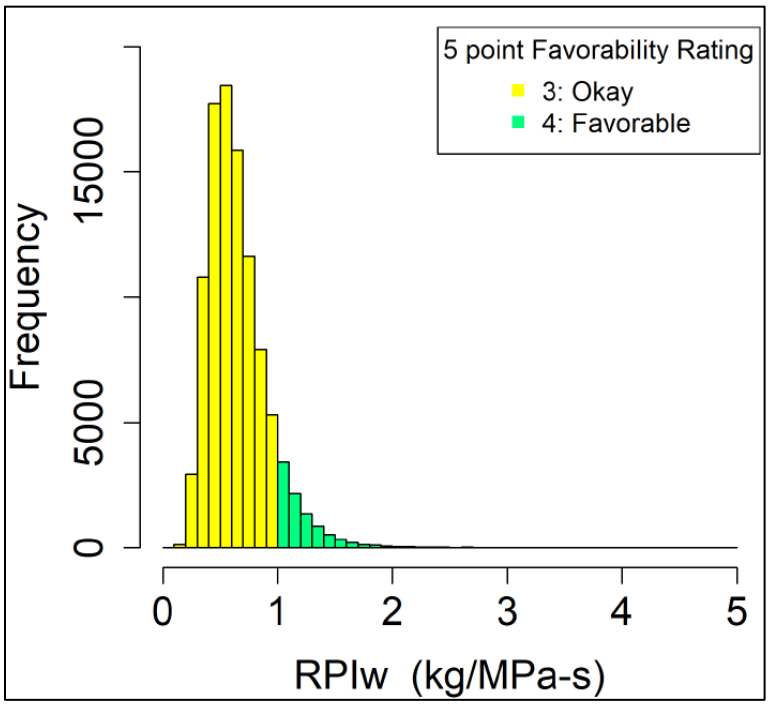

Figure 56: Reservoir Productivity Index for water (RPI_w) for matrix permeability only based on 100,000 Monte Carlo replicates of uncertain reservoir thickness, effective water permeability, and dynamic viscosity. The distribution is colored by the GPFA-AB favorability scale: 3: 0.1 kg/MPA-s – 1 kg/MPA-s, 4: 1 kg/MPA-s – 10 kg/MPA-s.

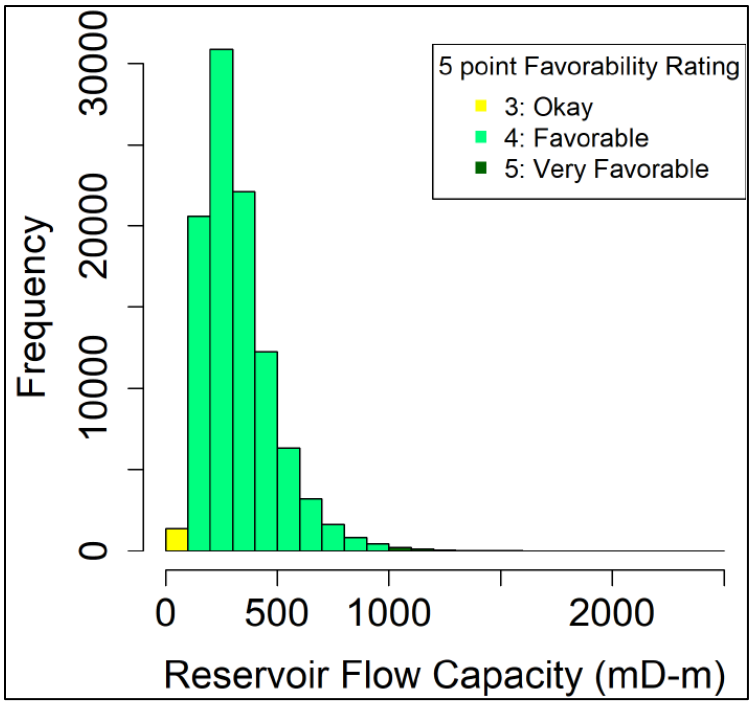

Figure 57: Reservoir flow capacity (RFC) for matrix permeability only based on 100,000 Monte Carlo replicates of uncertain reservoir thickness and effective water permeability. The distribution is colored by the GPFA-AB favorability scale: 3: 10 mD-m – 100 mD-m, 4: 100 mD-m – 1,000 mD-m, 5: >1,000 mD-m.

Fracture-based Reservoir Productivity

The distribution of Monte Carlo replicates for the RFC using the bootstrapped mean effective water permeability is provided in Figure 58. All Monte Carlo replicates are in the "Very Favorable" range.

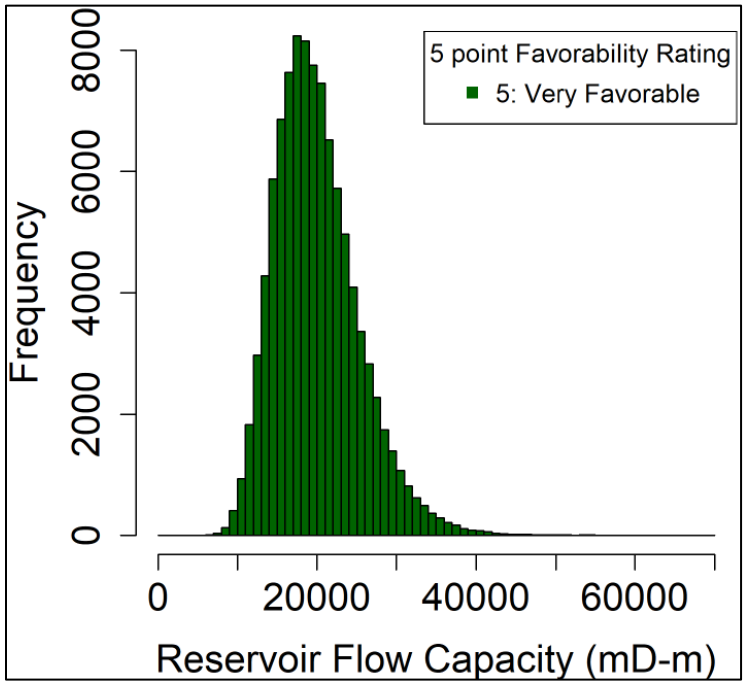

Figure 58: Reservoir flow capacity (RFC) for the Tuscarora based on 100,000 Monte Carlo replicates of uncertain reservoir thickness and mean effective water permeability. The distribution is colored by the GPFA-AB favorability scale. All these values fall within the >1,000 mD-m "Very Favorable" ranking.

Impact of well separation distance and reservoir thickness on the RPIw metric

Well separations of 400 m, 600 m, 800 m, and 1,000 m were evaluated to test the impact of well separation on the RPI_w metric. Two mean reservoir thicknesses were also evaluated: the expected thickness of 122 m, and the 83 m thickness observed for the Preston 119 well. The effect of both variables on the RPI_w metric is provided in Figure 59, which shows empirical CDFs of the RPI_w.

As expected, a thinner reservoir provides a smaller RPI_w, and shorter well spacing provides a larger RPI_w (Equation 2). The impact of well spacing is minimal for the values used in this analysis. For a 122 m thick reservoir, the percentage of replicates above 1 kg/MPa-s is about 9% for 1,000 m spacing, and about 14.5% for 400 m well spacing. The impact of mean reservoir thickness for the values selected is of greater importance than the well spacing. For a 1,000 m well spacing, the percentage of replicates above 1 kg/MPa-s is about 9% for a 122 m mean reservoir thickness, and about 1% for an 83 m mean reservoir thickness.

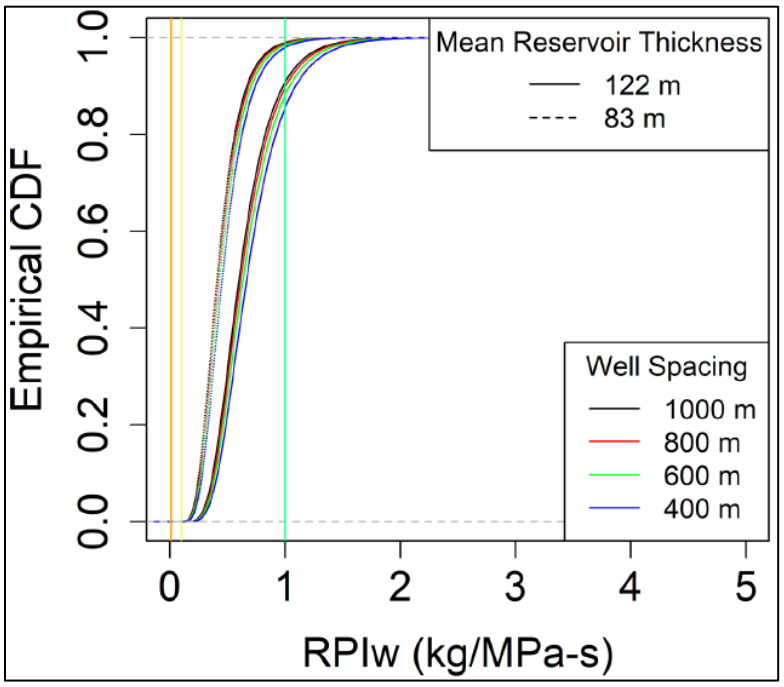

Figure 59: Empirical CDFs of the RPIw metric for matrix rock for various mean reservoir thicknesses and well spacings. Relevant favorability thresholds are shown as vertical lines. From left to right, they represent start of "unfavorable" region (orange), start of "okay" region (yellow), and start of "favorable" region (light green).

Impact of reservoir thickness and permeability uncertainty index for the RFC metric

Two uncertainty indices for the bootstrapped distribution of mean effective water permeability were evaluated for their impact of the resulting RFC distribution. The two mean reservoir thicknesses used in Figure 59 were also evaluated. Figure 60 provides the RFC metric as a function of the uncertainty index and mean reservoir thickness. Considering only the impact on favorability, it does not matter which mean reservoir thickness or permeability uncertainty is selected because all the Monte Carlo replicates are in the "very favorable" region.

Updated reservoir risk factor favorability and uncertainty maps

For matrix-dominated Tuscarora permeability, analysis of the reservoir productivity using the RPI_w metric shows the Tuscarora near Morgantown is okay, on average, and might be favorable (Figure 56). Figure 61 and Figure 62 provide the reservoir risk factor map and uncertainty map for the Appalachian Basin with the Morgantown Tuscarora added. The uncertainty is the coefficient of variation (CV) for the real-space data, not the uncertainty in favorability. For fracture-based Tuscarora permeability, analysis of the reservoir productivity using the RFC metric shows that Tuscarora near Morgantown is very favorable with no uncertainty in the favorability value (Figure 58). In the context of the Appalachian Basin, the Tuscarora reservoir near Morgantown is one of few very favorable reservoirs with low uncertainty (Figure 63 and Figure 64).

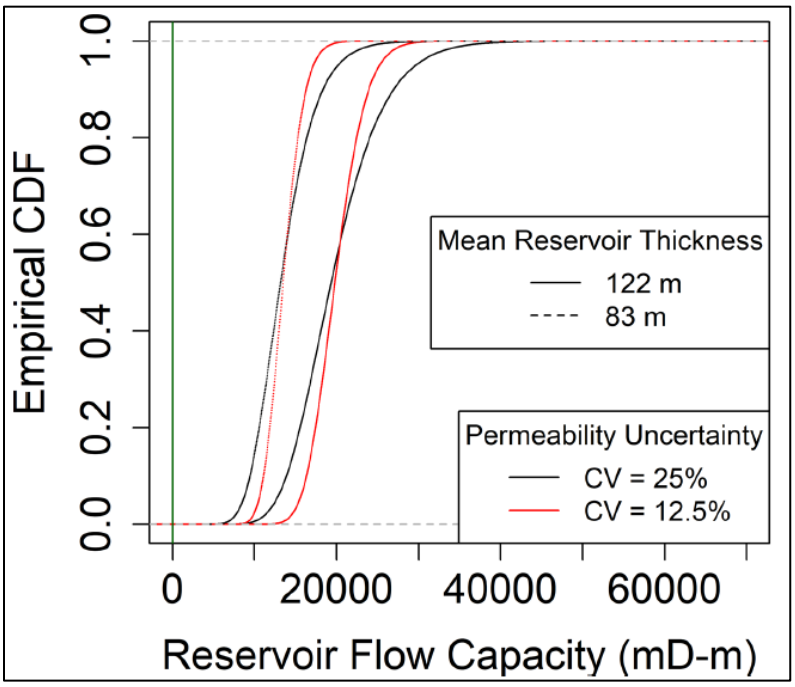

Figure 60: Empirical CDFs of the RFC metric for various mean reservoir thicknesses and permeability uncertainties. The "very favorable" threshold is shown as a dark green vertical line.

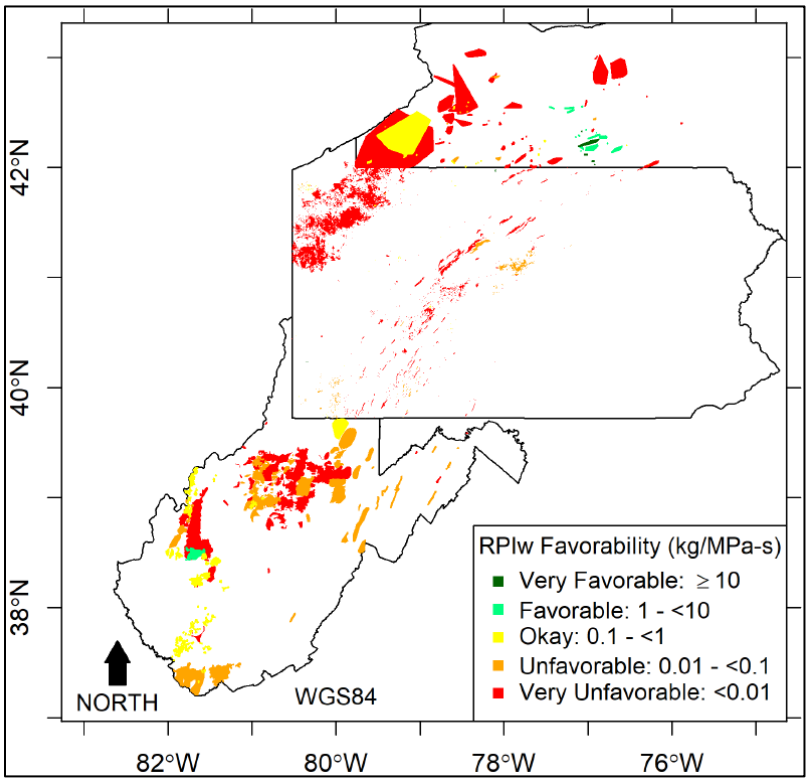

Figure 61: Map of the mean RPI_w for reservoirs identified in the GPFA-AB Reservoir Risk Factor Analysis, with the Morgantown Tuscarora added. Reservoirs are colored by their favorability. More favorable reservoirs are plotted on top of less favorable reservoirs. Locations without reservoirs in the database are shown as white.

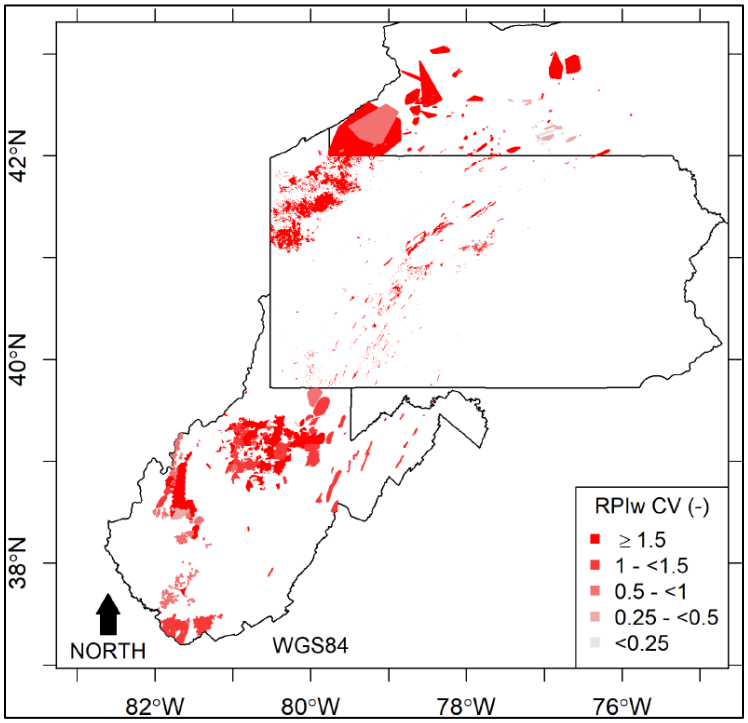

Figure 62: Map of the CV for RPIw for reservoirs identified in the GPFA-AB Reservoir Risk Factor Analysis, with the Morgantown Tuscarora added. More favorable reservoirs in Figure 61 are plotted on top of less favorable reservoirs.

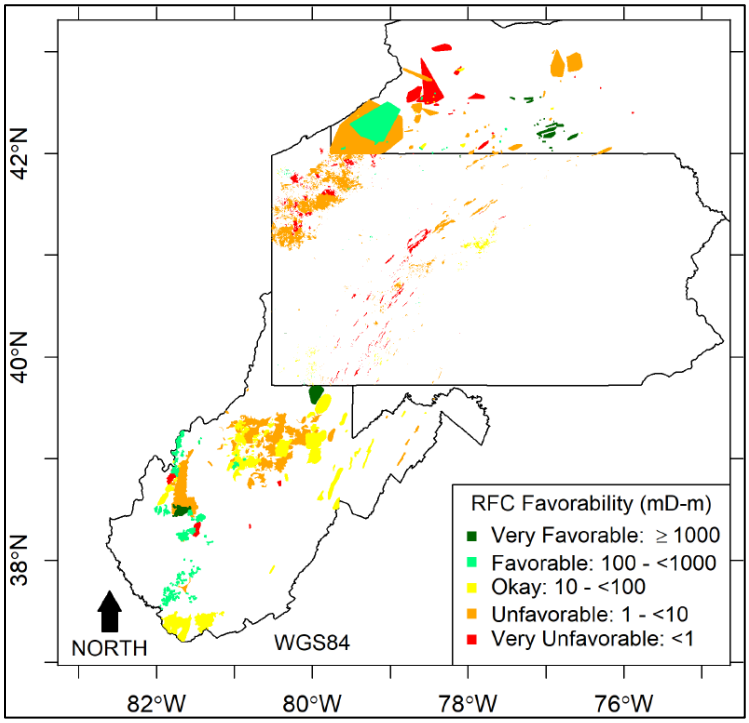

Figure 63: Map of the mean RFC for reservoirs identified in the GPFA-AB Reservoir Risk Factor Analysis, with the Morgantown Tuscarora added. Reservoirs are colored by their favorability. More favorable reservoirs are plotted on top of less favorable reservoirs.

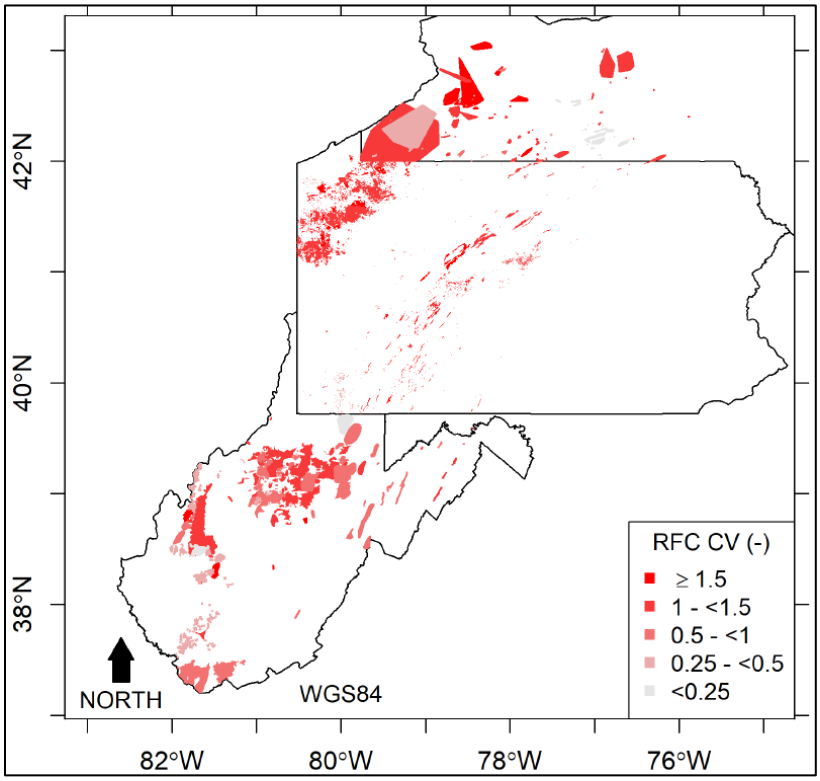

Figure 64: Map of the CV for RFC for reservoirs identified in the GPFA-AB Reservoir Risk Factor Analysis, with the Morgantown Tuscarora added. More favorable reservoirs in Figure 63 are plotted on top of less favorable reservoirs.

Objective 4 – Develop and Optimize Integrated Geothermal District Heating and Cooling (GDHC) System

Task 4.1: Estimate Base Case Levelized Cost of Heat (LCOH)

Capital cost for the centralized surface plant:

The direct costs for the heat exchanger, pumps, and new pipelines (connections to existing distribution pipelines) of the surface plant for both scenarios are calculated using ASPEN economic analyzer. For new pipelines, the material is carbon steel to prevent piping corrosion (Rafferty 1989; 1998) with an internal polyurethane insulation, while for PHE; the material is stainless steel (SS-304). The cost for a boiler is obtained as a quote from a vendor, Johnston Boiler Company. In order to account costs for existing distribution system, three cases are considered:

Case 1. MEA donates the pipelines to WVU,
Case 2. WVU purchases pipelines from MEA for $15M, and
Case 3. $25 M for installations of new distribution pipelines across the campus.

The surface plant capital cost is calculated as twice the direct capital costs using Equation 10. The total surface (surface plant +distribution) costs for both the scenarios in all the cases are listed in Table 18.

Table 18: Total surface capital costs including central plant and distribution pipelines.

Equipment type	Case 1		Case 2		Case 3	
	Scenario 1	Scenario 2	Scenario 1	Scenario 2	Scenario 1	Scenario 2
Heat Exchanger	0.17	0.15	0.17	0.15	0.17	0.15
Boiler (Vendor quote) *	1.83	1.75	1.83	1.75	1.83	1.75
Condensate Receiver Tank	0.27	0.24	0.27	0.24	0.27	0.24
Total Equipment	**2.27**	**2.15**	**2.27**	**2.15**	**2.27**	**2.15**
Pump Costs						
Hot water Pump	0.06	0.05	0.06	0.05	0.06	0.05
Condensate Pump	0.09	0.04	0.22	0.16	0.22	0.16
Total Pump Cost	**0.15**	**0.09**	**0.28**	**0.20**	**0.28**	**0.20**
Pipeline Costs						
Retrofitted Steam Pipeline	0.72	0.72	0.72	0.72	0.72	0.72
Retrofitted Condensate Pipeline	0.33	0.33	0.33	0.33	0.33	0.33
Natural Gas pipeline	0.18	0.18	0.18	0.18	0.18	0.18
Total Pipeline Cost	**1.23**	**1.23**	**1.23**	**1.23**	**1.23**	**1.23**
Total Costs						
Total Central Plant Direct Costs	3.65	3.47	3.65	3.47	3.65	3.47
Total Central Plant Capital Cost	**7.30**	**6.94**	**7.30**	**6.94**	**7.30**	**6.94**
Existing Pipeline Costs	**0**	**0**	**15**	**15**	**25**	**25**
Total Surface Capital Cost	**7.30**	**6.94**	**22.30**	**21.94**	**32.30**	**31.94**

*Vendor quote for 300 psig design pressure at a flow rate of 69,000 lbs/hr (8.7 kg/s) is 9.12 M$, and for 200 psig design pressure at a flow rate of 75,900 lbs/hr (9.5 kg/s) is 8.76 M$, therefore two boilers are considered for both scenarios to account for peak flow rates (Quotes are provided in Supporting information).

Economic analysis:

The LCOH for hybrid GDHC is evaluated using BICYCLE levelized cost model in GEOPHIRES. The current version of GEOPHIRES is edited to account for natural gas boiler and its heating duty and yearly cost for natural gas. The natural gas costs are assumed to be ~$4.12/MCF ($3.702/MCF plus monthly add-ons), the electricity price is considered as $0.067/kWh, and the heat price is estimated based on our current MEA price $15/MMBTU ($0.05/kWh). The technical parameters used for subsurface, and economic parameters are same as in Table 5 except for reinjection temperature (60°C) and reservoir impedance (0.752 GPa.s/m^3 and 0.1 GPa.s/m^3 for vertical and horizontal well, respectively). The total surface costs are taken from
Table 18, while natural gas boiler duty and pumping capacity is taken from Table 13 and Table 14. The LCOH is calculated for operating and maintenance costs of 2 M$/year and 4M$/year, respectively, and are tabulated in Table 19. LCOH is in the range of 7.5-11.6 $/MMBTU and 9.0 -15.7 $/MMBTU for scenario 1 and 2, respectively.

Table 19: LCOH for hybrid GDHC system.

O&M Cost = 2 M$/Year										
	Scenario 1	LCOH $/MMBTU				Scenario 2	LCOH $/MMBTU			
	Total Surface Plant Cost (M$)	Vertical Well Configuration		Horizontal Well Configuration		Total Surface Plant Cost (M$)	Vertical Well Configuration		Horizontal Well Configuration	
		NNE	Default	NNE	Default		NNE	Default	NNE	Default
Case 1	7.30	7.49	8.07	7.72	8.46	6.94	9.01	9.93	9.45	10.64
Case 2	22.30	8.42	8.99	8.64	9.38	21.94	10.49	11.42	10.93	12.12
Case 3	32.30	9.03	9.61	9.26	10.00	31.94	11.49	12.41	11.93	13.12
O&M Cost = 4M$/Year										
	Scenario 1	**LCOH $/MMBTU**				**Scenario 2**	**LCOH $/MMBTU**			
	Total Surface Plant Cost (M$)	**Vertical Well Configuration**		**Horizontal Well Configuration**		**Total Surface Plant Cost (M$)**	**Vertical Well Configuration**		**Horizontal Well Configuration**	
		NNE	**Default**	**NNE**	**Default**		**NNE**	**Default**	**NNE**	**Default**
Case 1	7.30	9.07	9.65	9.30	10.04	6.94	11.55	12.47	11.99	13.18
Case 2	22.30	10.00	10.57	10.22	10.96	21.94	13.04	13.96	13.48	14.67
Case 3	32.30	10.61	11.19	10.84	11.58	31.94	14.03	14.95	14.47	15.66

Task 4.2 – Optimize Integrated GDHC System

Improved steam-based system:

In order to improve the heat utilization, a heat pump is used to extract heat from the low temperature return condensate and is used to heat the geothermally preheated hot water before sending to the boiler. Thereby, enhancing the heat utilization and improving the geothermal heat extraction. The simulations with heat pump are repeated in HYSYS using the flow rate in January i.e., 15.2 kg/s for Scenario 1 and 10.1 kg/s for Scenario 2. The heat duty from PHE, heat pump and boiler are given in Table 20 and the geothermal contribution to the proposed hybrid GDHC system was calculated using Equation [13]. The pumping power required for hot water and condensate pumps along with the pressure head is tabulated in Table 21.

$$\%\, Geo = \frac{Q_{Geo}}{Q_{Geo} + Q_{Boiler} + Q_{HeatPump}} \qquad [13]$$

Table 20: The thermal contribution through different units to production of steam at required conditions for Hybrid GDHC system with heat pump.

Unit	Scenario 1	Scenario 2
PHE (Q_{Geo})	1.73 MWth	1.09 MWth
Boiler(Q_{Boiler})	39.33 MWth	23.61 MWth
Heat Pump ($Q_{HeatPump}$)	0.99 MWth	0.67 MWth
Total (Q_{Geo}+Q_{boiler}+$Q_{HeatPump}$)	42.05 MWth	25.37 MWth
%Geo	4.11	4.30

Table 21: The pumping capacity of hot water pump at central location and return condensate pumps at distribution points D and H for Hybrid GDHC system with heat pump.

Pump Type	Mass Flow (kg/s)		Pressure Head (ft)		Power (kW)	
	Scenario 1	Scenario 2	Scenario 1	Scenario 2	Scenario 1	Scenario 2
Hot water Pump	15.20	10.10	603.50	402.3	34.28	15.33
D	4.13	-	298.40	-	4.61	-
H	7.98	3.70	83.65	75.11	2.50	1.038

Heat Pump:

The Coefficient of Performance (*COP*) of heat pump is calculated as the ratio of the heat rejected by the condenser (q_c) to the work input (W) into the compressor using Equation 14 and are tabulated in Table 22.

$$COP_{heat\ pump} = \frac{q_c}{W} \qquad [14]$$

Table 22: Coefficient of performance (COP) of heat pump for both scenarios.

	Scenario 1	Scenario 2
Condenser Heat rejected, q_c (kW)	994.4	667.3
Compressor Work, W (kW)	221.3	221.3
COP	4.49	3.01

By addition of the heat pump, the geothermal contribution increased by about 1.6% in both scenarios.

Plate heat exchanger design:

Detailed design of the PHE is repeated for improved heat loads in Aspen EDR for Scenario 1and Scenario 2 using geothermal flow rates of 15.2 kg/s and 10.2 kg/s, respectively. The PHE geometry obtained for both scenarios from rigorous heat exchanger design along with inlet and outlet temperatures for the geothermal fluid and condensate water is shown in Figure 65 and the parameters are detailed in Table 23.

Table 23: Design of PHE in Hybrid GDHC system with heat pump.

Parameter	Parameter Value	
	Scenario 1	Scenario 2
Heat Duty (kW)	1,726	1,086
PHE Area (m^2)	303.3	170.1
Number of Plates	223.0	243
Plate length (mm)	2,469.45	1,595.55
Plate width (mm)	610.00	495.00
Overall heat transfer coefficient U (W/m^2-K)	1,103.00	1,470.20

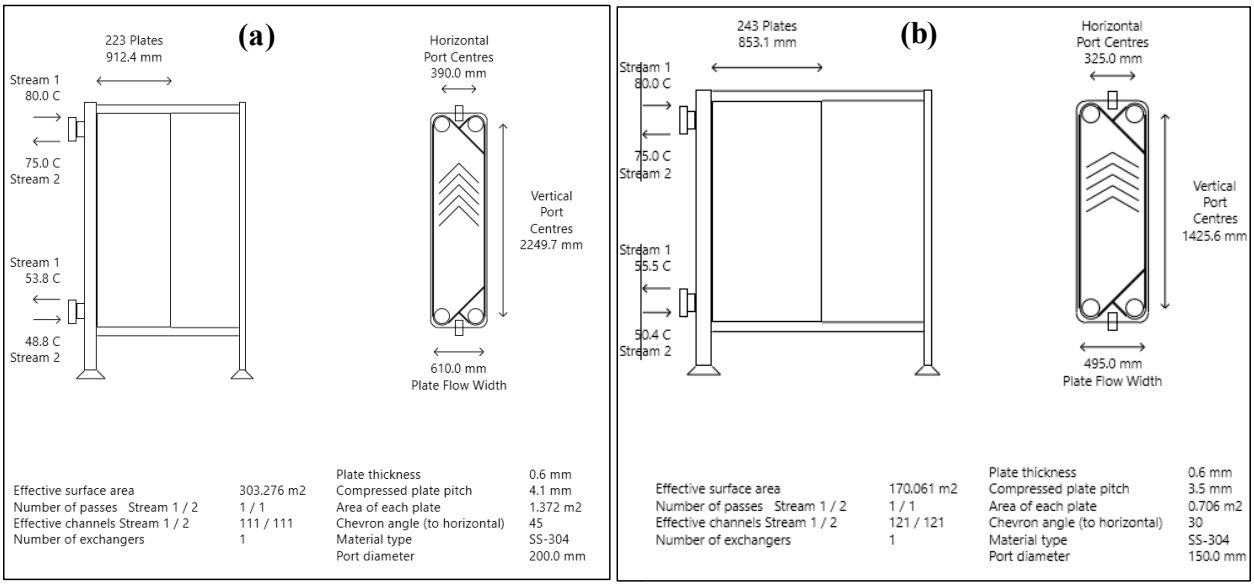

Figure 65: Geometry configuration of PHE in Hybrid GDHC system with heat pump.

Capital cost for the centralized surface plant:

Like the base case, the direct costs for the heat exchanger, pumps, and new pipelines connecting to existing distribution pipelines of the surface plant for both scenarios are calculated using ASPEN economic analyzer. The cost for boiler and heat pump are obtained from Johnston Boiler Company and Mayekawa USA, Inc., respectively. The surface capital costs calculated for both the scenarios in all the cases are listed in Table 24.

Table 24: Total surface capital costs including central plant and distribution pipelines for Hybrid GDHC system with heat pump.

Equipment type	Case 1		Case 2		Case 3	
	Scenario 1	Scenario 2	Scenario 1	Scenario 2	Scenario 1	Scenario 2
Heat Exchanger	0.22	0.17	0.22	0.17	0.22	0.17
Boiler (Vendor quote)	1.83	1.75	1.83	1.75	1.83	1.75
Heat Pump (Vendor quote)#	0.41	0.41	0.41	0.41	0.41	0.41
Condensate Receiver Tank	0.27	0.24	0.27	0.24	0.27	0.24
Total Equipment	**2.73**	**2.57**	**2.73**	**2.57**	**2.73**	**2.57**
Pump Costs						
Hot water Pump	0.06	0.05	0.06	0.05	0.06	0.05
Condensate Pump	0.09	0.04	0.22	0.16	0.22	0.16
Total Pump Cost	**0.15**	**0.09**	**0.28**	**0.20**	**0.28**	**0.20**
Pipeline Costs						
Retrofitted Steam Pipeline	0.72	0.72	0.72	0.72	0.72	0.72
Retrofitted Condensate Pipeline	0.33	0.33	0.33	0.33	0.33	0.33
Natural Gas pipeline	0.18	0.18	0.18	0.18	0.18	0.18
Total Pipeline Cost	**1.23**	**1.23**	**1.23**	**1.23**	**1.23**	**1.23**
Total Costs						
Total Central Plant Direct Costs	4.11	3.89	4.11	3.89	4.11	3.89
Total Central Plant Capital Cost	**8.22**	**7.78**	**8.22**	**7.78**	**8.22**	**7.78**
Existing Pipeline Costs	**0**	**0**	**15**	**15**	**25**	**25**
Total Capital Cost	**8.22**	**7.78**	**23.22**	**22.78**	**33.22**	**32.78**

Vendor quote for Mayekawa Plus Heat 4HS water source NH3 heat pump package with a capacity of 770 GPM (48.6 kg/s) is $414,000, therefore one heat pump is considered for both scenarios (Quotes are provided in Supporting information).

Economic analysis:

The LCOH for hybrid GDHC with heat pump is evaluated in modified GEOPHIRES. The technical parameters used for subsurface, and economic parameters are the same as in Table 5 except reinjection temperature (50°C) and reservoir impedance (0.82 GPa.s/m^3 and 0.11 GPa.s/m^3 for vertical and horizontal well, respectively). The natural gas boiler duty, heat pump work and pumping capacity are taken from Table 20 and Table 21, respectively. The total capital cost and surface operating and maintenance costs are varied between 10-40 M$ and 2-4 M$/year, respectively. The LCOH results are presented in Figure 66 and it is found that the LCOH is in the range of 7.1-12.4 $/MMBTU and 8.3 -16.7 $/MMBTU for scenarios 1 and 2, respectively. The LCOH for improved system is in same range as of the base case GDHC system with increased geothermal contribution.

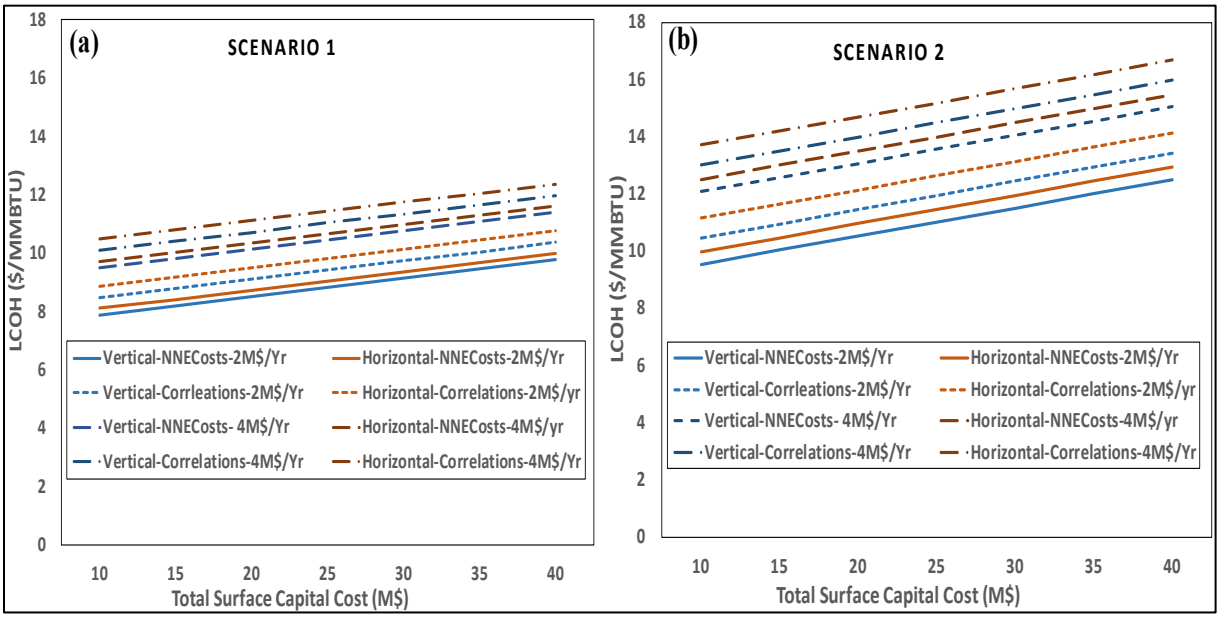

Figure 66: LCOH for hybrid GDHC system with heat pump for scenario 1 (a) and scenario 2 (b), using vertical and horizontal well configurations for different total surface capital and operating costs.

Hot water-based system:

The preliminary surface plant modeling of hot water system using maximum flow rate is performed in CHEMCAD for Evansdale and Health Sciences campuses. The heat exchanger design is performed using CCTHERM program and costs are calculated using ASPEN economic analyzer. The PHE geometry configuration along with costs obtained for all the cases are tabulated in Table 25.

Table 25: PHE geometry configuration obtained through CCtherm and costs from ASPEN economic analyzer.

Water/Steam →	**60/40**		**75/25**		**85/15**	
Campus →	**Evansdale**	**Medical**	**Evansdale**	**Medical**	**Evansdale**	**Medical**
Hot water flow rate (kg/s)	149.94	160.65	187.42	200.81	212.41	227.58
Heat Load MW_{th}	14.20	15.21	17.75	19.01	20.09	21.52
Gross Area (m^2)	768	828	960	1020	1080	1152
No. of Plates	64	69	80	85	90	96
Width (m)	3	3	3	3	3	3
Height (m)	4	4	4	4	4	4
Gap (mm)	2	2	2	2	2	2
Thickness (mm)	0.5	0.5	0.5	0.5	0.5	0.5
Direct Cost ($)	288,400	294,300	359,700	366,700	372,800	380,200

Heat pump COP is found to be 5.69 for all scenarios. Two options are available for heat pumps through Mayekawa, one with a hot water flow rate of 770 GPM (48.6 kg/s) and the other with 1,140 GPM (72 kg/s). The total number of heat pumps required is calculated based on the required hot water flow rate and rating of the commercially available heat pumps and is tabulated in Table 26.

Table 26: Total no. of heat pumps required and their corresponding costs.

Water/Steam →	**60/40**		**75/25**		**85/15**	
Campus →	**Evansdale**	**Medical**	**Evansdale**	**Medical**	**Evansdale**	**Medical**
Hot water flow rate (kg/s)	149.94	160.65	187.42	200.81	212.41	227.58
770 GPM heat pumps required	2	2	1	0	2	2
1140 GPM heat pumps required	1	1	2	3	2	2
Direct Costs[#] (M$)	1.26	1.26	1.28	1.31	1.70	1.70

Vendor quote for Mayekawa Plus Heat 4HS water source NH_3 heat pump package with a capacity of 770 GPM (48.6 kg /s) is $414,000 and 6HS water source NH_3 heat pump package with a capacity of 1140 GPM (72 kg/s) is $435,000 (Quotes are provided in Supporting information).

A central pump is used to deliver hot water to the buildings at a pressure of three bar (30 psig) and return condensate is also pumped back to the central plant at a pressure of three bar. The pumping capacity and costs are provided in Table 27.

Table 27: Pumping capacity and costs for hot water pump and the return condensate pumps for Evansdale and medical campuses.

Water/Steam →	**60/40**					
Campus →	**Evansdale**			**Medical**		
Pump	**Head (m)**	**Power (kW)**	**Cost (M$)**	**Head (m)**	**Power (kW)**	**Cost (M$)**
Central Plant Pump	21.4	39.3	0.11	22.6	44.5	0.11
G	2.9	4.0	0.08	-	-	-
F	13.5	18.5	0.09	-	-	-
I	18.4	8.7	0.06	-	-	-
H	58.3	107.1	0.15	-	-	-
HSC	-	-	-	23.8	46.9	0.12
Total Cost (M$)			0.48			0.23
Water/Steam →	**75/25**					
Campus →	**Evansdale**			**Medical**		
Pump	**Head (m)**	**Power (kW)**	**Cost (M$)**	**Head (m)**	**Power (kW)**	**Cost (M$)**
Central Plant Pump	26.1	60	0.13	24.6	60.6	0.14
G	2.9	5.1	0.09	-	-	-
F	15.0	25.6	0.10	-	-	-
I	18.6	11.0	0.06	-	-	-
H	67.8	155.8	0.12	-	-	-
HSC	-	-	-	30.4	74.9	0.14
Total Cost (M$)			0.50			0.28
Water/Steam →	**85/15**					
Campus →	**Evansdale**			**Medical**		
Pump	**Head (m)**	**Power (kW)**	**Cost (M$)**	**Head (m)**	**Power (kW)**	**Cost (M$)**
Central Plant Pump	29.8	77.7	0.15	26.7	74.6	0.15
G	2.9	5.7	0.10	-	-	-
F	16.2	31.3	0.11	-	-	-
I	18.7	12.5	0.07	-	-	-
H	75.3	196.1	0.14	-	-	-
HSC	-	-	-	35.1	98.0	0.16
Total Cost (M$)			0.56			0.30

The total surface capital costs are shown in Table 28 for all the cases considered. These costs do not include production of steam for Downtown campus and certain equipment at Evansdale and Health Sciences campuses.

Table 28: Preliminary equipment costs estimated for hot water-based system.

Water/Steam →	60/40		75/25		85/15	
Campus →	Evansdale	Medical	Evansdale	Medical	Evansdale	Medical
Heat Exchanger Costs (M$)	0.29	0.29	0.36	0.37	0.37	0.38
Heat Pump Costs (M$)	1.26	1.26	1.28	1.31	1.70	1.70
Domestic Hot Water heat exchangers (M$)	0.15	0.15	0.15	0.15	0.15	0.15
Pumps (M$)	0.48	0.23	0.50	0.28	0.56	0.30
Pipelines (M$)	5.00	5.00	5.00	5.00	5.00	5.00
Total Direct Cost (M$)	7.18	6.94	7.29	7.10	7.78	7.53
Total Capital Cost (M$)	14.36	13.88	14.59	14.21	15.56	15.06

Economic analysis:

Economic analysis for hot water system is performed using GEOPHIRES. For geothermal water production from the subsurface, multiple horizontal configurations are considered. Each configuration has two production wells and one injection well with a total production rate of 40 kg/s or 80 kg/s. Based on the hot water requirement total number of configurations are calculated. The LCOH ($/MMBTU) for central plant for both campuses (Scenario 2) with an operating and maintenance costs of 6 M$/year and total surface capital costs as 30 and 40 M$ are tabulated in Table 29. The LCOH obtained is in the range of 16-21 $/MMBTU and 21.4-24.6 $/MMBTU for a total geothermal flow rate from each configuration of 80 and 40 kg/s, respectively. In all the cases, the estimated LCOH is higher than the current heat price (~15 $/MMBTU); therefore, the hot water-based system is not feasible at the current estimations.

Table 29: LCOH calculation for hot water -based system using horizontal well configuration and total surface operating cost of 6M$/year.

Flow rate from each configuration	Water/ Steam Usage	Maximum Water Flow Rate (kg/s)	No. of Configurations	LCOH ($/MMBTU)	
				30 M$	40 M$
80 kg/s	60/40	310.6	4	19.75	20.76
	75/25	388.2	5	17.47	18.28
	85/15	440.0	6	15.95	16.62
40 kg/s	60/40	310.6	8	23.58	24.55
	75/25	388.2	10	21.38	22.16
	85/15	440.0	11	-	-

Task 4.3 – Quantify Minimized System Uncertainties & Development Risks

Economic analysis based on uncertainty quantification results from Task 3.3 are performed for hybrid GDHC system with heat pump for scenario 1 (entire campus supply) using horizontal well configuration and with a total surface capital cost and operating costs as $40 M and 4 M$/year, respectively. The normal probability plots for LCOH are plotted in Figure 67 using well drilling costs obtained through NNE quotes and default correlations and it is found that the uncertainty in the production temperature does not have much influence on the LCOH at a given flow rate.

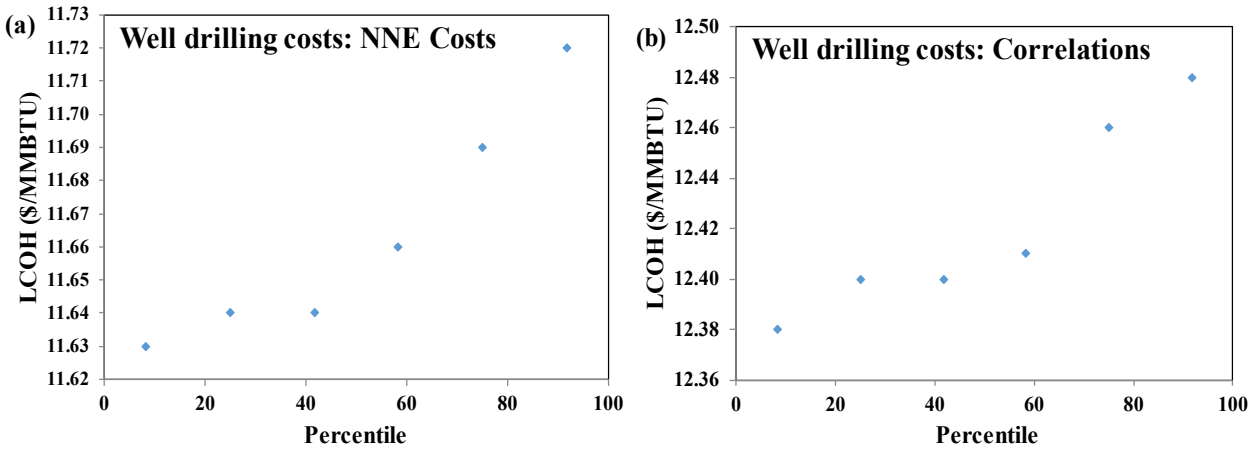

Figure 67: Normal probability plot of LCOH for hybrid GDHC with heat pump for scenario 1 using horizontal well configurations and costs obtained through NNE (a) and GEOPHIRES correlations (b) with a total surface plant cost of $40 M and operating and maintenance costs of 4 M$/year.

Objective 5.0 Maintain & Update Market Transformation Plan:

Task 5.1 – Maintain & Update Market Transformation Plan

The results from all the objectives above are unified and reported as appropriate through normal quarterly and final technical reports.

RECOMMENDATIONS FOR FURTHER ANALYSIS

At the closure of this first phase feasibility analysis of deep direct-use geothermal development on the West Virginia University campus - Morgantown, WV, significant announcements were made regarding the future of energy on the WVU Campus. The opportunities are significant, relative to system energy efficiency and environmental footprint for the campus and within the city of Morgantown, and the team is currently engaged with WVU Facilities Management regarding development of potential replacement concepts. Realizing this opportunity, the team has identified significant technical uncertainties that must be addressed to enable the potential implementation of a deep direct-use geothermal system. The most significant technical uncertainties, starting with the largest unknowns are: 1) reservoir parameters at the well location, 2) surface plant costs, 3) hot water requirements for each building, and 4) costs to retrofit existing buildings and infrastructure for hot water use, versus steam. Furthermore, in preparation for developing an operational geothermal heat supply and usage system on WVU campus, additional groundwork is needed that pertains to drilling an exploratory well with a full-logging program to obtain more information related to possible reservoir performance. Based on the subsurface parameters, full-fledged engineering analysis needs to be performed to evaluate conversion of the existing steam-based system to a hot water-based system.

Description of Recommended Activities

- **Exploratory well with an aggressive well logging program:** The goal of this task is to drill an exploratory well to a depth of 15,000 ft with a full logging and coring program to evaluate the geothermal gradient, petrophysics, and geochemistry at the proposed site to reduce the uncertainty in the reservoir parameters. A full-logging program would include a full suite of common logs [e.g., gamma ray (GR), resistivity, density, neutron, and full waveform sonic], specialty logs [e.g., a borehole imaging log, and a wireline testing tool (e.g., MDT),or a drill stem test (DST)], a temperature log, possibly a nuclear magnetic resonance (NMR), and an elemental capture spectroscopy (ECS) log. Additionally, borehole seismic profiling (VSP) data could also be acquired. Finally, the acquisition of drill core from the exploratory well, particularly from the upper Tuscarora, would enable a direct comparison to core previously analyzed. This, in turn, would provide confirmation of trends in porosity, permeability, petrology, and small-scale deformation (fracturing) developed for lithologic materials from outside of the WVU test area.

- **Potential of shallow reservoir for thermal energy storage using depleted wells:** The goal of this task is to evaluate the shallow reservoir at the potential DDU site for thermal energy storage. The additional energy produced during months of April-October will be stored in shallow reservoirs and will be extracted during the peak demand (December-January).

- **System engineering, design and technoeconomic assessment of the surface plant:** The current heating and cooling system on campus is based on steam. Each building heating demand, and temperatures needs to be measured. Potential of hybrid geothermal natural gas system for CHP system and conversion to a hot water system should be thoroughly analyzed to identify the best path going forward. Replacing existing steam-based equipment to high-efficiency equipment should be considered. Cascaded uses of geothermal heat need to be considered, for example the return water from the buildings

can be utilized to warm Personal Rapid Transit (PRT) guideways and melt the ice and snow on the guideway section, [which is currently heated by propylene glycol-water mixture at 60°C (140°F) produced using natural gas boilers] thereby improving geothermal utilization.

- **Seismic Survey:** A 2-D seismic survey done in the area of the WVU geothermal site location would be very helpful in designing horizontal wells in fracture zones or in regions with high permeability, for locating potential fault or fracture zones, and to steering the horizontal well completion within the target formation.

- **Updates to the initial feasibility study results:** All the information obtained for subsurface parameters through exploratory well-logging and surface utilization through first-order engineering analysis will be used to update the current feasibility analysis results. The reservoir dataset developed will help in updating the risk favorability map for Morgantown, WV. Thermal drawdown induced flow channeling is inevitable in a fracture dominant system, which will be studied by thermal-mechanical coupled modeling of the reservoir using TOUGH-FLAC and flow channeling due to the reaction chemistry will be performed using TOUGH-REACT. The first-order engineering analysis will help in updating capital and maintenance costs for surface design. The results of this effort will serve as the basis for a Go/No-Go decision point for significant investment of WVU financial resources to continue to pursue a GDHC system for the campus. This would be the first geothermal DDU project in the eastern U.S. and would serve as a demonstration of the potential for a low temperature geothermal energy industry in a region not currently served by DDU.

PROJECT OUTPUT

Publications

- Alonge, B. O., *"Design of Geothermal District Heating and Cooling system for the West Virginia University",* West Virginia University Libraries, 2019.
- Zhang, Y., Garapati, N., Doughty, C., Pierre, J., "*Modeling Study of Deep Direct Use Geothermal on the West Virginia University Campus-Morgantown, WV"*, Geothermics, , 87 (2020): 101848.
- Garapati, N., Irr, V. J., Lamb, B., "*Feasibility Analysis of Deep Direct-Use Geothermal on the West Virginia University Campus-Morgantown, WV*", 45th Workshop on Geothermal Reservoir Engineering, Stanford, CA, 2020.
- Garapati, N., Alonge, O.B., "*Development of Deep Direct-Use Geothermal system on West Virginia University Campus-Morgantown, WV*", AIChE Annual Meeting, Orlando, FL, 2019.
- Donnelly, K., Garapati, N., Zhang, Y., Pierre, J., "*Subsurface modelling of Deep Direct-Use (DDU) geothermal on the West Virginia University Campus - Morgantown, WV*", AIChE Annual Meeting, Orlando, FL, 2019, (Undergraduate Student Poster Session).
- McDowell, R. R., Lewis, J. E., Daft, G. W., Dinterman, P. A., Brown, S. A., and Moore, J. P., "*Silurian Tuscarora Sandstone in Western West Virginia: Will It Work as a Geothermal Reservoir Rock?*", Eastern Section American Association of Petroleum Geologists Convention, Columbus, OH, 2019, (Poster).
- Smith, J.D. "*A stochastic evaluation of geothermal reservoir potential for the Tuscarora Sandstone in Morgantown, West Virginia, USA"*. GRC Transactions, 43. p. 902-925. 2019. (Oral presentation and conference paper).
- Irr, V. J., Garapati, N., Zhang, Y., Pierre, J., Doughty, C., "*Subsurface Modeling and Well Configuration Design for Deep Direct-Use Geothermal Development at WVU*", 3rd Annual Undergraduate Spring Symposium, Morgantown, April 2019 (Poster).
- Irr, V. J., Garapati, N., Zhang, Y., Pierre, J., Doughty, C., "*Subsurface Modeling and Well Configuration Design for Deep Direct-Use Geothermal Development at WVU*", 16th Annual Undergraduate Research Day at the Capitol, Charleston, February 2019 (Poster).
- Garapati, N., Alonge, O.B., Hall, L., Irr, V. J., Zhang, Y., Smith, J. D., Pierre, J., Doughty, C., "*Feasibility of Development of Geothermal Deep Direct-Use District Heating and Cooling system at West Virginia University Campus-Morgantown, WV*", 44th Workshop on Geothermal Reservoir Engineering, Stanford, CA, 2019.
- Garapati, N., Alonge, O.B., Lemasters, D., Vozniak, S., Saurborn, L., Anderson, B.J., "*Development of integrated geothermal district heating and cooling (GDHC) system at West Virginia University Campus-Morgantown, WV*", AIChE Annual Meeting 2018.
- Irr, V. J., Zhang, Y., Pierre, J., Garapati, N., "*Subsurface Modeling and Well Configuration Design for Deep Direct-Use Geothermal Development at WVU*", AIChE Annual Meeting 2018 (Undergraduate Student Poster Session).
- Garapati, N., Zhang, Y., Irr, V. J., Pierre, J., Doughty, C., Anderson, B.J., "*Subsurface modeling and well configuration design for geothermal deep direct-use district heating system at West Virginia University Campus-Morgantown, WV*", TOUGH Symposium 2018, (Poster).
- McCleery, R. S., McDowell, R.R., Moore, J. P., Garapati, N., Carr, T.R., Anderson, B.J., "*Development of 3D geological model of Tuscarora Sandstone for feasibility of deep direct-*

use geothermal at West Virginia University's main campus", GRC Transactions, 42. p. 192-208. 2018. (Oral presentation and conference paper).

- Irr, V. J., Garapati, N., "*Subsurface modeling and well configuration design for deep direct-use geothermal development at WVU",* Summer Undergraduate Research Symposium, July 26, 2018 (Poster).
- Anderson, B.J., "*Feasibility of Deep Direct Use Geothermal on the WVU Campus-Morgantown, WV,*" Energy Transitions for Green Growth: A Conference by the West Virginia Office of Energy, Flatwoods, WV, June 5, 2018.
- Moore, J., Brown, S., Workman, S., Crandall, D., Dinterman, P., Moore, J. *"Computed Tomography of the Tuscarora Sandstone from the Preston 119 Well,"* NETL Technical Report Series, U.S. Department of Energy, National Energy Technology Laboratory, Morgantown, WV, 2018.
- Garapati, N., Anderson, B.J., Carr, T.R., "*Feasibility of Deep Direct Use Geothermal on the WVU Campus- Morgantown, WV*", 2018 SMU Power Plays conference, Dallas, TX, USA, January 10, 2018 (Poster).
- Garapati, N., Anderson, B.J., Carr, T.R., "*Feasibility of Deep Direct Use Geothermal on the WVU Campus- Morgantown, WV*", 2017 WVU Energy Institute / NRCCE Holiday Open House, Morgantown, WV, USA, December 8, 2017 (Poster).
- Garapati, N., Anderson, B.J., "*Feasibility of Deep Direct Use Geothermal on the WVU Campus- Morgantown, WV*", Geothermal Technologies Office 2017 Peer Review, Denver, CO, USA, November 13, 2017.

Status Reports

- First quarterly report is submitted to DOE EERE – Geothermal Technologies office, January 2018.
- Second quarterly report is submitted to DOE EERE – Geothermal Technologies office, April 2018.
- Third quarterly report is submitted to DOE EERE – Geothermal Technologies office, July 2018.
- Fourth quarterly report is submitted to DOE EERE – Geothermal Technologies office, October 2018.
- Fifth quarterly report is submitted to DOE EERE – Geothermal Technologies office, January 2019.
- Sixth quarterly report is submitted to DOE EERE – Geothermal Technologies office, April 2019.
- Seventh quarterly report is submitted to DOE EERE – Geothermal Technologies office, July 2019.

Media Reports

- WVU to study possible geothermal use thanks to DOE grant, November 6, 2017, WVU Energy Institute News. https://energy.wvu.edu/news-latest/2017/11/06/wvu-to-study-possible-geothermal-use-thanks-to-doe-grant.

Outreach Activities

- Garapati, N., "Geothermal Energy", Energy training for China Energy Executives, WVU Energy Institute, November 28, 2018.
- Garapati, N., Hall, L., Irr, V. J., "Geothermal Energy", Westwood Middle School, Morgantown, WV, November 30, 2018.

Networks/Collaborations Fostered

- NETL performed Computed Tomography (CT) scans on Preston-119 core resulting in a technical report. NETL also finished scans on Clay-513 and Harrison-79 core samples.

Other Products

- Server readings from four of the distribution points are collected monthly.
- Diagrams of the transmission lines and steam invoices were collected.
- Chain of Title for new proposed site locations were obtained.
- Cornell has provided data about Thermal Quality Analysis Maps and Structured Data from Low Temperature Geothermal Play Fairway Analysis for the Appalachian Basin.

REFERENCES

Adler, D.. (2005). vioplot: Violin plot. R package version 0.2. http://wsopuppenkiste.wiso.uni-goettingen.de/~dadler.

Aquaveo, LLC in Provo, Utah. GMS User Manual (v9.0) (2013) The Groundwater Modeling System.

Avary, K.L., (1996). The Lower Silurian Tuscarora Sandstone fractured anticlinal play. *In* J.B. Roen, and B.J. Walker. Eds. The atlas of major Appalachian gas plays. West Virginia Geological and Economic Survey, Publication V-25, Pp. 151 - 155.

Beckers, K. F., M. Z. Lukawski, T. J. Reber, B. J. Anderson, M. C. Moore, and J. W. Tester, (2013) Introducing GEOPHIRES v1. 0: Software package for estimating levelized cost of electricity and/or heat from enhanced geothermal systems, Proceedings, 38th Workshop on Geothermal Reservoir Engineering, Stanford University, Stanford, CA.

Beckers, K. F., M. Z. Lukawski, B. J. Anderson, M. C. Moore, and J. W. Tester, (2014) Levelized costs of electricity and direct-use heat from Enhanced Geothermal Systems, Journal of Renewable and Sustainable Energy, 6, p. 013141.

Beckers, K. F., (2016) Low-temperature geothermal energy: Systems modeling, reservoir simulation, and economic analysis. Cornell University Ph.D. Thesis.

Beckers, K. and K. McCabe. (2018). GEOPHIRES. Online GitHub Repository. https://github.com/kfbeckers/GEOPHIRES.

Bivand, R., T. Keitt, and B. Rowlingson. (2018). rgdal: Bindings for the 'Geospatial' Data Abstraction Library. R package version 1.3-3. https://CRAN.R-project.org/package=rgdal

Blackwell, D., M. Richards, and Z. Frone, (2010) Elevated Crustal Temperatures in West Virginia: Potential for Geothermal Power. Web.

Brunsdon, C., and H. Chen (2014). GISTools: Some further GIS capabilities for R. R package version 0.7-4. https://CRAN.R-project.org/package=GISTools

Camp, E., T.E. Jordan, M.J. Hornbach, and C.A. Whealton. (2018). A probabilistic application of oil and gas data for exploration stage geothermal reservoir assessment in the Appalachian Basin. *Geothermics*, *71*. Pp. 187 – 199.

Castle, J. and Byrnes, A., (2005). Petrophysics of Lower Silurian sandstones and integration with the tectonic-stratigraphic framework, Appalachian basin, United States: American Association of Petroleum Geologist Bulletin, v.89, no.1, p. 41-60.

Cornell University. (2017) *Final Report: Low Temperature Geothermal Play Fairway Analysis for the Appalachian Basin*: https://gdr.openei.org/submissions/899.

Craft, B.C., and M.F. Hawkins. (1959). Applied Petroleum Reservoir Engineering. Englewood Cliffs, NJ, Prentice Hall.

Deutsch, C.V., and A.G. Journel, (1992) GSLIB, Geostatistical Software Library and User's Guide, Oxford University Press, New York.

Dietz, D.N., (1965). Determination of average pressure from build-up surveys. *Journal of Petroleum Technologies*. p. 955-959.

Edwards, A.L. TRUMP, (1972) A Computer Program for Transient and Steady State Temperature Distributions in Multidimensional Systems, National Technical Information Service, National Bureau of Standards, Springfield, VA.

Finsterle, S., C. Doughty, M.B. Kowalsky, G.J. Moridis, L. Pan, T. Xu, Y. Zhang, and K. Pruess (2008). Advanced vadose zone simulations using TOUGH, Vadose Zone Journal, 7 pp. 601-609

Finsterle, S., Y. Jung, M. Kowalsky, L. Magnusdottir, G. Pau, H. Wainwright, And Y. Zhang, (2016), iTOUGH2 v7. 1, Lawrence Berkeley National Laboratory (LBNL), Berkeley, CA.

Frone, Z., and Blackwell, D., (2010) Geothermal map of the northeastern United States and the West Virginia thermal anomaly. Geothermal Research Council Transactions, 34.

Gagolewski, M., et al. (2018). R package stringi: Character string processing facilities. http://www.gagolewski.com/software/stringi/. DOI:10.5281/zenodo.32557.

Garapati, N., O. B. Alonge, L. Hall, V. J. Irr, Y. Zhang, J. D. Smith, P. Jeanne, and C. Doughty (2019). Feasibility of Development of Geothermal Deep Direct-Use District Heating and Cooling system at West Virginia University Campus-Morgantown, WV. PROCEEDINGS, 44th Workshop on Geothermal Reservoir Engineering. Stanford University, Stanford, California.

Gringarten, A.C., ed. (1978). Geothermics and Geothermal Energy. Springer. p. 297-308.

Hardie, R. W., (1981) BICYCLE II: A Computer Code for Calculating Levelized Life-Cycle Costs, LA-89089. Los Alamos National Laboratory, Los Alamos, New Mexico, United States.

Harrell, F.E., Jr., C. Dupont, et al., (2018). Hmisc: Harrell miscellaneous. R package version 4.1-1. https://CRAN.R-project.org/package=Hmisc

Hennen, R.V., D.B. Reger, and W.A. Price. (1914). Preston County: Geologic report and maps. West Virginia Geological and Economic Survey County Geologic Report CGR-24. p.566.

Hernandez-Galan, J. L., and Alberto Plauchu, L., (1989) Determination of·fouling factors for shell-and-tube type heat exchangers exposed to los azufres geothermal fluids, Geothermics, 18, p.121–128.

Honarpour, M. and Mahmood, S., (1988) Relative Permeability Measurements: An Overview, J. of Petroleum Technology, V. 40, no. 9, p. 963-966.

Jones, S.C., (1987). Using the inertial coefficient, β, to characterize heterogeneity in reservoir rock. SPE Annual Technical Conference and Exhibition, Dallas, Texas, Sept. 27–30. SPE-16949-MS. http://dx.doi.org/10.2118/16949-MS.

Jones, F.O. and W.W. Owens. (1980). A laboratory study of low-permeability gas sands. *J. Pet. Technol. 32 (9)*. pp. 1631–1640. SPE-7551-PA. http://dx.doi.org/10.2118/7551-PA.

Jordan, T.E., F.G. Horowitz, J.R. Stedinger, J.W. Tester, E.R. Camp, C.A. Whealton, J.D. Smith, B.J. Anderson, K. Welcker, X. He, M.C. Richards, C. Chickering-Pace, M. Hornbach, Z.S. Frone, C. Ferguson, R. Bolat, and M.B. Magnani. (2016). Low temperature geothermal play fairway analysis for the Appalachian Basin: Phase 1 Revised Report. U.S. Dept. of Energy Award No. DE-EE0006726.

Killick R., and I.A. Eckley. (2014). changepoint: An R package for changepoint analysis. *Journal of Statistical Software*, *58(3)*. Pp. 1-19. http://www.jstatsoft.org/v58/i03/

Killick R., K. Haynes, and I.A. Eckley. (2016). changepoint: An R package for changepoint analysis. R package version 2.2.2. https://CRAN.R-project.org/package=changepoint>

Lowry, T.S., J.T. Finger, C.R. Carrigan, A. Foris, M.B. Kennedy, T.F. Corbett, C.A. Doughty, S. Pye, and E.L. Sonnenthal. (2017). Reservoir maintenance and development task report for the DOE geothermal technologies office GeoVision study. Sandia National Labs Report SAND2017-9977. 81 p.

Marcellus Shale Energy and Environment Laboratory (MSEEL). (2018). [dataset] DTS_Data.zip from Research – Well Datasets – Fiber Optics. http://mseel.org/Data/Wells_Datasets/MIP_3H/Fiber_Optics/DTS/DTS_Data.zip

McCleery, R.S., J.P. Moore, R.R. McDowell, N. Garapati, T.R. Carr, and B.J. Anderson. (2018). Development of 3-D geological model of Tuscarora Sandstone for feasibility of deep direct-use geothermal at West Virginia University's main campus. *GRC Transactions*, *42*. Pp. 192-208.

McDowell, R., compiler. (2018). Summary of petrographic observations, Silurian Tuscarora Sandstone interval - Clay 513 drill core [dataset]. West Virginia Geological and Economic Survey (personal communication).

McDowell, R., J. Lewis, and G. Daft, compilers. (2018). Permeability data acquired by direct air injection from the Silurian Tuscarora Sandstone interval – Preston 119 drill core [dataset]. West Virginia Geological and Economic Survey.

McKay, M. D., W. J. Conover, and R. J. Beckman, (1979) A comparison of three methods for selecting values of input variables in the analysis of output from a computer code, Technometrics, 21, 239– 245.

Narasimhan, T.N. and P.A. Witherspoon., (1976) An Integrated Finite Difference Method for Analyzing Fluid Flow in Porous Media, Water Resour. Res., 12(1), p.57 – 64.

Nasir, Q., Sabil, K. M., and Nasrifar K., (2014) Measurement and Phase Behavior Modeling (Dew Point+Bubble Point) of CO_2 Rich Gas Mixture, J. Appl. Sci., 14(10), p.1061–1066.

Ooms, J. (2018). writexl: Export data frames to Excel 'xlsx' format. R package version 1.0. https://CRAN.R-project.org/package=writexl

Page, E.S.. (1954). Continuous inspection schemes. *Biometrika*, *41(1/2)*. Pp. 100-115.

Patchen D. G. et al. (2006) A geologic Play Book for Trenton-Black River Appalachian Basin Exploration, Final Report. NETL, DOE : West Virginia University Research Corp.

Pebesma, E.J., and R.S. Bivand. (2005). Classes and methods for spatial data in R. *R News 5 (2)*, https://cran.r-project.org/doc/Rnews/

Peters, M.S., Timmerhaus, K.D., West, R.E., (2003) Plant Design and Economics for Chemical Engineers. McGraw- Hill Chemical Engineering Series.

Pruess, K., and T.N. Narasimhan., (1982) On Fluid Reserves and the Production of Superheated Steam from Fractured, Vapor-Dominated Geothermal Reservoirs, J. Geophys. Res., 87, p. 9329 – 9339.

Pruess, K. and T.N. Narasimhan., (1985) A Practical Method for Modeling Fluid and Heat Flow in Fractured Porous Media, Soc. Pet. Eng. J., 25(1), p.14 - 26.

Pruess, K., C. Oldenburg, and G. Moridis, (1999) *TOUGH2 User's Guide, Version 2.0*, Report LBNL-43134, Lawrence Berkeley National Laboratory, Berkeley, CA.

Pruess, K., C. Oldenburg, and G. Moridis, (2011) T*OUGH2 User's Guide, Version 2.1,* LBNL-43134 (revised)*:* Lawrence Berkeley National Laboratory, Berkeley, CA.

QGIS Development Team (2018). QGIS Geographic Information System. Open-Source Geospatial Foundation Project. http://qgis.osgeo.org

R Core Team. (2018). R: A language and environment for statistical computing. R Foundation for Statistical Computing. Vienna, Austria. https://www.R-project.org/

Rafferty, K., (1989) Geothermal District Piping - A Primer, Geo-Heat Center, Klamath Fall, OR.

Rafferty, K., (1998) Chapter 11 Heat Exchangers, in Geothermal Direct Use Engineering and Design Guidebook, 3rd ed., p. 1–32.

Rafferty, K., (1998) Piping, Geo-Heat Cent. Oregon Inst. Technol., p.241–259.

Rasband, W. S. ImageJ. U.S. National Institutes of Health: Bethesda, MD, 1997–2016, http://imagej.nih.gov/ij/ (accessed 2018).

Ryder, R.T., Crangle, R.D., Jr., Trippi, M.H., Swezey, C.S., Lentz, E.E., Rowan, E.L., and Hope, R.S., (2009) Geologic cross section D–D' through the Appalachian basin from the Findlay arch, Sandusky County, Ohio, to the Valley and Ridge province, Hardy County, West Virginia: U.S. Geological Survey Scientific Investigations Map 3067, 2 sheets, 52-p. pamphlet

Ryder, R., and Zagorski, W. (2003). Nature, origin, and production characteristics of the Lower Silurian regional oil and gas accumulation, central Appalachian basin, United States. AAPG Bulletin, 87(5), pp.847~872, 2

Sminchak, Joel R. (2018) Final Technical Report: Integrated Wellbore Integrity Analysis Program for CO_2 Storage Applications. United States: N. p., Web. doi:10.2172/1481775.

Smith, J.D., (2016). Analytical and geostatistical heat flow modeling for geothermal resource reconnaissance applied in the Appalachian Basin. Cornell University MS Thesis. 254 p.

Smith, J.D., (2019). Exploratory spatial data analysis and uncertainty propagation for geothermal resource assessment and reservoir models. Cornell University PhD Thesis. 255 p.

Sommer, C.; Strähle, C.; Köthe, U.; Hamprecht, F.A., (2011) ilastik: Interactive Learning and Segmentation Toolkit; 2011 IEEE international symposium on biomedical imaging: From nano to macro, PP 230-233.

West Virginia GIS Technical Center. (2010). Census Incorporated Places. WV State GIS Data Clearinghouse. http://wvgis.wvu.edu/data/data.php.

Whealton, C.A., Stedinger, J.R., Horowotiz, F.G., (2015) Application of Generalized Least Squares Regression in Bottom-Hole Temperature Corrections, in: Final Report: Low Temperature Geothermal Play Fairway Analysis for the Appalachian Basin. pp. 130–144.

Wickham, H., (2018). stringr: Simple, consistent wrappers for common string operations. R package version 1.3.1. https://CRAN.R-project.org/package=stringr

Wickham, H., and J. Bryan (2018). readxl: Read Excel files. R package version 1.1.0. https://CRAN.R-project.org/package=readxl

Wilson, T. H, Carr, T., et al., (2018). Marcellus Shale model stimulation tests and microseismic response yield insights into mechanical properties and the reservoir discrete fracture network. Interpretation, V.6, No. 2, May 2018. T-231-T243.

Zhang, Y., and G. Pinder, (2003) Latin hypercube lattice sample selection strategy for correlated random hydraulic conductivity fields, Water Resour. Res., 39(8), 1226, doi:10.1029/2002WR001822.

Zhou, Q., Oldenburg, C. M., & Rutqvist, J. (2019). Revisiting the analytical solutions of heat transport in fractured reservoirs using a generalized multirate memory function. Water Resources Research, 55, 1405–1428. https://doi. org/10.1029/2018WR024150.

APPENDIX A

Contents:

Figure A-1:

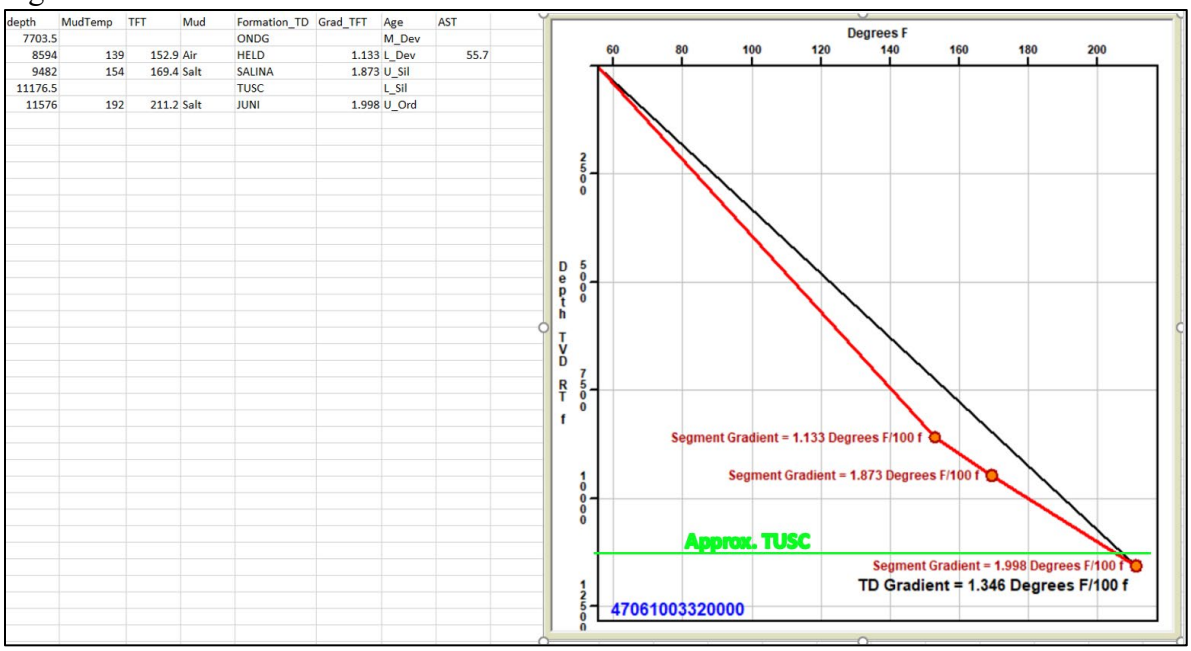

depth	MudTemp	TFT	Mud	Formation_TD	Grad_TFT	Age	AST
7703.5				ONDG		M_Dev	
8594	139	152.9	Air	HELD	1.133	L_Dev	55.7
9482	154	169.4	Salt	SALINA	1.873	U_Sil	
11176.5				TUSC		L_Sil	
11576	192	211.2	Salt	JUNI	1.998	U_Ord	

Figure A-1: Temperature data and GTG (geothermal temperature gradient) plot for Greer Steel #11646, 47061003320000, Monongalia, Co.

Figure A-2:

depth	MudTemp	TFT	Mud	Formation_TD	Grad_TFT	Age	AST
8087.5				ONDG		M_Dev	55.7
8964	176	193.6	Air	SALINA	1.543	U_Sil	
10886				TUSC		L_Sil	
11400	217	238.7	Air	JUNI	1.863	U_Ord	

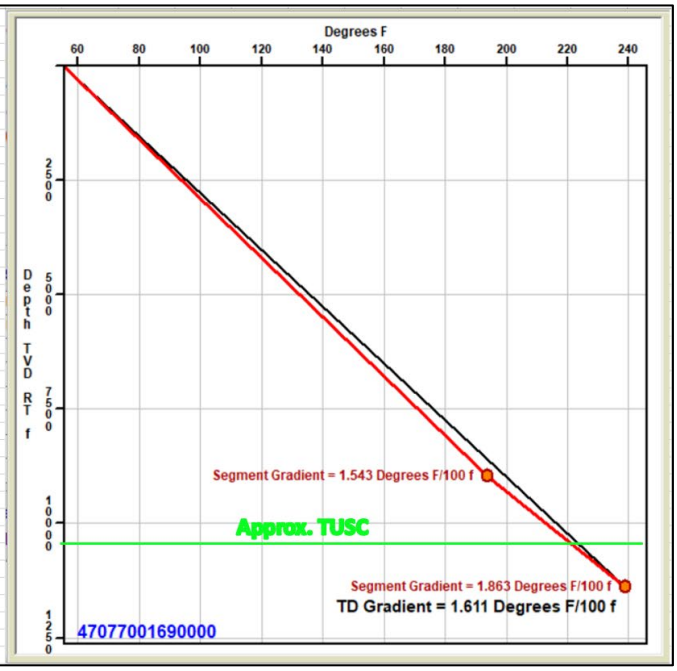

Figure A-2: Temperature data and GTG plot for Huggins #11537, 47077001690000, Preston, Co.

Figure A-3:

depth	MudTemp	TFT	Mud	Formation_TD	Grad_TFT	Age	AST
7520				ONDG		M_Dev	55.7
7828	160	176	Air	HELD	1.541	L_Dev	
10472				TUSC		L_sil	
14593	238	261.8	Salt	TRENT	1.269	L_Ord	

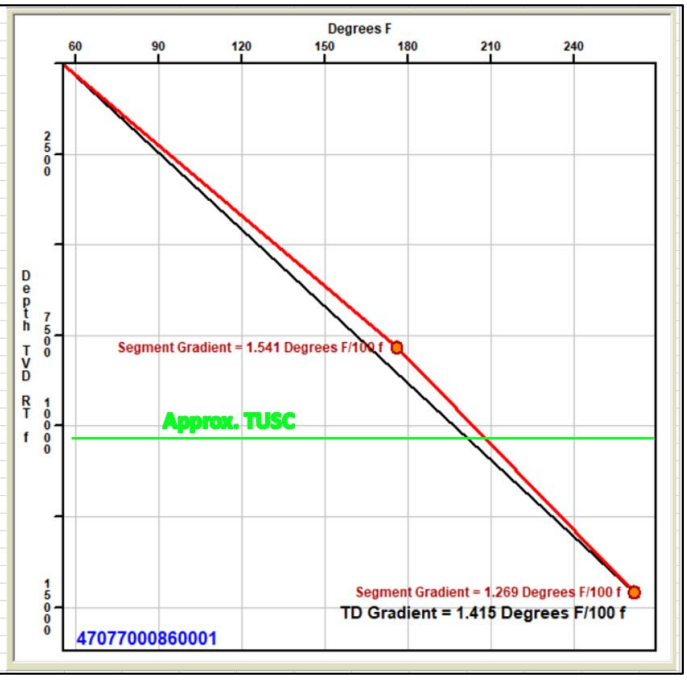

Figure A-3: Temperature data and GTG plot for Walls #1, 47077000860001, Preston, Co.

Figure A-4:

depth	MudTemp	TFT	Mud	Formation_TD	Grad_TFT	Age	AST
7191.5				ONDG		M_Dev	55.7
7499	141	155.1	Emul	HELD	1.331	L_Dev	
10062.5				TUSC		L_Sil	
12089	208	228.8		MRTNS	1.604	U_Ord	
14961	248	272.8	Salt	STP	1.536	M_Ord	
16057	234	257.4	Salt	BEEK	-1.405	L_Ord	
17033	262	288.2	Salt		3.146		
17119	266	292.6	Salt		5.176		

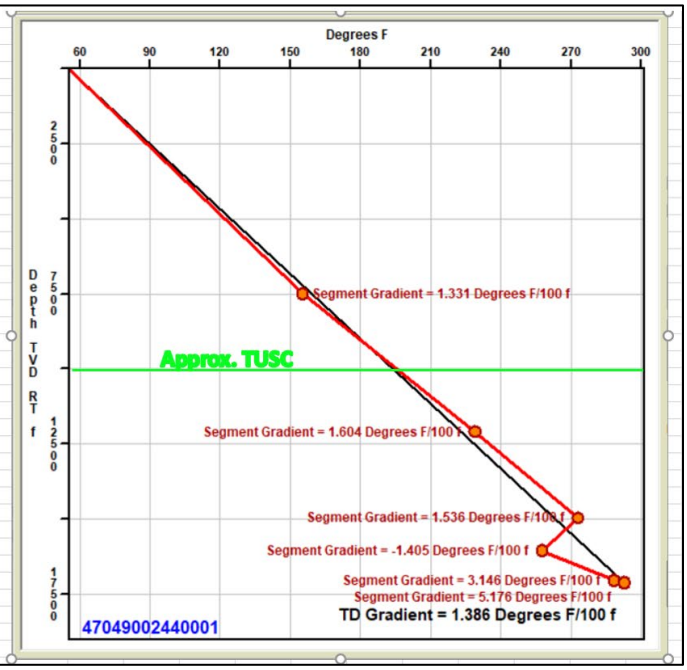

Figure A-4: Temperature data and GTG plot for Finch #A-1, 47049002440001, Marion, Co.

APPENDIX B

How Porosity Assumptions Affect the Klinkenberg Correction

The Klinkenberg correction will be greatest for the smallest air permeability. The correction will be larger for larger porosities than for smaller porosities. It is likely that a small permeability will have a small porosity; but, below the effect is tested for small and large porosities relative to the assumed average porosity of 3%.

$$b_{small} = 15.61\left(\frac{0.4}{0.005}\right)^{-0.447} = 2.20 \text{ psig}$$

$$b_{avg} = 15.61\left(\frac{0.4}{0.03}\right)^{-0.447} = 4.90 \text{ psig}$$

$$b_{large} = 15.61\left(\frac{0.4}{0.15}\right)^{-0.447} = 10.07 \text{ psig}$$

$$k_{w_{small}} = \frac{0.4}{1 + \frac{2.20}{26}} = 0.369 \text{ mD}$$

$$k_{w_{avg}} = \frac{0.4}{1 + \frac{4.9}{26}} = 0.337 \text{ mD}$$

$$k_{w_{large}} = \frac{0.4}{1 + \frac{10.07}{26}} = 0.288 \text{ mD}$$

$$\frac{k_{w_{small}}}{k_{w_{avg}}} = 1.09$$

$$\frac{k_{w_{avg}}}{k_{w_{large}}} = 1.17$$

APPENDIX C

Blue-Stain Visual Porosity Reference Chart and Methodology

Porosity was estimated by comparison of thin section view(s) at lowest available magnification (1x objective – 10x eyepiece).

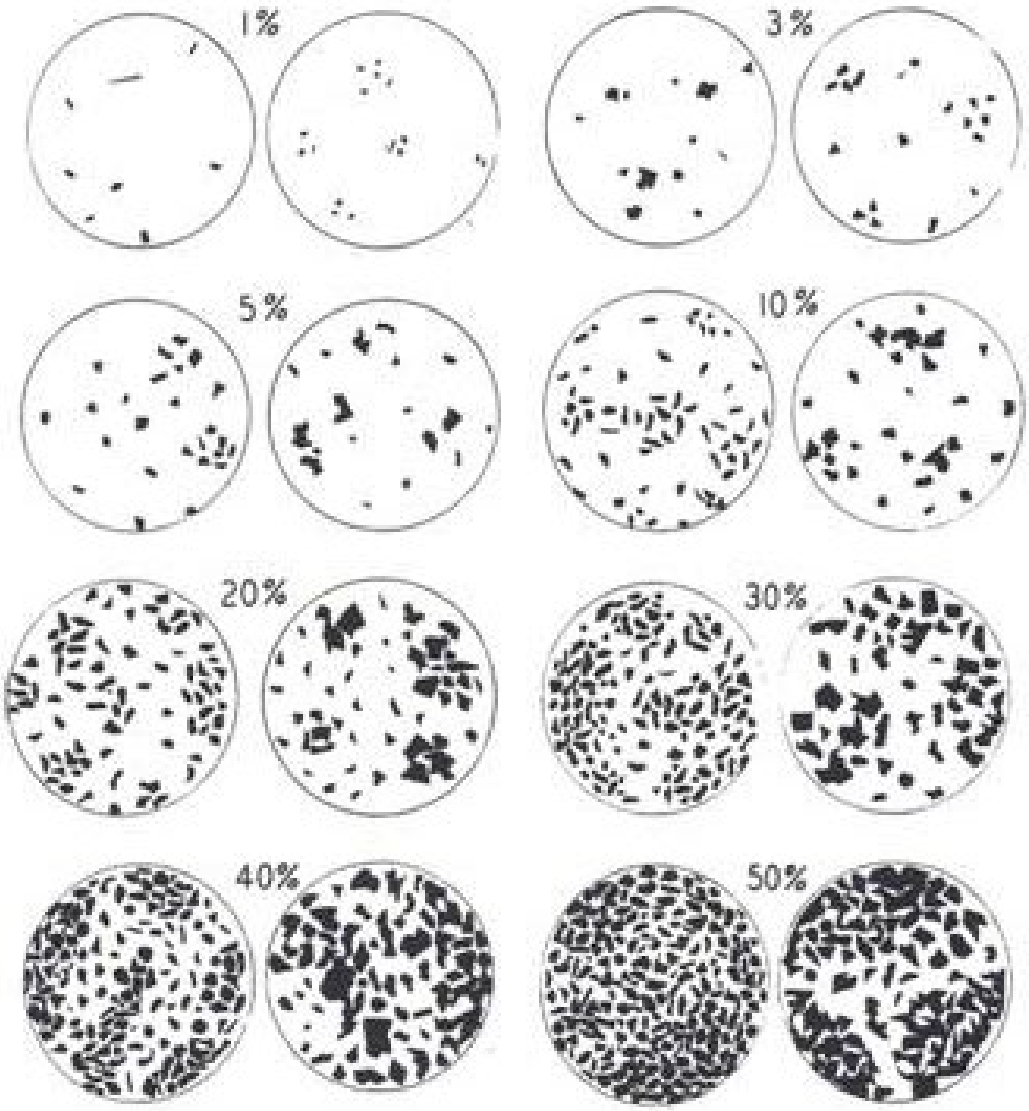

Figure C-1: Comparison Chart for Visual Percentage Estimation (After Terry and Chillingar, 1955)

APPENDIX D

Vertical Spatial Autocorrelation for Effective Water Permeability

The vertical (1D) spatial autocorrelation of the calculated Klinkenberg corrected effective water permeability was evaluated by computing the semivariance of each point pair in the dataset and computing the bin (lag) estimates of average semivariance in increments of 5 ft. Figure 1C provides the variogram cloud of semivariance point-pairs, and the bin mean estimates. A separation distance tolerance of ±2.5 ft. was used to gather point-pairs to estimate the bin means.

Based on the variogram cloud, the permeability data are similarly variable over separation length scales ranging from 0 to 130 feet. The bin means fluctuate about 2e+5 for the entire 130 ft. range, indicating that spatial autocorrelation does not influence these permeability data at the length scales considered.

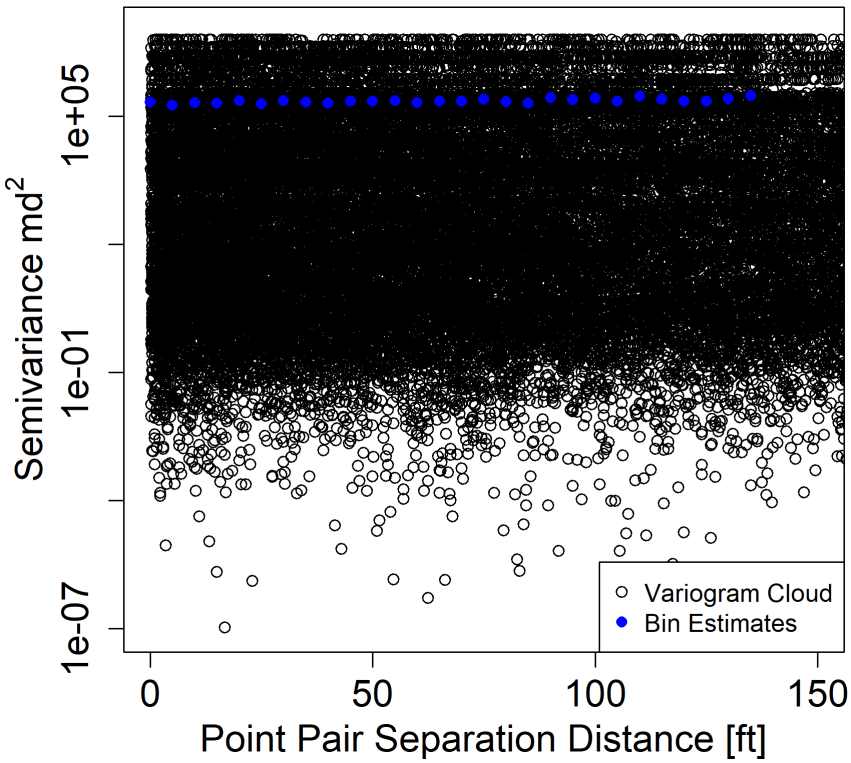

Figure D-1: Variogram cloud and bin (lag) estimates for effective water permeability at 5 ft. intervals from 0 to 150 ft. vertical separation distance.

CATALOG OF SUPPORTING FILES

Tuscarora Sandstone Geophysical Log Digitization: provides details about the well logs digitized, structural maps collected, and information related to oilfield brine geochemistry in West Virginia and Pennsylvania.

Computed Tomography (CT)-scanned data Analysis for the Tuscarora Sandstone: contains details and files related to CT-scan data and methodology used to analyze the Preston 119 well for fracture density estimations.

Estimation of Reservoir Properties for the Tuscarora Sandstone: provides description of the files of porosity and permeability estimations using thin section analysis and minipermeameter, respectively.

Development of 3-D Structural surface model for the Tuscarora Sandstone, Morgantown, WV: provides information of the grid files used to create subsurface maps in GES interpretation software and exported as Zmap-formatted grid files.

Numerical Modeling and Model Uncertainty Analysis for the Potential DDU Geothermal on the WVU Campus-Morgantown, WV: provides details of the numerical simulations to investigate reservoir impedance and thermal production including the input files and output files generated using iTOUGH2/EOS1 simulation.

Reservoir Productivity Uncertainty Analysis for the Tuscarora Sandstone, Morgantown, WV: provides details of the reservoir parameter used along with the stochastic analysis for uncertainty analysis to estimate reservoir productivity for the currently unexplored Tuscarora Sandstone below Morgantown, WV. The results are summarized in figures, spreadsheets, and maps.

Temperature-Depth Estimates for West Virginia University, Morgantown, WV: provides data spreadsheets and figures that summarize the results of a stochastic analysis of temperatures at depth below the West Virginia University campus in Morgantown, WV.

Energy Demand Characterization and Surface Plant Modeling: provides information gathered to determine end-use load and assessment of existing DHS. It also provides Aspen simulation files used to model the hybrid geothermal natural gas GDHC system along with Exchange Design and Rating (EDR) files to design a Plate Heat Exchanger (PHE) and Capital cost estimator project set-up used for capital cost evaluation of surface plant and retrofit distribution lines. In addition, ChemCAD files used for preliminary analysis of conversion of steam-based to hot water-based system are included.

Economic Analysis using GEOPHIRES: contains all the inputs used and outputs produced from the economic analysis for base case, improved system with heat pump and hot water GDHC.

Environmental Calculations: contains all the codes used and results obtained for calculations amount of CO_2 reduction by using a hybrid geothermal system for production of steam over the current coal-based system and natural gas boiler system.

Tuscarora Sandstone Geophysical Log Digitization

The purpose of this document is to describe the contents of information contained within a submission to the Geothermal Data Repository (GDR) node of the National Geothermal Data System (NGDS) in support of Feasibility of Deep Direct-Use Geothermal on the West Virginia University Campus-Morgantown, WV.

Abstract: This dataset contains well log files collected from wells penetrating the Tuscarora Sandstone, structural geologic map of West Virginia and salinity information based on brine geochemistry in West Virginia and Pennsylvania. Detailed descriptions of the contents of this repository are provided below.

Key Words: Appalachian Basin, West Virginia University, Tuscarora Sandstone, LAS Files, Ordovician, Salinity.

Citation: When referencing this data, please use the following citation information:

Title: WVU DDU: Tuscarora Sandstone Geophysical Log Digitization
Author(s): West Virginia Geological and Economic Survey
Date: September 22, 2021

Software Requirement Note:

A combination of proprietary and free software may be required to view some of the information provided. Software used for data analysis and figure creation include ESRI ArcGIS. For GIS map files, you will have to change the directories of the files to match your computer. LAS files were digitized using IHS Petra software, but may be viewed in Microsoft Notepad, or converted to .csv files in Microsoft Excel.

Contents of Submission:

Folder: LAS Files

Contains 90 LAS well log files for wells, in ASCII format. Wells were selected based upon penetration of the Tuscarora Sandstone and log curves were digitized via Petra subsurface mapping software. Geophysical traces will differ from well to well, but normally contain a gamma ray and caliper curves and may also contain a combination of density, porosity, and temperature logs. Logs are sources from the WVGES Oil and Gas wells database. Some of these LAS files are converted to formats that are easier to manipulate and are in the "Modified LAS Files" folder.

Folder: MRS_8_Ordovician Structure

WVGES Publication MRS (Map Reporting Series), Number 8. *West Virginia Gas Development in the Tuscarora and Deeper Formations (with Structural Maps Contoured on Top of Ordovician and Precambrian*: D.H. Cardwell, 1977, 38 p., 1 map, 1:500,000 40"x36". Presents data from about 150 West Virginia wells. Includes "Structural Geologic Map of West Virginia, Datum: Top of Ordovician". Project work performed by the GIS Technical Center at West Virginia University.

1. **Scanned Map Folder**
   Contains scans of original two hard copy maps of Structural Map of West Virginia Datum: Ordovician in TIF format.

2. **Mosaicked Map Folder**
   Contains mosaicked Structural Map of West Virginia Datum: Ordovician in TIF format in compressed folder.

3. **Georeferenced Map Folder**
   Contains georeferenced TIF and clipped georeferenced TIF of Structural Map of West Virginia Datum: Ordovician. Clipped TIF contains less extraneous information but needs color symbology imported from non-clipped georeferenced TIF.

4. **Digitized Map Folder**
   Contains final digitized Structural Map of West Virginia Datum: Ordovician.

5. **Geodatabase Folder**
   Contains a geodatabase of all contour feature datasets for Structural Map of West Virginia Datum: Ordovician.

6. **Documentation Folder**
   Contains Metadata and Methodology for Structural Map of West Virginia Datum: Ordovician and a pdf for the final map.

7. **ReadMe File**
   Contains the information described above.

Folder: Salinity of Oilfield Brines
Contains references and tabular data related to oilfield brine geochemistry in West Virginia and Pennsylvania.

1. **File:Chemistry of Oil and Gas Well Brines in Western Pennsylvania (Drexel, 1985).xlsx**
   Contains data transcribed from Tables 2 and 3 of Dresel and Rose, 2010, which were originally published by Dresel (1985) as an internal Pennsylvania Geological Survey publication.

2. **File: Dresel and Rose_2010_Geochemical Origin of Oilfield_Brines_PA**
   PAGS Publication, *Chemistry and origin of oil and gas well brines in western Pennsylvania*: Dresel, P. E., and Rose, A. W., 2010, Pennsylvania Geological Survey, 4th ser., Open-File Report OFOG 10–01.0, 48 p., Portable Document Format (PDF). URL:https://www.fwspubs.org/doi/suppl/10.3996/052013-JFWM-033/suppl_file/patnodereference+s3.pdf.

3. File: Vol 8_ Salt Brines of WV

WVGES publication V-8, *Salt Brines of West Virginia*: P. H. Price, C. E. Hare, J. B. McCue, and H. A. Hoskins, 1937, 203 p, 23 pl, 18 f. History of the salt brine industry in West Virginia, geology of the brine-bearing regions, and chemical analyses of 189 brines.

Computed Tomography (CT)-scanned data Analysis for the Tuscarora Sandstone

The purpose of this document is to describe the contents of information contained within a submission to the Geothermal Data Repository (GDR) node of the National Geothermal Data System (NGDS) in support of Feasibility of Deep Direct-Use Geothermal on the West Virginia University Campus-Morgantown, WV.

Abstract: This dataset contains CT scan images collected from the cores obtained from Clay 513, Harrison 79, and Preston 119 wells. Additional processing of the CT scan data from Preston 119 well is performed to semi-quantitatively assess fracture volume. These results are summarized in figures, and spreadsheets. Detailed descriptions of the contents of this repository are provided below.

Key Words: Appalachian Basin, West Virginia University, Tuscarora Sandstone, Computed Tomography, Image J.

Citation: When referencing this data, please use the following citation information:

Title: WVU DDU: Computed Tomography (CT)-scanned data Analysis for the Tuscarora Sandstone

Author(s): West Virginia Geological and Economic Survey

Date: September 22, 2021

Software Requirement Note:

Free software may be required to view some of the information provided. Software used for data analysis include ilastik, FIJI and ImageJ2.

Contents of Submission:

Folder: DDU Geothermal_Clay 513_CT scans

Contains image files for Medical CT scans of the Clay 513 well. These images are a reslice through the center of the core and represent a 2D image of the core. Color variations are a proxy for density differences in the core. Each image represents a scan from one core box, ~ 3 feet in length.

Folder: DDU Geothermal_Harrison 79_CT scans

Contains an image file for a Medical CT scan of the Harrison 79 well. This image is a reslice through the center of the core and represent a 2D image of the core. Color variations are a proxy for density differences. The image represents a scan from one core box, ~ 3 feet in length.

Folder: Preston_119_CT scan data

Contains Characterization data collected from analysis of the Preston 119 core. CT scanning was collected with a Toshiba® Aquilion TSX-101A/R medical scanner. The CT scanner generates images with a resolution in the millimeter range, with scans having voxel resolutions of 0.43 x 0.43 mm in the XY plane and 0.50 mm along the core axis. The scans were conducted at a voltage of 135 kV and at a current of 200 mA. Subsequent processing and combining of stacks were performed to create three-dimensional (3D) volumetric representations using ImageJ to produce Tiff stacks. The variation in grayscale values

observed in the CT images indicates changes in the CT number obtained from the scans, which is directly proportional to changes in the attenuation and density of the scanned rock. Darker regions are less dense and absorb less x-rays.

i. Exported segmented files

Contains the files produced after segmentation in ilastik. They can be viewed in several image processing programs including ImageJ2 or FIJI. After importing the segmented tiff stack for a core section into one of the image processing programs you can view the volumes and calculate the percentages by following the instructions in the '% volume by CT calc' PowerPoint. The background (air/outside) is subtracted, and the percent volume of fractures can be determined for the entire sample. These segmentations and associated calculations were performed on entire scans (2-to-3-foot sections of core, one length of core box); these can be refined if a small subset is chosen. With a smaller subset, additional artifacts can be removed such as beam hardening and edge effects.

ii. ilastik segmented files

Contains files produced using the interactive learning and segmentation toolkit ilastik. The premise of isolating features is to first segment out the feature based on its unique grayscale value. Once this isolation has occurred, the next steps are to differentiate multiple isolated features and then combine them into one coherent visual representation.

iii. Tiff stacks

The 'Tiff stacks' folder contains the original stacks collected from the medical scanner in a .h5 format which is easier to use in ilastik. The grayscale values in the Tiff stacks were used to isolate and visually differentiate objects of interest in the scans (in this case: matrix, fractures and air/outside).

iv. % volume by CT calc.pptx

Contains explanation of how volume percentages were calculated in FIJI/imageJ2 after segmentation.

v. CT summary.docx

Contains explanation of the parameters used in CT data collection and how segmentation was used to produce volume percentages.

vi. CT_Read_me.txt

Contains explanation of the files in this folder.

vii. Netl-trs-9-2018-ct-of-the-tuscarora-sandstone-from-the-preston-119-weel-final-20180509

Contains technical report produced by NETL on the CT scanning of the Preston 119 core.

viii. Tusc fracture volumes by CT v3 all boxes.xlsx

Contains fracture volume percentage of the Preston 119 well after filtering to remove edge effects. The data is listed by tiff stack, which represents one core box or approximately 3 feet of core.

ix. Preston 119 CT scan fracture estimation.xlsx

Contains early version of fracture volume percentage of the Preston 119 well after filtering to remove edge effects. The data is listed by tiff stack, which represents one core box or approximately 3 feet of core.

Estimation of Reservoir Properties for the Tuscarora Sandstone

The purpose of this document is to describe the contents of information contained within a submission to the Geothermal Data Repository (GDR) node of the National Geothermal Data System (NGDS) in support of Feasibility of Deep Direct-Use Geothermal on the West Virginia University Campus-Morgantown, WV.

Abstract: This dataset contains black-and-white photographic images of individual core segments from well Preston 119 and photomicrographs taken of petrographic thin sections from well Clay 513. Minipermeameter measurement results of 2,260 samples for fracture and matrix permeability on core segments for well Preston 119. These results are summarized in figures, spreadsheets, and PowerPoints. Detailed descriptions of the contents of this repository are provided below.

Key Words: Appalachian Basin, West Virginia University, Tuscarora Sandstone, minipermeameter, thin section analysis.

Citation: When referencing this data, please use the following citation information:

Title: WVU DDU: Estimation of Reservoir Properties for the Tuscarora Sandstone
Author(s): West Virginia Geological and Economic Survey
Date: March 19, 2020

Software Requirement Note:

Proprietary software may be required to view some of the information provided. Microsoft Excel will be necessary to examine the permeability data and software capable of reading a .PDF file will be needed to view the file of annotated core CT scans. Microsoft PowerPoint will be necessary to view the photomicrograph presentation.

Contents of Submission:

File: Preston-119_FINAL_core_permeability_illustrated.xlsx
Excel spreadsheet containing experimental results of 2,260 samples of fracture and matrix permeability on core segments for well Preston 119. Includes measurements of fracture orientation, fracture length, and hyperlinked photographic images of individual core segments. NOTE: hyperlinked images are all resident in folder **/Preston_119/permeability_photos**.

File: Tus_XZ_slices_scaled_Preston-119_annotated.pdf
Standard PDF file containing black-and-white photographic images of individual core segments from well Preston 119. Each segment has a scale with the image. In addition, visible fractures have been annotated by tracing them in red.

File: Clay_513 Thin Section Photos_RMcDowell.pptx
PowerPoint slide presentation of color photomicrographs taken of petrographic thin sections from well Clay 513. Seventeen (17) slides with scale and explanation of content – features of special interest have been annotated.

Folder: Preston_119

1. **permeability_photos**

Collection of 335 color JPG images of the permeability sampling locations for each individual core segment from well Preston 119 examined for fracture permeability. NOTE: these images are referenced by hyperlink in file Preston-119_FINAL_core_permeability_illustrated.xlsx. This folder/subfolder arrangement and naming convention must be maintained for hyperlink access to work correctly from the Excel file.

References

McCleery, R.S., J.P. Moore, R.R. McDowell, N. Garapati, T.R. Carr, and B.J. Anderson. (2018). Development of 3-D geological model of Tuscarora Sandstone for feasibility of deep direct-use geothermal at West Virginia University's main campus. *GRC Transactions*, *42*. Pp. 192-208.

Development of 3-D Structural surface model for the Tuscarora Sandstone, Morgantown, WV

The purpose of this document is to describe the contents of information contained within a submission to the Geothermal Data Repository (GDR) node of the National Geothermal Data System (NGDS) in support of Feasibility of Deep Direct-Use Geothermal on the West Virginia University Campus-Morgantown, WV.

Abstract: This dataset contains grid files for subsurface maps created in GES interpretation software and exported as Zmap formatted grid files. Depth values in SSTVD (subsea true vertical depth). Detailed descriptions of the contents of this repository are provided below. The methods used for analysis and a detailed discussion of the results are presented in a paper by McCleery et al., (2018).

Key Words: Appalachian Basin, West Virginia University, Tuscarora Sandstone, 3-D structural surface, Conformable gridding

Citation: When referencing this data, please use the following citation information:

Title: WVU DDU: 3-D Structural Surface Model of Tuscarora Sandstone for Morgantown, WV

Author(s): West Virginia University

Date: March 19, 2020September 22, 2021

Contents of Submission:

Folder: SubsurfaceGridfiles

Contains grid files for surface tops of the six key tops identified. The tops picked were LNG (unnamed marker-bed), TLLY (Tully Fm.), ONDG (Onondaga Fm.), ORISK (Oriskany Fm.), TUSC (Tuscarora Fm.), and JUNI (Juniata Fm.).

Contents

1. **File: LNG_ SSTVD_TopSurface.txt**
   LNG marker is the shallowest (youngest) horizon and has the most well control.

2. **File: TLLY_after_LNG_SSTVD.txt**
   Tully formation is the next deepest horizon and was gridding using the previous grid as a trend-grid, influencing the shape of this grid, which has fewer data points.

3. **File: ONDG_after_TLLY_SSTVD.txt**
   Onondaga formation is the next deepest horizon and was gridding using the previous grid as a trend-grid, influencing the shape of this grid, which has fewer data points.

4. **File: ORSK_after_ONDG_SSTVD.txt**
   Oriskany formation is the next deepest horizon and was gridding using the previous grid as a trend-grid, influencing the shape of this grid, which has fewer data points.

5. **File: TUSC_after_ORSK_SSTVD.txt**
   Tuscarora formation is the next deepest horizon and was gridding using the previous grid as a trend-grid, influencing the shape of this grid, which has fewer data points.

6. **File: JUNI_after_TUSC_SSTVD.txt**
   Juniata formation (base of Tuscarora): is the next deepest horizon and was gridding using the previous grid as a trend-grid, influencing the shape of this grid, which has fewer data points.

7. **File: TUSC_to_JUNI_ISOCHORE.txt**
   Isochore of top Tuscarora to top Juniata, i.e., Tuscarora isochore.

8. **File: README.txt**
   provides details about the files in the folder.

References

McCleery, R.S., J.P. Moore, R.R. McDowell, N. Garapati, T.R. Carr, and B.J. Anderson. (2018). Development of 3-D geological model of Tuscarora Sandstone for feasibility of deep direct-use geothermal at West Virginia University's main campus. *GRC Transactions*, *42*. Pp. 192-208.

Numerical Modeling and Uncertainty Analysis for the Potential DDU Geothermal on the WVU Campus-Morgantown WV

The purpose of this document is to describe the contents of information contained within a submission to the Geothermal Data Repository (GDR) node of the National Geothermal Data System (NGDS) in support of Feasibility of Deep Direct-Use Geothermal on the West Virginia University Campus-Morgantown, WV.

Abstract: To reduce the geothermal exploration risk, a feasibility study is performed for a deep direct-use system proposed at the West Virginia University (WVU) Morgantown campus. This study applies numerical simulations to investigate reservoir impedance and thermal production. Because of the great depth of the geothermal reservoir, few data are available to characterize reservoir features and properties. As a result, the study focuses on the following three aspects: 1. model choice for predicting reservoir impedance and thermal breakthrough: after investigating three potential models (one single permeability model and two dual permeability models) for flow through fractured rock, it is decided to use single permeability model for further analysis; 2. well placement (horizontal vs. vertical) options: horizontal well placement seems to be more robust to heterogeneity and the impedance is more acceptable; 3. Prediction uncertainty: the most influential parameters are identified using a First-Order-Second-Moment uncertainty propagation analysis, and the uncertain range of the model predictions is estimated by performing a Monte Carlo simulation. Heterogeneity has a large impact on the perdition, therefore, is considered in the predictive model and uncertainty analysis. The numerical model results and uncertainty analysis are used for economic analysis. The dataset submitted here support the described study.

Key Words: Direct-Use Geothermal, West Virginia University, Tuscarora Sandstone, reservoir flow model, permeability, matrix, fracture, uncertainty analysis.

Citation: When referencing this data, please use the following citation information:

Title: Modeling Study of Deep Direct Use Geothermal on the West Virginia University Campus-Morgantown, WV

Author(s): Yingqi Zhang[1], Nagasree Garapati[2], Christine Doughty[1], Pierre Jeanne[1]

1. Lawrence Berkeley National Laboratory, Berkeley
2. Department of Chemical and Biomedical Engineering, West Virginia University

Date: March 19, 2020September 22, 2021

Contents of Submission:

Description: This dataset contains input/output data used in the model study of the potential deep direct-use geothermal on the West Virginia University Campus-Morgantown, WV, and data used in the model uncertainty analysis. The data and result figures are described in the final report (as well as in manuscript that will be submitted to Geothermics). Here we provide a brief description of each set of data:

1. **SingleK_Figure3.zip:** contains input/output files for the base case single permeability with vertical well layout model analysis. Figure 3 and part of Figure 2 (the plot for single K) of the manuscript and final report is produced from the output data in this set. This set also contains the post-processing python file to extract data in 2D for plotting purpose.

2. **DualK1.zip and DualK2.zip:** contain the input/output files for the two-dual permeability with vertical well layout models described in the manuscript and final report. Part of Figure 2 (the two lines for dual K) the manuscript and final report is produced from the output data in this set.

3. **Mtest_Figure4_5.zip:** contains the input/output files of the Mtest case with vertical well layout described in the manuscript and final report. It also contains the result data files for Figures 4 and 5 in the manuscript.

4. **Figure6_7.zip:** contains the input/output files for the single K model with horizontal well layout described in the manuscript and final report. The results from this set of simulation appeared in the final report and manuscript Figure 6 and part of Figure 7 in the manuscript.

5. **Figure7.zip:** contains the input/output files for the single K heterogeneous model with horizontal well layout described in the manuscript and final report. The results are used to produce Figure 7.

6. **Fosim_horizontal.zip:** contains input/output files for the FOSM analysis described in input/output files for the single K model with horizontal well layout described in the manuscript and final report. The results are summarized in Table 3.

7. **MC_allPara2_input.7z_AppendixFigure8:** contains input files used in the Monte Carlo simulation analysis described in the manuscript and final report.

8. **MC_allPara2_output.7z_AppendixFigure8:** contains output files used in the Monte Carlo simulation analysis. Results are used in generating Figure 8 in the manuscript and final report.

9. **BaseCase_run_F9.zip, HighG_run_F9.zip, LowG_run_F9.zip:** contains input/output used in the initial temperature uncertainty analysis described in the manuscript and final report. Results are used in generating Figure 9 of the manuscript. HighG represent high geothermal gradient case and LowG represents low geothermal gradient case.

References

Finsterle, S. (2004). Multiphase inverse modeling: review and iTOUGH2 applications. Vadose Zone Journal, 3 (2004), pp. 747-762.

Reservoir Productivity Uncertainty Analysis for the Tuscarora Sandstone, Morgantown, WV

The purpose of this document is to describe the contents of information contained within a submission to the Geothermal Data Repository (GDR) node of the National Geothermal Data System (NGDS) in support of Feasibility of Deep Direct-Use Geothermal on the West Virginia University Campus-Morgantown, WV.

Abstract: This dataset contains figures that summarize the Tuscarora Sandstone core permeability data collected from the Preston 119 well in Preston County, WV, and summary results of a stochastic analysis that was used to estimate reservoir productivity for the currently unexplored Tuscarora Sandstone below Morgantown, West Virginia. Uncertainties in reservoir productivity considered the thickness of the reservoir, rock permeability, and fluid viscosity. A Monte Carlo analysis of these uncertain properties was used to predict reservoir flow productivity for the case of a matrix-dominated reservoir, and a fracture-dominated reservoir. These results are summarized in figures, spreadsheets, and maps. Detailed descriptions of the contents of this repository are provided below.

Supporting data for this analysis was provided by the West Virginia Geologic and Economic Survey (McDowell et al., 2018). The methods used for analysis and a detailed discussion of the results are presented in a paper by Smith (2019). Some of the information used for this uncertainty analysis are provided in other data and code repositories that describe methods for Monte Carlo uncertainty analysis of natural reservoir productivity in the Appalachian Basin (Camp et al., 2018), natural reservoir productivity analysis results for the Appalachian Basin (GDR submission #881; Cornell University, 2016), and the original code used for that analysis (Whealton and Smith, 2015). The code was updated for use in this analysis, and the updated code is provided in this repository.

The Appalachian Basin reservoir productivity maps provided in Cornell University (2016) are updated in this repository by adding the Morgantown Tuscarora to the maps. In contrast to all other reservoirs, the Morgantown Tuscarora is not yet known to exist with the properties assumed in this study because a well has not been drilled to the Tuscarora depth below Morgantown.

Key Words: Appalachian Basin, West Virginia University, Tuscarora Sandstone, sedimentary reservoir, reservoir flow geometry, reservoir productivity assessment, permeability, matrix, fracture, uncertainty analysis.

Citation: When referencing this data, please use the following citation information:

Title: WVU DDU: Tuscarora Sandstone Flow Productivity Uncertainty Analysis Results for Morgantown, WV

Author(s): West Virginia University, Cornell University

Date: March 19, 2020September 22, 2021

Dependencies:

The MATLAB code depends on the function “csvwrite_with_headers.m” by Keith Brady (n.d.).

Contents of Submission:

Folder: AppalachianBasinReservoirShapefiles

Contains a shapefile of the Appalachian Basin reservoirs that were evaluated as potential geothermal reservoirs in the Geothermal Play Fairway Analysis of the Appalachian Basin (Camp et al., 2018; original shapefile from Cornell University, 2016). To this shapefile, a polygon for the Morgantown Tuscarora Sandstone was added. A figure of that polygon is provided. The attribute table for the shapefile is described in the Cornell University (2016) GDR submission and associated content links.

Contents

1. **Shapefile: GPFAReservoirs2018.dbf, GPFAReservoirs2018.prj, GPFAReservoirs2018.qpj, GPFAReservoirs2018.shp, and GPFAReservoirs2018.shx**
   The Appalachian Basin reservoir dataset updated with information for Morgantown Tuscarora.

2. **File: Figure1_Map_MorgantownTuscaroraEstimatedSpatialExtent.png**
   Map of the estimated spatial extent of the Tuscarora reservoir for Morgantown. A description of the assumptions made to determine the spatial extent is provided in Smith (2019).

Folder: Preston119_PermeabilityDataAnalysis

Contains figures illustrating the permeability data collected from core measurements sampled from the Preston 119 well in Preston County, WV. Raw air permeability-depth data were provided by the West Virginia Geologic and Economic Survey (WVGES) (McDowell et al., 2018).

Contents:

1. **File: WaterPermeabilityDepthPreston119_NoClosedFracs_Avg_log.png**
   Figure of the Klinkenberg-estimated water permeability for the Preston 119 well's Tuscarora core permeability measurements. This plot provides only those measurements that were sampled on fractures that would likely be open at depth, corresponding to dips greater than 20° (colored points) and other features, like matrix rock (black points). The plotted points correspond to the average of the three measurements that were taken in each location. It is plotted in log-space on the x-axis.

2. **Files: WaterAvgPermBreakdown_NoClosedFracs_NewLegend.png, and WaterAvgPermBreakdown_NoClosedFracs.png**
   Histograms of the Preston 119 permeability data colored by the type of feature. The plot with "NewLegend" in the title appears in Smith (2019).

3. **File: LNfitAvgWaterPerm_Mat.png**
   Lognormal distribution fits to the observed matrix rock permeability in the Preston 119 Tuscarora core.

4. **Files: LNfitAvgWaterPerm_All_OpenFracs.png, and LNfitGeomWaterPerm_All_OpenFracs.png**

Lognormal distributions fit to the average (LNfitAvg) or geometric mean (LNfitGeom) of bootstrapped random samples of the Preston 119 permeability data. All features were considered, and only likely open fractures at depth were considered.

5. **File: PermVario_OpenFracs_log.png**
   Variogram cloud and mean estimates of log(water permeability) along the core of the Preston 119 Tuscarora. Only likely open fractures at depth were considered.

Folder: TuscaroraReservoirProductivityAnalysis
Contains the code used for analysis (modified from Whealton and Smith, 2015), input data, and output results for the reservoir productivity uncertainty analysis.

Contents

1. **Folder: Code**
   a. **File: GenRandNums.m**
      Random number generation file modified from Whealton and Smith (2015) to meet the requirements of the Morgantown Tuscarora analysis.
   b. **File: Main_Productivity.m**
      Main script used to run the uncertainty analysis, modified from Whealton and Smith (2015) to meet the requirements of the Morgantown Tuscarora analysis.
   c. **File: MonteCarloApprox.m**
      Monte Carlo script modified from Whealton and Smith (2015) to meet the requirements of the Morgantown Tuscarora analysis.

2. **Folder: InputDatasets**
   a. **File: UncertaintyLevels09-09-16.csv**
      File describing the uncertainty levels, as described in Camp et al. (2018).
   b. **File: RPIw_MorgantownTuscarora_Mat.csv**
      File describing the distributions and parameters for the uncertainty analysis of the RPIw flow productivity metric for matrix rock.
   c. **File: RFC_MorgantownTuscarora_Mat.csv**
      File describing the distributions and parameters for the uncertainty analysis of the RFC flow productivity metric for matrix rock.
   d. **File: RFC_MorgantownTuscarora_All.csv**
      File describing the distributions and parameters for the uncertainty analysis of the RFC flow productivity metric for all features observed in the Preston 119 core permeability dataset. Only likely open fractures were considered in this analysis.

3. **Folder: Results**
   a. **Folder: RFC_MatOpenFracs**
      RFC for "all" permeability data, which considers the permeability distribution for matrix rock and fractures likely to be open at depth (Smith, 2019)
      i. **File: RFC_MorgantownTuscarora_Results_All.csv**
         contains summary information, including the mean, standard deviation, coefficient of variation, and percentiles of the Monte Carlo distributions

for the RFC for all permeability data with likely open fractures for each RsvNum (scenario).

ii. **File: RFC_MorgantownTuscarora_ResultsAll_All.csv**
contains all Monte Carlo replicates for each RsvNum (scenario). The summary data were computed from this spreadsheet.

iii. **Files: MorgantownTuscaroraAllRFCs.png, and MorgantownTuscaroraAllRFCs_GeomMean.png**
Histogram of the RFC Monte Carlo replicates from the RFC_MorgantownTuscarora_ResultsAll_All.csv results corresponding to the geometric mean (GeomMean file) and the average fracture-dominated permeability.

iv. **Files: EcdfPlot_RFCAll_ArithGeoMean.png**
Empirical cumulative distribution plots for the RFC replicates corresponding to arithmetic mean and geometric mean fracture-dominated permeability. Results are plotted for different probability distribution assumptions, and different average reservoir thicknesses.

v. **Files: RiskMap_RFC_AllOpenFracs.png, and RiskMap_RFC_All_CV.png**
Maps of the Appalachian Basin reservoir mean and coefficient of variation (CV) for the RFC. For Morgantown, these maps display the arithmetic mean fracture-dominated permeability results.

vi. **Files: RiskMap_RFC_AllOpenFracs_GeoMean.png, and RiskMap_RFC_All_CV_GeoMean.png**
Maps of the Appalachian Basin reservoir mean and coefficient of variation (CV) for the RFC. For Morgantown, these maps display the geometric mean fracture-dominated permeability results.

b. Folder: RFC_Matrix

RFC for matrix permeability data only.

i. **File: RFC_MorgantownTuscarora_Results_Mat.csv**
contains summary information, including the mean, standard deviation, coefficient of variation, and percentiles of the Monte Carlo distributions for the RFC for matrix rock for each RsvNum (scenario).

ii. **File: RFC_MorgantownTuscarora_ResultsAll_Mat.csv**
contains all Monte Carlo replicates for each RsvNum (scenario). The summary data were computed from this spreadsheet.

iii. **File: MorgantownTuscaroraMatrixRFCs.png**
Histogram of the RFC Monte Carlo replicates from RFC_MorgantownTuscarora_ResultsAll_Mat.csv.

c. Folder: RPIw_Matrix

RPIw for matrix permeability data only.

i. File: RPIw_MorgantownTuscarora_Results_Mat.csv
contains summary information, including the mean, standard deviation, coefficient of variation, and percentiles of the Monte Carlo distributions for the RPI for matrix rock for each RsvNum (scenario).

ii. File: RPIw_MorgantownTuscarora_ResultsAll_Mat.csv
contains all Monte Carlo replicates for each RsvNum (scenario). The summary data were computed from this spreadsheet.

iii. Files: EcdfPlot_RPIwMat.png, and EcdfPlot_RPIwMat_newCols.png
Empirical cumulative distribution plot for the RPIw replicates. Results are plotted for different well separations and different probability distribution assumptions. The color scheme is different between these two files.

iv. File: MorgantownTuscaroraMatrixRPIw.png
Histogram of the RPIw Monte Carlo replicates from RPIw_MorgantownTuscarora_ResultsAll_Mat.csv.

v. Files: RiskMap_RPIw_Mat.png, and RiskMap_RPIw_Mat_CV.png
Maps of the Appalachian Basin reservoir mean and coefficient of variation (CV) for the RPIw. For Morgantown, these maps display the matrix dominated RPIw results.

d. Files: RPIResults_Morgantown_2018.csv, and RPIResults_Morgantown_2018_Geom.csv
Results of the reservoir productivity index (RPI) and reservoir flow capacity (RFC) for Appalachian Basin reservoirs, including one row for the Morgantown Tuscarora (number 1964). For the Morgantown Tuscarora, both spreadsheets have the RPI for matrix rock. For the Morgantown Tuscarora, the RFC for the geometric mean fracture-dominated permeability is reported in the Geom file, and the RFC for average fracture-dominated permeability is provided in the other file. Other reservoirs have the productivity as reported in Camp et al. (2018) (from Cornell University, 2016).

References

Brady, K. (n.d.). csvwrite_with_headers.m [code]. Retrieved on Nov. 17, 2019 from https://www.mathworks.com/matlabcentral/fileexchange/29933-csv-with-column-headers?focused=5176300&tab=function.

Camp, E., T.E. Jordan, M.J. Hornbach, and C.A. Whealton. (2018). A probabilistic application of oil and gas data for exploration stage geothermal reservoir assessment in the Appalachian Basin. Geothermics, 71. Pp. 187 – 199.

Cornell University. (2019). Appalachian Basin Temperature-Depth Maps and Structured Data in support of Feasibility Study of Direct District Heating for the Cornell Campus Utilizing Deep Geothermal Energy [data set]. Retrieved from http://gdr.openei.org/submissions/1182.

Cornell University. (2016). Natural Sedimentary Reservoirs Data Geothermal Play Fairway Analysis 2016 Revision [data set]. Retrieved from http://gdr.openei.org/submissions/881.

McDowell, R., J. Lewis, and G. Daft, compilers. (2018). Permeability data acquired by direct air injection from the Silurian Tuscarora Sandstone interval – Preston 119 drill core [dataset]. West Virginia Geological and Economic Survey.

Smith, J.D.. (2019). A stochastic evaluation of geothermal reservoir potential for the Tuscarora Sandstone in Morgantown, West Virginia, USA. 43rd GRC Annual Meeting & Expo, Palm Springs, CA. Sept. 16.

Whealton, C.A., and J.D. Smith. (2015). geothermal_pfa/reservoir_ideality [code]. GitHub repository commit from Apr 7, 2015 with label cfea0214311535f9c16272ce825f3550fdfc5ec1 retrieved from https://github.com/calvinwhealton/geothermal_pfa/tree/master/reservoir_ideality.

Temperature-Depth Estimates for West Virginia University, Morgantown, WV

The purpose of this document is to describe the contents of information contained within a submission to the Geothermal Data Repository (GDR) node of the National Geothermal Data System (NGDS) in support of Feasibility of Deep Direct-Use Geothermal on the West Virginia University Campus-Morgantown, WV.

Abstract: This dataset contains data spreadsheets and figures that summarize the results of a stochastic analysis of temperatures at depth below the West Virginia University campus in Morgantown, WV. These results are extracted from a study by Smith (2019), whose results are included in a GDR submission that provides rasters and shapefiles for the Appalachian Basin states of New York, Pennsylvania, and West Virginia (GDR submission #1182). Uncertainties considered included geologic properties, thermal properties, and uncertainty from geostatistical interpolation of the surface heat flow. A Monte Carlo analysis of these uncertain properties was used to predict temperatures at depth using a 1-D heat conduction model. For the pixel corresponding to West Virginia University, a .csv file containing the 10,000 temperature-depth profiles estimated from a Monte Carlo analysis is provided. Temperatures are provided for depths from 1-5 km in 0.5 km increments. These data are summarized in a figure containing violin plots that illustrates the probability of obtaining certain temperatures at depth for Morgantown. Detailed descriptions of the contents of this repository are provided below.

Key Words: Appalachian Basin, West Virginia, West Virginia University, low-temperature geothermal, resource assessment, uncertainty analysis.

Citation: When referencing this data, please use the following citation information:

Title: WVU DDU: Temperature-Depth Estimates
Author(s): West Virginia University, Cornell University
Date: March 19, 2020September 22, 2021

Contents of Submission:

Main Folder: WVUMorgantown_TemperaturesDepthData

Contents:

1. **File: 355347_MorgantownTemperatureDepthReplicates.csv**
   File containing the 10,000 replicates of temperature-depth estimates for the pixel corresponding to West Virginia University in Morgantown, WV, from the Appalachian Basin temperature-depth resource assessment by Smith (2019). The number 355347 is the pixel index number on the maps in the Appalachian Basin Temperature Depth Maps in GDR submission #1182.
   Columns:
   rep: the replicate ID number, from 0 – 9999.
   TXkm, TXp5 km, TBase: temperature estimated at X km, X.5 km, and basement depth, respectively.

2. **File: MorgantownTemperaturesAtDepth.png**
   Violin plots of the temperatures at depth for WVU campus-Morgantown. Data for the violin plots are from the 355347_MorgantownTemperatureDepthReplicates.csv file.

References

Cornell University. (2019). Appalachian Basin Temperature-Depth Maps and Structured Data in support of Feasibility Study of Direct District Heating for the Cornell Campus Utilizing Deep Geothermal Energy [data set]. Retrieved from http://gdr.openei.org/submissions/1182.

Cornell University. (2016). Appalachian Basin Play Fairway Analysis Thermal Risk Factor and Quality Analyses [data set]. Retrieved from http://gdr.openei.org/submissions/879.

Cornell University. (2015). Appalachian Basin Play Fairway Analysis: Thermal Quality Analysis in Low-Temperature Geothermal Play Fairway Analysis (GPFA-AB) [data set]. Retrieved from http://gdr.openei.org/submissions/638.

Smith, J.D. (2019). Exploratory spatial data analysis and uncertainty propagation for geothermal resource assessment and reservoir models. PhD Thesis, Cornell University, Ithaca, NY.

Smith, J.D. (2016). Analytical and geostatistical heat flow modeling for geothermal resource reconnaissance applied in the Appalachian Basin. MS Thesis, Cornell University, Ithaca, NY.

Energy Demand Characterization and Surface Plant Modeling

The purpose of this document is to describe the contents of information contained within a submission to the Geothermal Data Repository (GDR) node of the National Geothermal Data System (NGDS) in support of Feasibility of Deep Direct-Use Geothermal on the West Virginia University Campus-Morgantown, WV.

Abstract: This dataset provides information gathered to determine end use load and assessment of existing DHS. It also provides Aspen simulation files used to model hybrid geothermal natural gas GDHC system along with Exchange Design and Rating (EDR) files to design Plate Heat Exchanger (PHE) and Capital cost estimator project set up used for capital cost evaluation of surface plant and retrofit distribution lines. In addition, ChemCAD files used for preliminary analysis of conversion of steam-based to hot water-based system are included. Detailed descriptions of the contents of this repository are provided below.

Key Words: Appalachian Basin, West Virginia University, Hybrid Geothermal natural gas system, Deep direct-use, ASPEN HYSYS, ACCE, ChEMCAD.

Citation: When referencing this data, please use the following citation information:

Title: WVU DDU: Surface Plant Analysis for GDHC at WVU campus, Morgantown, WV

Author(s): West Virginia University

Date: March 19, 2020September 22, 2021

Software Requirement Note:

A combination of proprietary and free software may be required to view some of the information provided. Software used for surface modeling, capital cost analysis includes ASPEN Suite (HYSYS, EDR, ACCE). For ACCE template files, you will have to change the directories of the files to match your computer.

Contents of Submission:

Folder: Facilities

Contains files gathered to determine end use load.

Contents

1. **Folder: SteamMeterReadings**
   Contains monthly recorded data of steam temperature, pressure flowrate along with condensate flow rate and temperature at four (Med center, Towers, Ag. Science, Downtown) distribution points along with gas data at the buildings where natural gas boilers are located.

2. **File. MEA OneLine.pdf**
   One-line drawing of current Morgantown Energy Association's (MEA) distribution pipelines with meter points along with linear pipe distances, and pipe sizes.

3. **File: Pipeline elevations_GoogleMaps.docx**
   Contains figures of google map estimations of the pipeline elevations between the distribution points.

4. **File: MEA Meter Points Google Maps.xlsx, Evansdale Campus Distances.xlsx**
   Google map showing the current locations of meter points and the distribution pipeline path, pipelines in red are owned by MEA and in green are owned by WVU.

Folder: ASPEN
Contains ASPEN files related to hybrid geothermal natural gas system.
Contents

1. **Folder: HYSYS**
   a. **File: scenario1.hsc, scenario2.hsc**
      Aspen HYSYS files for modeling hybrid GDHC system to produce steam at 250 PSIG and 500°F for entire campus (Scenario1), and to produce saturated steam for supplying Evansdale and Health Science campus (Scenario 2).
   b. **File: scenario1_heatpump.hsc, scenario2_heatpump.hsc**
      Aspen HYSYS files for modeling improved hybrid GDHC system with a heat pump to produce steam at 250 PSIG and 500°F for entire campus (Scenario1), and to produce saturated steam for supplying Evansdale and Health Science campus (Scenario 2).

2. **Folder: EDR**
   a. **File: GEO-PHE_Sceanrio1.EDR, GEO-PHE_Sceanrio2.EDR**
      Aspen Exchange Design and Rating (EDR) files to design plate and heat exchanger (PHE) for scenario 1 and scenario 2 for hybrid GDHC system.
   b. **File: GEO-PHE_Sceanrio1_HeatPump.EDR, GEO-PHE_Sceanrio2_HeatPump.EDR**
      Aspen EDR files to design PHE for scenario 1 and scenario 2 for improved hybrid GDHC system with heat pump.

3. **Folder: ACCE**
   a. **Folder: Distribution**
      Aspen ACCE template file used to calculate the capital cost of pipelines for distribution network.
   b. **Folder: Equipment**
      Aspen ACCE template file used to calculate the capital cost of PHE and condensate tank.

Folder: ChemCAD
Contains files related to hot water-based geothermal system.
Contents

1. **File: Total Integrated Design_Hotwater.cc7**
   ChemCAD file used to model the hot water geothermal system for Evansdale and Health Science campuses.

2. **File: Hotwater_Results table.xlsx**
   ChemCAD results along with capital costs are presented in this excel file.

Economic Analysis using GEOPHIRES

The purpose of this document is to describe the contents of information contained within a submission to the Geothermal Data Repository (GDR) node of the National Geothermal Data System (NGDS) in support of Feasibility of Deep Direct-Use Geothermal on the West Virginia University Campus-Morgantown, WV.

Abstract: This dataset contains all the inputs used and output produced from the modified GEOPHIRES for the economic analysis of base case hybrid GDHC system, improved hybrid GDHC system with heat pump and for hot water GDHC. Detailed descriptions of the contents of this repository are provided below.

Key Words: Appalachian Basin, West Virginia University, GEOPHIRES, LCOH, Hybrid Geothermal natural gas system, Deep direct use.

Citation: When referencing this data, please use the following citation information:

Title: WVU DDU: GEOPHIRES Analysis Results for GDHC at WVU campus, Morgantown, WV

Author(s): West Virginia University

Date: March 19, 2020September 22, 2021

Software Requirement Note:

GEOPHIRES open-source code, Microsoft Notepad, Microsoft Excel.

Contents of Submission:

Folder: GEOPHIRES

Contains the input data, and output results for the economic analysis.

Contents

1. **File: GEOPHIRES Parameter.docx**
   The subsurface, surface, financial, capital cost and O&M parameters used in this study are listed.
2. **Folder: HybridGDHC**
   - **c. Folder: GDHC**
     - i. Correlations
       Input and output files of LCOH analysis for hybrid GDHC system using GEOPHIRES correlations for well drilling and completion costs, with an adjustment factor of 1.5 for horizontal wells.
     - ii. NNECosts
       Input and output files of LCOH analysis for hybrid GDHC system using well drilling and completion costs obtained through the quotes from Northeast Natural Energy (NNE).
   - **d. Folder: GDHC_HeatPump**
     - i. Correlations:
       Input and output files of LCOH analysis for improvised hybrid GDHC system using GEOPHIRES correlations for well drilling and completion costs, with an adjustment factor of 1.5 for

horizontal wells.

ii. NNECosts
Input and output files of LCOH analysis for improvised hybrid GDHC system using well drilling and completion costs obtained through the quotes from Northeast Natural Energy (NNE).

e. File: UQAnalysis

i. Correlations
Input and output files of LCOH analysis for improvised hybrid GDHC system using the temperature profile obtained in uncertainty analysis using iTOUGH2 and using default well drilling and completion costs.

ii. NNECosts
Input and output files of LCOH analysis for improvised hybrid GDHC system using the temperature profile obtained in uncertainty analysis using iTOUGH2 and using the NNE quotes for well drilling and completion costs.

3. Folder: HotWaterSystem

a. Folder: 40
Input and output files for LCOH analysis of hot water system with a production flow rate from each well as 20 kg/s and for every two-production wells, one injection well is considered. The wells are horizontal and well drilling and completion costs is obtained through the quotes from Northeast Natural Energy (NNE).

b. Folder: 80
Input and output files for LCOH analysis of hot water system with a production flow rate from each well as 40 kg/s and for every two-production wells, one injection well is considered. The wells are horizontal and well drilling and completion costs is obtained through the quotes from Northeast Natural Energy (NNE).

4. Files: Economics_BaseCase.xlsx; Economics_Improved.xlsx; Economics_HotWater.xlsx
Results of LCOH analysis for base case hybrid GDHC, improved hybrid GDHC system and preliminary analysis for hot water system.

Environmental Calculations

The purpose of this document is to describe the contents of information contained within a submission to the Geothermal Data Repository (GDR) node of the National Geothermal Data System (NGDS) in support of Feasibility of Deep Direct-Use Geothermal on the West Virginia University Campus-Morgantown, WV.

Abstract: This dataset contains all the inputs used and output produced from Matlab for the environmental analysis of an improved hybrid GDHC system with a heat pump, without a heat pump and for a hot water GDHC. Detailed descriptions of the contents of this repository are provided below.

Key Words: Appalachian Basin, West Virginia University, Hybrid Geothermal natural gas system, Deep direct-use, and Environmental effects.

Citation: When referencing this data, please use the following citation information:

Title: WVU DDU: Environmental Analysis Results for GDHC at WVU campus, Morgantown, WV

Author(s): West Virginia University

Date: September 22, 2021

Software Requirement Note:

Matlab.

Contents of Submission:

Folder: Environmental Calculations

Contains the input data, and output results for the calculations to determine the decrease in the amount of CO_2 emissions

Contents

1. **File: Environmental calculations.docx**
   Word document describing the methodology used along with the amount of CO_2 emissions reduced for production of hot water and steam using GDHC system when compared to natural gas and coal as energy source.

2. **Folder: Hybrid Coal**
   a. **File: A1_H.m, A2_H.m**
      Scripts used to calculate the decrease in the amount of CO_2 emissions between the hybrid geothermal system with a heat pump for a horizontal well configuration and a coal-based system for scenario 1 and scenario 2 respectively.
   b. **File: A1_V.m, File: A2_V.m**
      Scripts used to calculate the decrease in the amount of CO_2 emissions between the hybrid geothermal system with a heat pump for a vertical well configuration and a coal-based system for scenario 1 and scenario 2 respectively.

c. **File: S1_H.m, S2_H.m**
Scripts used to calculate the decrease in the amount of CO_2 emissions between the hybrid geothermal system without a heat pump for a horizontal well configuration and a coal-based system for scenario 1 and scenario 2 respectively.

d. **File: S1_V.m, S2_V.m**
Scripts used to calculate the decrease in the amount of CO_2 emissions between the hybrid geothermal system without a heat pump for a vertical well configuration and a coal-based system for scenario 1 and scenario 2 respectively.

3. **Folder: Hybrid Natural Gas**
   a. **File: A1_H.m, A2_H.m**
   Scripts used to calculate the decrease in the amount of CO_2 emissions between the hybrid geothermal system with a heat pump for a horizontal well configuration and a natural gas system for scenario 1 and scenario 2 respectively.
   b. **File: A1_V.m, A2_V.m**
   Scripts used to calculate the decrease in the amount of CO_2 emissions between the hybrid geothermal system with a heat pump for a vertical well configuration and a natural gas system for scenario 1 and scenario 2 respectively.
   c. **File: S1_H.m, S2_H.m**
   Scripts used to calculate the decrease in the amount of CO_2 emissions between the hybrid geothermal system without a heat pump for a horizontal well configuration and a natural gas system for scenario 1 and scenario 2 respectively.
   d. **File: S1_V.m, S2_V.m**
   Scripts used to calculate the decrease in the amount of CO_2 emissions between the hybrid geothermal system without a heat pump for a vertical well configuration and a natural gas system for scenario 1 and scenario 2 respectively.

4. **Folder: Water Coal**
   a. **File: Total_60_peak_H_40.m, Total_60_peak_H_80.m**
   Scripts used to calculate the decrease in the amount of CO_2 emissions between the 60/40 water/steam ratio hybrid geothermal system using peak energy demand with a 40 kg/s and 80 kg/s injection rates and a horizontal well configuration and a coal-based system.
   b. **Total_75_peak_H_40.m, Total_75_peak_H_80.m**
   Scripts used to calculate the decrease in the amount of CO_2 emissions between the 75/25 water/steam ratio hybrid geothermal system using peak energy demand with a 40 kg/s and 80 kg/s injection rates and a horizontal well configuration and a coal-based system
   c. **Total_85_peak_H_80.m**
   Script used to calculate the decrease in the amount of CO_2 emissions between

the 85/15 water/steam ratio hybrid geothermal system using peak energy demand with an 80 kg/s injection rate and a horizontal well configuration and a coal-based system

5. **Folder: Water Natural Gas**
    a. **File: Total_60_peak_H_40.m, Total_60_peak_H_80.m**
    Scripts used to calculate the decrease in the amount of CO_2 emissions between the 60/40 water/steam ratio hybrid geothermal system using peak energy demand with a 40 kg/s and 80 kg/s injection rates and a horizontal well configuration and a natural gas system.
    b. **Total_75_peak_H_40.m, Total_75_peak_H_80.m**
    Scripts used to calculate the decrease in the amount of CO_2 emissions between the 75/25 water/steam ratio hybrid geothermal system using peak energy demand with a 40 kg/s and 80 kg/s injection rates and a horizontal well configuration and a natural gas system.
    d. **Total_85_peak_H_80.m**
    Script used to calculate the decrease in the amount of CO_2 emissions between the 85/15 water/steam ratio hybrid geothermal system using peak energy demand with an 80kg/s injection rate and a horizontal well configuration and a natural gas system.